UILU-ENG 87-3605

Report No. 139

FATIGUE CRACK CLOSURE AND CRACK GROWTH OUTSIDE THE SMALL SCALE YIELDING REGIME

by

R. Craig McClung

Materials and Design Division
Department of Mechanical and Industrial Engineering

A Report of the

MATERIALS ENGINEERING - MECHANICAL BEHAVIOR

College of Engineering, University of Illinois at Urbana-Champaign

December 1987

FATIGUE CRACK CLOSURE AND CRACK GROWTH OUTSIDE THE SMALL SCALE YIELDING REGIME

Robert Craig McClung, Ph.D
Department of Mechanical and Industrial Engineering
University of Illinois at Urbana-Champaign, 1988

ABSTRACT

The changes in crack opening stresses and the effects of these changes on crack growth rates are investigated for several problems in fatigue cracking outside the regime where small-scale yielding assumptions are strictly valid. The primary tool used here for the determination of opening stress, S_{open}, is an elastic-plastic finite element simulation of fatigue crack growth. Computations are performed on a CRAY X-MP/48 supercomputer. Several modeling issues are investigated, including the effects of mesh design, crack advance scheme, material properties, and constitutive model on the resulting values of S_{open}. Special attention is given to the dependency of S_{open}/S_{max} on S_{max}, the maximum stress. Crack opening behavior is interpreted and explored in terms of information about crack opening displacements, crack-tip plastic zones, and stress-strain histories. Parameters which might be used to correlate crack growth rates under these conditions are critically reviewed, and the potential role of closure in these parameters is explored. Fatigue crack growth data obtained under conditions of intermediate- and large-scale yielding and biaxial loading are successfully correlated only when closure-modified parameters are employed. The changes in S_{open} for a crack growing from a hole are investigated. Simple models are developed to correlate this particular crack opening behavior and the associated accelerated crack growth rates.

ACKNOWLEDGMENTS

This research was supported financially by the Fracture Control Program, College of Engineering, University of Illinois at Urbana-Champaign (UIUC). Supercomputer access was made possible by grants from the National Center for Supercomputing Applications, UIUC. Experimental portions of the work were performed in the Materials Engineering Research Lab, College of Engineering, UIUC.

Special appreciation is extended to my advisor, Professor Huseyin Sehitoglu, whose friendship, encouragement and insightful suggestions over the past five years stimulated the research. He is especially thanked for the freedom and trust granted to me, enabling me to aggressively pursue independent initiatives. My M.S. thesis co-advisors, Professor JoDean Morrow and Professor Herb Corten, are thanked for similar contributions, especially during the first half of my graduate career.

The work would not have been possible without the technical contributions of fellow students. Paul Lalor provided essential assistance with the finite element software. A number of undergraduate student workers played key roles: Louis Lundell, Gary Fenn, Peter Nelson, Tom Leone, and especially Chris Kuhlman completed large quantities of tedious work with great attention to quality.

Many professional colleagues around the world are thanked for their swift replies to questions and requests for data. Special appreciation is extended to Dr. P. Truyens of the University of Ghent, Belgium, who made available his unpublished doctoral thesis.

The Publications Office of the Department of Mechanical and Industrial Engineering, UIUC provided extraordinarily friendly, prompt and high quality service in typing the manuscript and preparing the figures. June Kempka, Suzanne Palmer, Cel Daniel, and Tammy Lawhead are thanked for these contributions.

Finally, the strength to conceive and complete the work was provided by God through Jesus Christ and members of His Body on earth: my parents, who loved and encouraged me unconditionally; dear Christian friends who revived me weekly and daily, especially Dick, King, Ray, and Ken; and most of all my wife Becky, who gave herself fully to me in service and loving devotion.

TABLE OF CONTENTS

LIST OF FIGURES

NOMENCLATURE

a	crack length
a'	plasticity-modified crack length, equal to $(a + r_y)$
$\Delta a, da$	crack growth increment
A	constant in expression for power-law constitutive model
b	half-height of an elliptical hole (one-half of the minor axis)
B	specimen thickness
c	half-width of a center notch or hole or (rarely) Coffin's exponent in strain-life equation
C	coefficient in a Paris law crack growth relationship
C_p	coefficient of the plastic term in an elastic-plastic fatigue crack growth parameter
C_t, C', C_o	coefficient of the entire expression for an elastic-plastic fatigue crack growth parameter
COD	crack opening displacement
CST	constant strain triangle
e, e_e, e_p	remote or far-field strain, elastic component, plastic component
E	modulus of elasticity
f	yield function
F	elastic geometry correction factor for stress intensity factor
FCG	fatigue crack growth
FEM	finite element method
H	plastic modulus, equal to $d\bar{\sigma}/\bar{\varepsilon}_p$
$h(n), h_o$	function of strain hardening exponent, appearing in expressions for J_p and ΔJ_p
ISY	intermediate scale yielding
$J, \Delta J$	J-integral, range of J-integral
J_e, J_p	elastic, plastic components of J-integral

ΔJ_{eff}	effective range of J-integral
J_2	second invariant of stress, equal to 1/2 $S_{ij}S_{ij}$
k	yield stress in simple shear
K	stress-intensity factor or strength coefficient
K'	cyclic strength coefficient
ΔK	range of stress intensity factor
K_{max}	maximum value of stress intensity factor
ΔK_{mod}	plasticity-modified ΔK (a replaced by a')
ΔK_{eff}	effective range of stress intensity factor
K_t	theoretical elastic stress concentration factor
K^σ	Neuber concentration factor for local stress
K^ε	Neuber concentration factor for local strain
ΔK_ε	range of strain intensity factor
$\Delta K'$	range of equivalent stress intensity factor
K_γ	intensity factor of Bhanderi, et al.
ℓ	crack length, measured from notch
ℓ_o	initial crack length
ℓ_t	transition crack length between short crack and long crack solutions
LCF	low cycle fatigue
LSY	large scale yielding
m	exponent in a Paris law crack growth relationship
n, n'	strain hardening exponent, cyclic strain hardening exponent
N	constant in expression for power-law constitutive model
N, dN	number of cycles, increment in number of cycles
N_f	number of cycles to failure
P, P_o	load, limit load

r_p	width of the crack tip plastic zone along the crack line, generally at maximum load
Δr_p	width of the crack tip reversed plastic zone along the crack line, generally at minimum load
R	stress ratio, equal to S_{min}/S_{max}
S, S_x, S_y	stress, usually far-field or remote value
ΔS	range of stress
S_{max}	maximum stress
S_{min}	minimum stress
S_{clos}	stress at which crack tip first closes
S_{open}	stress at which crack tip first opens completely
ΔS_{eff}	effective range of stress, equal to $(S_{max} - S_{open})$
S_{ij}	stress deviator
S^c_{ij}	center of the yield surface in stress deviator space
SSY	small scale yielding
U	effective stress range ratio, equal to $(\Delta S_{eff}/\Delta S)$
W	half-width of plate
ΔZ	range of an elastic-plastic fatigue crack growth parameter

Greek

δ	displacement, usually load-line deflection
δ_{resid}	residual displacements in wake of crack tip
δ_t	crack tip opening displacement
$\varepsilon, \varepsilon_{yy}$	strain, usually at a local position
$\Delta\varepsilon$	total strain range
$\varepsilon_p, \Delta\varepsilon_p$	plastic strain, range of plastic strain
$\Delta\varepsilon^e_N, \Delta\varepsilon^p_N$	range of elastic and plastic strain, based on net section stresses

$\dot{\varepsilon}^{P}_{ij}$	plastic strain rate
ε'_f	fatigue ductility coefficient in strain-life equation
λ	biaxial stress ratio, generally S_x/S_y
ν	Poisson's ratio
ρ	radius of center hole at position y = 0
σ, σ_{yy}	stress, usually at a local position
σ_o	yield stress, usually intersection of elastic and plastic lines in a bilinear representation
σ_{ys}	0.2% offset yield stress
σ_u	ultimate strength
σ_z	out-of-plane stress
ϕ	coefficient of r_y in expressions for plasticity-modified crack length

1. INTRODUCTION

1.1 Background

Under certain conditions, a large percentage of the total useful service life of a component or structure subjected to cyclic loading coincides with the slow, steady growth of a small fatigue crack. Successful engineering analysis and design for these conditions, then, may depend on the availability of an accurate model to correlate and predict the rate of growth of cracks for a given combination of load history, component geometry, and material properties. Most such models in current use are based on the concept, first proposed by Paris [1,2], that the average crack growth per cycle can be described as a power-law function of the crack tip linear elastic stress intensity factor, K. This principle, with certain occasional modifications, has been successfully applied to explain and predict crack growth behavior for a wide range of stress levels, stress states, crack lengths, materials, variable amplitude histories, and geometric configurations.

One of the most significant advances in the study of fatigue crack growth was the discovery by Elber [3,4] of the crack closure phenomenon. He found that the tip of a fatigue crack was, in general, closed during some portion of the loading cycle. He proposed that only the portion of the loading cycle during which the crack tip was open was actually "effective" in propagating the crack. This concept has since been used extensively to explain stress ratio effects and variable amplitude loading effects, and it has further been proposed as a possible factor in other apparently anomalous crack propagation behaviors.

Nevertheless, there remain a number of important problems in fatigue crack growth which have not been solved by traditional applications of K-based parameters. These include the growth of very short cracks, thickness effects, stress biaxiality effects, and notch effects. In addition, when stresses are high and plastic deformations become large, linear elastic fracture mechanics ultimately loses its validity. Analogous elastic-plastic parameters have been proposed and have met with some success, but several critical questions remain.

The phenomenon of crack closure also involves many unresolved issues. For example, debate continues over whether closure occurs at all in plane strain, and what implications this may have for crack growth in real components. Both experimental measurement and analytical estimation of accurate crack opening levels are difficult tasks, and as a result there is not yet a clear picture of which parameters have the most significant impact on crack opening stresses.

1.2 Purpose and Scope of this Research

The present research has two parallel thrusts. The first is an analytical investigation of crack closure and the factors which control its magnitude. Special attention will be given to the influence of maximum stress, constitutive relationships, and stress biaxiality. The primary tool used here for the determination of opening stresses under various conditions is an elastic-plastic finite element simulation of fatigue crack growth. Insight is also drawn from simpler analytical models and original experimental measurements. Chapter 2 presents details of the finite element formulation, a discussion of several

crucial modeling issues, and the basic results of the analysis for uniaxially stressed center cracks.

The second thrust of the research is the application of this closure information to the correlation of experimental crack growth data. Attention is focused on problems which have not been resolved by traditional applications of ΔK and closure-modified ΔK. Considered primarily are those problems in which the assumptions of small scale yielding (SSY) are not strictly satisfied, including both intermediate scale yielding (ISY) and the large scale yielding (LSY) typically associated with low cycle fatigue.

Chapter 3 begins with a critical review and analysis of parameters which have been proposed to correlate crack growth data associated with ISY and LSY. The possible role of closure in these parameters is discussed. Correlations are attempted for crack growth data from two steels over a wide range of stresses and crack lengths. The importance of crack closure information for these correlations is evaluated.

Cyclic biaxial stressing of mode I cracks is considered in Chapter 4. Finite element simulations of closure under these conditions are presented and discussed. Three sets of crack growth data from the literature are correlated with and without consideration of closure behavior, and the correlations are compared.

The problem of crack growth from notches is the focus of Chapter 5. The opening behavior of these cracks is characterized with the finite element analysis. A simple model is developed to explain the behavior to a first approximation. The model is compared with experimental crack growth data for notches of various sizes and shapes.

Chapter 6 provides a summary of the research and further discussion of the significance of crack closure for engineering analysis and design.

2. FINITE ELEMENT FORMULATION AND BASIC RESULTS

2.1 Background

The first finite element modeling of fatigue crack growth may have been carried out by Miyamoto et al. [5]. They compared monotonic and cyclic loading with special attention to changes in the stress and strain distributions and crack opening displacements upon release of the crack tip node. Premature contact of the crack surfaces during unloading in a tension-tension cycle was observed but not investigated in depth.

The first major study of crack closure with the finite element method was published by Ohji, Ogura, and Ohkubo beginning in 1974 [6-10]. They applied their model to the study of crack growth from notches (especially the non-propagating crack problem), variable amplitude loading, and biaxial loading. At about the same time Newman published the results of his independent investigations [11-14], giving more attention to the details of the model itself.

In the following ten years, only a handful of papers gave attention to this technique. Shiratori et al. [15] published a detailed analysis of stresses, strains, and displacements near the fatigue crack under simple constant amplitude and overload histories. Socie [16] considered crack closure under constant and variable amplitude loading of the SAE keyhole specimen, although more of his attention was directed to the total life prediction problem. Nakagaki and Atluri [17,18] took a radically different approach to the problem, employing special crack-tip elements and translation of the near-tip mesh, and studying mixed mode configurations in addition to the standard mode I case. Nakamura et al.

[19,20] evaluated closure in the compact tension (CT) specimen with special attention to the comparison between ideal and fatigue cracks. Blom and Holm [21] studied closure in the CT specimen at different stress ratios under plane stress and plane strain.

Interest in the finite element modeling of fatigue crack closure has surged in recent years, however, including four papers presented at the May 1986 ASTM International Symposium on Fatigue Crack Closure.* Fleck [22,23] adapted Newman's original formulation to examine closure under plane strain, and Chermahini [24,25] expanded Newman's formulation to consider a simple three-dimensional problem. Nicholas, Palazotto, and Bednarz [26] employed a more general constitutive model and analyzed short cracks at high stresses. Finally, Lalor and Sehitoglu [27-29] have published research which is a direct predecessor of the present thesis, and which is described in more detail in the next section.

2.2 Finite Element Formulation

2.2.1 Formulation of Lalor and Sehitoglu

Lalor and Sehitoglu developed an original elasto-plastic finite element code for their study of fatigue crack closure. A small deformation formulation was employed. Iteration to the correct solution of the nonlinear equations at each load step was carried out according to the direct Newton-Raphson method, which is based on the tangent stiffness matrix. While this requires a complete solution of the full system of equations at each iteration, which can be computationally

*The edited proceedings are being published by ASTM as Special Technical Publication (STP) 982.

expensive, convergence is generally very rapid. This technique also permitted updating of the nodal coordinates at each increment, which represents a first approximation to a large deformation formulation.

The material model was based on concepts of incremental, rate-independent classical plasticity. The von Mises criterion was used to identify the yield surface. Kinematic hardening was chosen as the best simple simulation of the Bauschinger effect associated with reversed yielding. Ziegler's modification of Prager's hardening rule was observed. The stress-strain relationship was modeled as bilinear. The constitutive equation was numerically integrated according to a mean normal method with subincrementation and radial return.

The changing boundary conditions associated with intermittent opening and closing of the crack surfaces and with crack advance were accommodated through a series of truss elements along the crack line, following the concept of Newman [11-14]. The stiffness of a given truss was set to an extremely large value when the crack was "closed" at that location, and set to a negligibly small value when the crack was "open." Stresses and displacements along the crack line were monitored on each load increment to determine if boundary conditions should be changed at any location. Crack advance was accomplished by a similar sharp decrease in the stiffness of the truss at the crack tip node at some specified time in the loading history, typically at maximum load.

The meshes were composed of four-noded isoparametric elements (Q4 elements), which permit linear strain distributions. This represented a significant advance over the constant strain elements used in a majority of the previous research [5-16,19,20,22,23,26]. True higher-order

elements are generally not feasible due to the computational expense associated with the additional degrees-of-freedom required.

The majority of the actual computation involved in the research of Lalor and Sehitoglu was carried out on a dedicated HP-9000 super-minicomputer. Typical execution times for a single simulation were on the order of 100 hours.

Further details of the formulation can be found in Refs. 27-29.

2.2.2 Formulation used in the Present Research

All finite element analyses conducted as a part of the present research were based on the formulation and computer codes developed by Lalor and Sehitoglu. Significant modifications fall into four categories: optimization and vectorization, pre- and post-processing, constitutive relationships, and mesh development.

Optimization and Vectorization. The lengthy execution times characteristic of the earlier research made more advanced studies unfeasible. To overcome this limitation, access was obtained to the CRAY X-MP/48 supercomputer at the National Center for Supercomputing Applications, University of Illinois at Urbana-Champaign. In order to make optimal use of the new machine, the entire program was extensively rewritten to reduce redundancies and streamline execution. Special attention was given to vectorization of all matrix operations. Reduction of the stiffness matrix and back-substitution to obtain nodal displacements were identified as particularly time-consuming portions of the program. The simple Gaussian scheme of the original program was replaced by highly vectorized routines, based on Choleski decomposition,

from a commercial software package. As a result of these changes, a reference problem that required 100 hours to execute on the HP-9000 required fewer than 20 minutes on the CRAY, corresponding to a decrease in execution time of approximately 300x.

Pre- and Post-Processing. Special attention was given to the format of information input to and output from the program. Input files were designed to be compact and easily modified in only a few minutes. Each run of the program generated six lengthy output files of standard format. A series of post-processing graphics programs were developed to be able to read and visually display any desired information from the raw output files quickly and with a minimum of user input. Many of the figures in this thesis were taken directly from computer-generated plots based on the raw output files.

Constitutive Relationships. In addition to the bilinear stress-strain relationship used in the previous research, a power-law hardening model was developed and installed as an optional alternative. Details are given later in this chapter.

Mesh Development. Eight new meshes were developed for the present research with the aid of original mesh generation programs. Most are conceptually similar to the meshes of Lalor and Sehitoglu, in that they simulate mode I cracks growing from a central hole in a remotely loaded two-dimensional plate. The meshes differ primarily in the size and shape of the central hole, the size and number of the elements along the crack line, and the uniformity of element size and shape.

A typical mesh is shown in Fig. 2.1. Note that one-quarter symmetry is observed. Strictly speaking, the dimensions of the mesh are

unitless, since loads are directly applied as stresses along the remote boundaries. The half-widths of the central holes range from 8 to 32 units. Final crack lengths typically range from a = 100 to a = 125, or a/W ratios of 0.1 to 0.125. A closer look at a typical fine mesh region is given in Fig. 2.2. Here the element width along the crack line (and hence the crack growth increment, Δa) corresponds to $\Delta a/W = 0.002$. The truss elements along the x-axis are not shown in these figures.

2.3 Modeling Issues

One of the great dangers of the finite element technique is that nearly any run of a program will produce a great many numbers, and the complexity of the problem being solved makes it virtually impossible to tell at a quick glance whether those numbers actually give a correct solution. The danger emerges when those numbers are accepted as being correct without any study of the accuracy and sensitivity of the model itself. This is especially true in the finite element analysis of fatigue crack closure. This is a complex nonlinear problem with reversed plasticity in which primary attention is focused not on the usual quantities of stress and strain but on displacement histories as loads and boundary conditions continuously change. Unfortunately, only a handful of the previous researchers in the area have exhibited any serious study of how their model design might be influencing the quantitative or qualitative nature of their results.

In this section, careful attention is given to a series of critical decisions about mesh design and crack advance techniques. The possible effect of each of these decisions on the accuracy of the final result is

evaluated. These discussions serve not only as background to the present research, but also as a critique of previously published research and as suggested guidelines for future researchers.

2.3.1 Mesh Refinement

The refinement of the mesh along the crack line is important for at least two reasons. First, the mesh must be fine enough to capture the severe stress concentration at the crack tip. Second, the element spacing defines the crack growth increment, which should be as small as possible in order to simulate "real" crack growth. In opposition to these arguments for an abundance of tiny elements, however, are considerations of time and cost. Extensive mesh refinement leads to large stiffness matrix bandwidths and many total degrees-of-freedom, both of which multiply computer execution times, and also requires many increments of crack growth (many cycles, many more load steps). A balance between these two sets of considerations is required which does not seriously degrade the reliability of the results.

Newman [13] was the first to identify and examine the problem of mesh refinement. Working with three meshes composed of constant strain triangles of varying refinement along the crack line, he identified critical mesh spacings necessary for dependable solutions at different stress levels. He described this mesh spacing in terms of the ratio of crack growth increment to the plastic zone size at maximum load.

The design of the current research was to determine opening levels at a fixed final crack length for two different mesh spacings at a wide range of stress levels and two stress ratios, and to observe when the

different meshes gave markedly different opening levels. The results are shown in Fig. 2.3. The symbol "S" is used to represent stress here and often throughout this thesis to emphasize that far-field stress levels are being quantified, not stresses at the crack tip. Here the stress-strain relationship is bilinear and σ_o is the yield stress, the point of intersection of the elastic and plastic lines. The values H and E represent the slopes of the plastic line and the elastic line, respectively. Material properties and constitutive relationships are discussed in more detail later in the chapter. Each individual data point in this figure (and other figures like it throughout the text) corresponds to one (or more) specific finite element simulations. The lines connecting the points represent the author's judgment about general trends and are included as an aid to visualization.

Observe first that above a certain stress level at each R-ratio, the two meshes give reasonably similar results. There is a consistent tendency for the finer mesh to yield slightly higher opening levels, although the difference is not always significant. A remaining question is whether successively finer meshes (e.g., $\Delta a/W$ = 0.001, 0.0005,...) would give continuously higher values of S_{open} or whether an upper bound value would be quickly reached. An important side note is that at this crack length (a = 100, a/W = 0.1), cracks experiencing R = -1 cycling at maximum stresses above 0.6 σ_o have not yet grown out of the influence of the circular hole, and so opening levels are lower than final stable values. This phenomenon will be discussed in more detail in the next section.

Observe second that at intermediate values of maximum stress, normalized opening levels sharply increase and then sharply decrease with S_{max}/σ_o. This "false peak" is an artifact of the modeling process, and is not indicative of any significant physical behavior. In this region the mesh is not sufficiently fine to capture reversed yielding at the crack tip upon unloading. Since there is no reduction of the forward (tensile) plastic deformations (which lead to residual deformations in the wake of the crack tip), these deformations are artificially large and induce artificially high opening levels.

Finally, observe that as the maximum stress approaches zero, opening levels rapidly drop off towards zero. In this region the mesh is insufficiently fine to capture a significant amount of forward plastic deformation. In the absence of substantial crack tip plastic strains, the basic mechanism of plasticity-induced crack closure is absent, and so opening levels will be artificially low.

It is reasonable, instead, to postulate that normalized opening levels should continuously decrease as maximum stresses increase. This is observed in the present model when major mesh defectiveness is eliminated. Based on this postulate, and based also on the earlier observation that opening levels may increase slightly with mesh refinement even at high stress levels, it is possible to construct a schematic representation of an idealized "correct" solution independent of any artificial mesh effects. Such a representation is given by the dashed line in Fig. 2.3, and is intended only for qualitative consideration.

Each of these same three observations appears to hold true for the data of Newman, replotted as Fig. 2.4 from Fig. 11 of Ref. 13. Here

meshes I, II, and III are progressively more finely divided; mesh I corresponds to $\Delta a/W = 0.0028$, mesh II to $\Delta a/W = 0.0007$, and mesh III to $\Delta a/W = 0.00035$. Note the artificially low opening levels for coarse meshes and low maximum stresses, the apparent "false peak" at intermediate stresses, and the convergence to mesh-independent stable values at higher maximum stresses.

The data of Newman suggest a simple criterion for mesh sufficiency based on the ratio of the element size to the forward crack-tip plastic zone size. Estimating the width of the plastic zone along the crack line at maximum load according to a simple Irwin-type relationship for center-cracked panels under plane stress,

$$\frac{r_p}{a} = \left(\frac{S_{max}}{\sigma_o}\right)^2 \qquad (2.1)$$

a value of $\Delta a/r_p \leq 0.05$ seems to be a good rule of thumb for reliable results with Newman's constant strain triangle elements. This ratio also corresponds approximately to the inflection point in the data of Ogura et al. ([9], Fig. 5) below which closure levels decrease with decreasing S_{max}. Such a criterion also suggests that some of the results published in Refs. [5,15,19,20,26], all using constant strain triangles, may have been adversely influenced by insufficient mesh refinement.

Returning to the present research and Fig. 2.3, and comparing results at the two R-ratios, it appears that a single criterion based only on the forward plastic zone size is not sufficient. For the Q4 elements used in this work, $\Delta a/r_p \leq 0.10$ seems to be an indicator of

mesh sufficiency for R = 0, and $\Delta a/r_p \leq 0.15$ for R = -1. The more generous criterion at R = -1 is due to the important role of reversed plasticity in modeling the crack closure phenomenon.

The curves in Fig. 2.3 are composites drawn from the results of several different crack growth simulations at a fixed final crack length. The same trends could be observed, however, in a single test at constant S_{max} as crack length increases. Consider a hypothetical simulation in which the initial crack length in an unnotched mesh is zero. Early in the test the strain intensity at the crack tip will be insufficient to cause forward yielding in the finite-sized crack tip elements, and opening levels will be low. Note that this phenomenon is distinctly different from the well-known "short crack" problem, although the results would appear similar. As the test proceeds and crack length increases, the forward plastic zone will be sufficiently captured by the mesh but the reversed plastic zone will not be, and so opening levels will be artificially high. Finally, as the crack length increases enough to satisfy a $\Delta a/r_p$ criterion, the opening levels will decrease slightly to reach a stable level. While no such test with initial crack length equal to zero was conducted in the present research, the phenomenon of artificially high opening levels at intermediate crack lengths was observed in a number of simulations. In several cases this would have led to erroneous conclusions about opening behavior had not the phenomenon been recognized as a modeling defect.

Comparisons of the mesh-independent results of Newman and the present research in Fig. 2.5 (based on similar strain-hardening behavior) suggest that higher-order elements (Q4 vs. CST) will predict

higher opening levels. This seems to be consistent with the trend in Fig. 2.3 towards higher opening levels with increasing mesh refinement at sufficiently large stresses. A higher-order element should better capture the crack-tip singularity in forward loading and hence develop larger tensile plastic strains (i.e., larger residual deformations).

2.3.2 Initial Defect Size and Stabilization Behavior

The conclusions of the previous discussion suggest that there is no benefit in starting with a zero-length crack analogous to a "naturally" occurring microcrack. In addition to being very computationally expensive due to the large number of load increments required, the results at short crack lengths are likely to be unreliable. A more economical approach is to start with some initial crack length large enough to satisfy the criteria for mesh sufficiency, and then grow the crack only long enough to insure that a stable opening level has been reached.

The nonzero initial crack length can be developed in at least two ways. First, the crack can be initiated from the root of a hole or notch in the mesh. Although the initial crack length is still actually zero in this case, the plasticity caused by the notch is generally sufficient to bypass the types of mesh problems discussed earlier. An added bonus is that this mesh design simulates a real-world fatigue problem: initiation and propagation of fatigue cracks from local stress concentrations.

An alternative approach is simply to start with the crack tip at some arbitrary initial position in an unnotched mesh. A possible dis-

advantage here is mesh economy: a hole or notch represents some large number of elements and nodes which do not have to be included in the mesh, thus reducing the total degrees-of-freedom in the system of equations. In addition, the nature and possible symmetry of the hole or notch may provide a unique opportunity to design the mesh in such a way as to sharply reduce the bandwidth of the stiffness matrix. Since solution times for matrix reduction are typically proportional to the square of the bandwidth, this can be a significant source of cost reduction. Design of a mesh with a large region of extremely fine elements and a narrow bandwidth is something of a difficult artistic problem in its own right, even with the aid of renumbering schemes and other optimization tools. The notched meshes used in the present research typically had bandwidths of 22 to 29 node numbers for meshes with 800 to 1000 total nodes. For two degrees-of-freedom per node, this corresponds to stiffness matrix bandwidths of 44 to 58 and total stiffness matrix orders of 1600 to 2000.

The danger involved in either of these schemes for developing initial crack lengths is that the final stable opening levels (or perceived stable levels) might be artificially influenced by the scheme itself. This is clearly a possible problem with the use of notches: the notch introduces a significant redistribution of stress which can significantly perturb the crack-tip stress and strain fields. Even without a notch, the problem may remain. If crack closure is dependent on the previous history of crack tip deformations, then arbitrarily throwing away a large portion of that previous history is philosophically suspect.

Results of the present finite element analysis demonstrating the effects of notches on stabilization behavior are shown in Figs. 2.6 and 2.7. Results at R = -1 for three different stress levels and two different notch acuities are shown in Fig. 2.6. Here each of the six piecewise linear curves describes a single run of the finite element program. In each case opening levels start low and gradually increase, rising rapidly at first and then more slowly as a stable level is attained.

Several general observations should be interjected at this point. First, note that in the present research the minimum "step size" between normalized opening levels is 0.04, because the load range between zero and maximum load was always broken down into 25 equal load steps. Actually, however, the resolution of opening levels was somewhat finer. A common phenomenon was for the stable opening stress in a given run to smoothly oscillate between two adjacent levels. This was taken as an indication that the true opening stress was at some intermediate level, proportional to the relative amount of time spent at each standard level. Second, note that once a stable level is reached, opening stresses do not further increase with crack length. This suggests that opening levels are not a function of the stress intensity factor K. Instead, it seems clear that opening levels are primarily a function of the normalized maximum remote stress. And third, note that although it is not clear from this picture, opening levels at S_{max}/σ_o = 0.6 and 0.8 have not yet fully stabilized at a = 100.

What does this figure tell us about the effect of notches on stabilization behavior? First, it suggests that stabilization is

relatively rapid at low stress amplitude but somewhat slow at higher stress amplitudes. The initial notch here has a half-width of 32; stabilization at $S_{max}/\sigma_o = 0.4$ occurs after a total Δa of about 28 (14 crack growth steps of $\Delta a = 2$ each), but stabilization at $S_{max}/\sigma_o = 0.8$ has not yet occurred after the crack has grown a distance equal to twice the initial notch half-width. Second, these required distances for stabilization do not change significantly with notch acuity. Results for a mild circular notch ($K_t = 3$) and a moderately sharp elliptical notch ($K_t = 7$) are systematically but only subtly different.

Similar results for crack growth from a circular hole at R = 0 are given in Fig. 2.7. Note that stabilization is relatively more rapid, occurring even at $S_{max}/\sigma_o = 0.8$ by the time the crack has grown a distance equal to one notch radius, but still requiring at least eight crack growth steps (one-half the notch radius) at $S_{max}/\sigma_o = 0.5$. Note also that the $S_{max}/\sigma_o = 0.5$ run shown here exhibits the "false peak" behavior discussed in the previous section on mesh refinement.

This last observation points out that it is important to distinguish between true notch effects and the simple effects of insufficient mesh refinement. Such a distinction can be made by comparing the behaviors of cracks initiated at holes of different sizes. Such a comparison is made in Fig. 2.8. The crack opening curves corresponding to circular holes with radii of 8, 16, and 32 are geometrically similar, indicating that a true notch effect is involved.

A more detailed explanation of this notch effect is given in a later chapter. Here it is sufficient to note that a significant effect does exist and must be considered when interpreting finite element

closure data. Unfortunately, such a consideration does not seem to have been taken into account in some published research. Ogura et al. [8], for example, report stable values for cracks which have grown only about 10 percent of the original notch depth.

The effect of initial crack length, independent of any notch, on stabilization behavior is illustrated in Fig. 2.9. Several analyses were conducted at different stress ratios and stress amplitudes; the results shown here are typical. Opening levels for a crack growing from a notch have stabilized by the time total $\Delta a = 32$. Another crack started at an initial length of 32 units beyond the initial notch (total $a_o = 64$) still required another 24 units (12 steps) of crack growth to reach the same stable level. Other analyses suggested that, as for notches, stabilization lengths increased with increasing S_{max}/σ_o. This same trend was noted earlier by Newman [13].

In general, cracks begun from an initial crack length eventually reached the same opening level as naturally occurring ($\ell_o = 0$) cracks experiencing the same loading history. The only apparent exceptions to this rule are cases where one or both crack growth simulations being compared fell victim to problems of insufficient mesh refinement; this caused some confusion in Refs. [28,29].

What conclusions can be drawn about the use of notches and initial crack lengths to reduce computational expense? Both techniques are valid and eventually give accurate stable opening levels. Unfortunately, in those cases where economizing is most needed (negative R-ratios and large maximum stresses), stabilization is relatively slow. Special care must be given to verify that the crack has grown beyond the region of influence of the initial defect.

A final note on the topic is that the concept of a "stable" level is unfortunately somewhat vague. How long must the opening level remain unchanged before it can be consider "stable"? At low stresses "stable" behavior may be relatively obvious; opening levels rapidly rise to a level from which they do not change for thirty or more crack growth increments. At higher stress levels the issue is cloudier. Opening levels may remain constant for ten or fifteen steps before smoothly rising to the next higher level. Since the fine mesh region is necessarily small and therefore the total number of possible crack growth steps limited, it may not always be possible to identify the "stable" level with full confidence. No definitive answer or empirical criterion is suggested here as a resolution of this dilemma, only a caveat to the future researcher and the interpreter of past research.

2.3.3 Crack Tip Node Release Scheme

A limitation of the finite element model for fatigue crack growth is that crack advance must occur in relatively large discrete jumps corresponding to element sizes rather than in the relatively smooth, continuous series of infinitesimally small "da" values occurring in the physical situation. Another limitation is that there is no quantitative consensus about the mechanism that actually causes crack advance. Even in the research community, crack growth rates are typically correlated as an average over large numbers of cycles with empirical models based primarily on quantities remote from the crack tip. The combined result of these two limitations is that crack advance schemes are typically arbitrary and are perhaps the most unrealistic feature of the model as a whole.

The most common scheme is that originally suggested by Newman [11-13], who released the crack-tip node (and hence extended the crack) at the maximum load in each cycle. Newman completed redistribution of loads due to the node release before beginning the next unloading increment. A similar technique was employed by Fleck, Chermahini, and Blom and Holm. Ogura et al. released the crack tip node numerically at the minimum load in the cycle. Since the crack tip was closed at that point, the node was effectively released during the ensuing loading cycle, at the moment when the usual criterion for crack opening was satisfied at the crack tip node. This pattern was also followed by Nakamura et al. Nakagaki and Atluri released the crack tip node at different points along the forward loading excursion and found, for their formulation, that the apparent opening level was heavily dependent on the timing of the node release. They arbitrarily chose a release point along the loading ramp in order to give an opening stress similar to certain reported experimental values. Lalor and Sehitoglu employed a node release scheme in which the crack tip was advanced immediately after the point of maximum load, during the first increment of unloading. Nicholas, et al., released the node gradually during the unloading excursion, beginning at maximum load, and completing the process by the time the mean load was reached.

Since no comparative study of node release schemes had been reported for standard finite element schemes, and in view of the large effects reported by Nakagaki and Atluri with their nontraditional scheme, such a study was carried out with the present formulation. Three primary node release schemes were compared: node release at

maximum load with stabilization (after Newman), node release at minimum load (after Ogura, et al.), and node release immediately after maximum load (after Lalor). Each of these schemes involved release of a node on every cycle. It was further postulated that the sudden release of a node at or near maximum load could result in artificial residual strains or stresses which would not be eliminated before the next node release occurred. For this reason, further node release schemes were investigated in which the crack tip node was released just after maximum load, but two or more full cycles were completed at a given crack length before the next node was released.

The results of such a study for R = 0 are shown in Fig. 2.10. Observe first that there is not an extremely large effect of node release scheme. All four schemes shown gave similar results, especially at higher stresses. Observe second that the scheme involving node release immediately after maximum load gave the "smoothest" and most consistent results, both in terms of final stable opening stress (shown) and in terms of transient closure behavior (not shown here). This scheme also gave the highest crack opening stresses.

Allowing two cycles per crack growth increment (as opposed to only one) resulted in a slight decrease in opening levels. This is apparently due to a minor redistribution of stress around the crack tip: normal stresses in the one or two elements immediately behind the crack tip increased slightly, while stresses immediately ahead of the crack tip relaxed slightly. No significant changes in COD, plastic zone size, etc., occurred. For the bilinear hardening model, these changes in opening level essentially occurred only during the second cycle

following node release. Alternative schemes in which three or more cycles were allowed per crack growth increment did not result in still lower values for S_{open}.

One small difficulty exists with either of the schemes in which a node is released at or near maximum load on every cycle. The immediately previous crack tip node, now the first node behind the new crack tip, nearly always closes during the very first unloading increment. This happens because a complete redistribution of loads and plastic strains does not occur immediately upon node release; the COD actually changes very little. A similar behavior was previously reported by Fleck [23]. This problem was dealt with here by simply ignoring the closure of this node and treating the crack conceptually as if it did not extend until the next forward loading excursion had begun. This means that crack closing levels were generally determined by the behavior of the second node behind the real crack tip, while crack opening levels were based on the behavior of the first node behind the crack tip. The other crack advance schemes in which this problem did not occur (release at minimum load, or two cycles per crack growth increment), however, showed that the first two nodes behind the crack tip tended to close naturally at the same increment. Ignoring the first node upon unloading, then, should cause no difficulty.

Throughout the remainder of this thesis, the crack advance scheme involving node release immediately after maximum load on each cycle was chosen as the standard technique, due to its general efficiency and consistent performance. Alternate schemes do not appear to give particularly different results in many cases. The fact that the chosen

scheme gave the highest S_{open} values was also of some attraction, noting the general tendency observed earlier to slightly higher S_{open} values with increasing mesh refinement.

2.4 Basic Results

In this section the basic results of the analysis will be presented and briefly discussed. Stable opening levels, crack tip plastic zones, and crack opening displacements will be examined for mode I center cracks under uniaxial plane stress tension. Attention will be focused on the effects of maximum stress in the cycle, material properties, and constitutive model. Differences in opening and closing levels will be considered.

2.4.1 Effect of Maximum Stress

Stable crack opening levels, normalized by the maximum stress in the cycle, are presented as a function of S_{max}/σ_o for a single set of material properties in Fig. 2.11. These results, and others throughout the remainder of the thesis, are based on meshes with $\Delta a/W = 0.002$ and are independent of any significant notch or initial crack length effects. Two primary features should be noted. The first is the strong stress ratio effect, the difference in opening levels between R = 0 and R = -1. This also corresponds to a pronounced difference in the effective stress range ratio, U, where

$$U = \frac{\Delta S_{eff}}{\Delta S} = \frac{S_{max} - S_{open}}{S_{max} - S_{min}} = \frac{1 - (S_{open}/S_{max})}{1 - R} \qquad (2.2)$$

This R-ratio effect was a primary focus of the earliest crack closure studies [4].

The second important feature to be noted is the pronounced decrease in normalized opening stress with increasing maximum stress, which is especially prominent for R = -1. This phenomenon, which motivates a majority of the applications of crack closure concepts in this thesis, is clearly supported by all previous finite element closure models which have considered more than one stress level. Unfortunately, it is a phenomenon which has been largely ignored or assumed not to exist in a great deal of experimental research and a great many applications of closure concepts to life prediction. It has been common, for example, to develop formulas for U as a function of R without any consideration or definition of S_{max} [4,30].

This phenomenon is also supported by a number of simple analytical models for crack closure. All are generally based on a Dugdale [31] or Bilby-Cottrell-Swinden [32] type of strip yield model which has been modified to leave material in the wake of the advancing crack tip. These include the early efforts of Dill and Saff [33], Shiratori, et al. [34], Fuhring and Seeger [35], and Budiansky and Hutchinson [36]; the more well-known Newman model [37-39] which considers constraint effects in addition to R and S_{max} effects; and the more recent contributions of Sehitoglu [40-41] and Ibrahim, et al. [42]. Several of the more general and more accessible models are compared with the present FEM results in Fig. 2.12. Since the simple analytical models assume elastic-perfectly plastic material response characterized by the limit stress σ_o, for comparison purposes the FEM results given correspond to nearly

negligible linear hardening characterized by H/E = 0.01 above a yield stress σ_o.

At first glance the decrease in opening level with S_{max} appears to be paradoxical. Plasticity-induced crack closure is a result of inelastic deformations at the crack tip, which are left behind as residual deformations in the wake of the crack tip. It would seem, then, that when inelastic deformations are significantly larger (higher maximum stresses), crack closure should be more pronounced. This paradox seems to be resolved, however, by a careful examination of Fig. 2.13. In this figure the crack opening displacement (COD) at maximum load is shown as a function of distance behind the crack tip, giving the profile of the crack surfaces (note the major difference in the scales for ordinate and abscissa). Two types of cracks are represented. The solid line corresponds to a fatigue crack which has been grown in short steps from a very small initial length to a length of a = 100, and which has therefore developed a wake of residual deformations. The dashed line is also generated from finite element analysis (with the same meshes), but in these cases the initial crack length was set to a = 100 and the cracked body was loaded once from zero to maximum load. The difference between the "stationary" crack profile and the "fatigue" crack profile is a reasonable first estimate of the residual deformations, δ_{resid}. The comparison should, in reality, be a more complex one involving a general multiaxial problem in reversed plasticity. However, the original concept of residual deformations as an easily visualized and quantified entity is something of an idealization itself. The present comparison as a definition of δ_{resid} has also been suggested by previous

finite element researchers [13,19,20]. There are some changes in plastic zones and stress and strain distributions ahead of the crack tip for corresponding stationary and fatigue cracks, but the most significant reason for the major differences in COD appears to be the displacements caused by previous crack tip strain histories.

What, then, can be learned from this comparison of COD values at various maximum stresses? First note that, as expected, as the maximum stress increases, the residual deformations increase (the difference between the stationary and fatigue cracks increases). Overcoming this effect, however, is the large increase in total COD with increasing S_{max}. The crack opening event can be idealized as a competition between (1) the total "ideal" COD, which increases during a loading cycle with the remote stress, and which is loosely suggested by the behavior of the stationary crack, and (2) δ_{resid}, which is essentially constant during the loading cycle. When the "ideal" COD at or near the crack tip first exceeds δ_{resid} at that location, the crack tip "opens". If two cracks have the same "ideal" COD but different deformation histories, the one with the larger δ_{resid} will open later. On the other hand, if two cracks have the same δ_{resid} but different loading, the one with the larger "ideal" COD will open earlier. In Fig. 2.13, the residual deformations at higher S_{max} values are a smaller percentage of the total corresponding COD, and so normalized (not necessarily absolute) opening stresses are lower. Again, remember that these arguments are idealizations intended to develop an intuitive feel for crack opening behavior, and are not presented as rigorous analytical mechanics.

Comparisons between R = 0 and R = -1 behavior can be made in the same context. Total ideal COD values are essentially the same in both cases, but the clearly larger δ_{resid} values for R = 0 lead to higher opening stresses. Examination of the R-ratio effect also points out the significant role of reversed plastic deformation; the large δ_{resid} values encountered in R = 0 histories (where forward loading and tensile plastic deformations are dominant) have been significantly reduced in R = -1 histories by the compressive yielding at and behind the crack tip.

2.4.2 Effect of Material Properties

2.4.2.1 H/E Ratio

The constitutive model used in a majority of this research is based on a bilinear representation of the stress-strain curve. The first linear portion represents elastic behavior, and is characterized by a Young's Modulus of E = 205410 MPa. The elastic Poisson's ratio, ν, is taken as 0.3. The second linear portion represents strain hardening behavior, and may be characterized by the plastic modulus H, where $H = d\bar{\sigma} / d\bar{\varepsilon}_p$. The intersection of the two lines defines the yield stress σ_o. In the present research, σ_o is typically 430 MPa and H is chosen to be 13670 MPa, so that the non-dimensional ratio H/E is nominally about 0.07. These properties correspond to a 1070 Class U railroad wheel steel which was the subject of earlier crack closure research [40,41] and which is typical of a much wider class of moderately strong steels. The properties input to the finite element program can be easily changed, however, and this provides the opportunity to systematically examine possible effects on closure.

High values of H/E correspond to materials with appreciable strain hardening, such as soft steels. Low values of H/E, approaching zero, are representative of high strength steels and many aluminum alloys. Here a value of H/E = 0.01 was generated by changing H but leaving E and σ_o unchanged. The basic results for crack opening stresses at the two H/E ratios are shown in Fig. 2.14. At both R-ratios, crack opening levels are higher for H/E = 0.01 at low maximum stresses and lower for H/E = 0.01 at high maximum stresses. Another possible summary statement is that opening levels are similar at intermediate stresses, but the effect of maximum stress on opening levels is more pronounced for low hardening materials.

These effects can be more easily understood in the context of Fig. 2.15, which shows COD values at maximum load for fatigue and stationary cracks at the two H/E ratios. At low maximum stresses, δ_{resid} is larger for H/E = 0.01 because plastic strains are more easily developed at the crack tip. Total COD values for the two H/E values at low S are relatively similar, however, because at low stress levels the COD is more controlled by the remote stress-strain behavior, which is predominantly elastic and hence unchanged with H/E. Put another way, elastic constraint is high, and so increases in local plasticity are more significant. At higher remote stresses, however, (such as S_{max}/σ_o = 0.8) constraint is beginning to be lost due to the onset of general yielding. In this case the dominant event is the larger total COD generated for H/E = 0.01 because of larger tensile plastic deformations generated at intermediate distances from the crack tip. Residual deformations for H/E = 0.01 may even be smaller than for H/E =

0.07 because of the increased role of reversed plasticity at higher stress amplitudes.

2.4.2.2 σ_o/E Ratio

Another significant material property is characterized by the nondimensional form σ_o/E. For steels, this ratio is typically 0.001 - 0.003, while for aluminums, the large change in E results in ratios often around 0.005 - 0.007. Does this affect crack closure? Several finite element simulations suggest that the answer is "no". One example is shown in Fig. 2.16. Here H, E, and S_{max}/σ_o values are the same in both cases, but σ_o is changed by a factor of three. Results for the two runs, expressed in customary normalized form, are essentially identical. Other studies in which σ_o remained constant but H and E changed by factors of three led to the same conclusion.

2.4.3 Crack Tip Plastic Zones

The finite element provides useful information about forward and reversed plastic zones which can lead to a broader perspective on fatigue crack growth and closure as a whole. Figure 2.17 shows typical forward plastic zone sizes and shapes at maximum load for a common crack length (a = 100, a/W = 0.1) and different S_{max} values. At lower maximum stresses plastic zones are approximately circular or lobe-shaped and their sizes are small compared to crack lengths, so plasticity is confined and "small scale yielding" criteria are generally satisfied. At higher maximum stresses, the characteristic shape of the plastic zone changes to more closely resemble an intense shear band, aligned at an

angle to the crack line not far from 45°. There is no major difference between the two H/E values, other than a general tendency to larger plastic zones at H/E = 0.01.

A typical characteristic dimension of the plastic zone ahead of a crack tip is its width along the crack line at maximum load, commonly denoted as r_p. This quantity was estimated by Irwin [43] and later by Rice [44] for an elastic-perfectly plastic material (H/E = 0) in plane stress as

$$r_p = \frac{1}{\pi} \left(\frac{K_{max}}{\sigma_o}\right)^2 \qquad (2.3)$$

For a reference center crack in an infinite plate, $K_{max} = S_{max}\sqrt{\pi a}$ and so

$$\frac{r_p}{a} = \left(\frac{S_{max}}{\sigma_o}\right)^2 \qquad (2.4)$$

Shih [45] later extended Eq. (2.3) to include strain hardening materials by introducing the factor (1-n)/(1+n), where n is the strain hardening exponent in an equation of the form

$$\sigma = K(\varepsilon_p)^n \qquad (2.5)$$

This factor implies that plastic zone sizes will be smaller for materials that strain harden more.

Information about forward plastic zone widths is summarized in Fig. 2.18. Here sizes are quantified with the non-dimensional ratio $(r_p/a)/(S_{max}/\sigma_o)^2$, where a value of 1.0 implies an exact correlation

with the Irwin estimate. Each point on the figure represents the average of 10 to 20 different measurements of r_p (from finite element results at different crack lengths), so a total of over 200 plastic zones are represented here. Values for r_p/a were remarkably constant with crack length outside of the region of significant notch effects (which data were excluded from this analysis).

Observe several interesting features of this figure. First, for the low hardening material, the numerical results are remarkably similar to the perfectly plastic estimates of Irwin. Second, as expected, plastic zone sizes are slightly smaller for higher hardening materials. Third, forward plastic zone sizes for R = 0 and R = -1 cases are similar but not identical (although maximum stresses are identical). Plastic zones are preferentially larger for R = -1, which may suggest a slight closure effect. Fourth, as maximum remote stresses approach yield and the characteristic shape of the plastic zone changes, the current definition of r_p becomes less significant as a descriptor of overall plastic zone size, and r_p/a begins to decrease sharply. This is most obvious for H/E = 0.01, R = -1, S_{max}/σ_o = 0.8, where non-normalized r_p is actually less than for S_{max}/σ_o = 0.7. See again Fig. 2.17.

Typical sizes and shapes for reversed plastic zones, or active plastic zones at minimum load, are shown in Fig. 2.18 for a single H/E value but two R-ratios. Note the significant difference in scale between this figure and Fig. 2.17. Again, at lower maximum stresses the region of reversed plastic strains tends to be approximately circularly shaped, while for large maximum stresses and R = -1, the reversed plastic zone more closely resembles an intense shear band.

The width of the reversed plastic zone, denoted here as Δr_p, was predicted by Rice [44] to have a width equal to 1/4 of the width of the forward plastic zone for zero-max (R = 0) cycling, based on the doubling of the stress-strain curve for simple reversed uniaxial loading. Rice's model was based on an elastic-perfectly plastic material, and no closure effects were considered.

Values of Δr_p, normalized by the forward plastic zone size r_p, are shown in Fig. 2.20. Again, each open or filled point represents the average of measurements at many different crack lengths. Observe first the crossed points and dashed line corresponding to a stationary crack. These values were obtained from the finite element model by setting the initial crack length equal to a = 100, loading once to maximum load, unloading to zero remote load without advancing the crack, and measuring the plastic zone widths at both max and zero load. In these cases the crack tip had not closed when zero load was reached, so crack closure was not a factor. These crossed circles represent only one pair of measurements each. Different circles at the same S_{max}/σ_o value correspond to the two different H/E values, which had little effect on these particular results.

Rates of Δr_p to r_p for the stationary crack were remarkably constant with S_{max} at around $\Delta r_p/r_p = 0.2$, a slightly lower value than that predicted by Rice. Ratios at R = 0 for the fatigue crack, where closure plays a significant role, were sharply lower, generally no greater than 0.15 and approaching 0.1 at lower applied stress levels. This observation, and the observation that the ratio $\Delta r_p/r_p$ is slightly different for different H/E (with a systematic crossover), suggests that crack

closure has a significant impact on reversed plastic zone sizes. This conclusion is strengthened by a look at $\Delta r_p/r_p$ values for R = -1, where opening levels change more dramatically with S_{max}/σ_o, and $\Delta r_p/r_p$ ratios also change more dramatically. This conclusion is also in keeping with physical intuition about crack behavior. When the crack prematurely closes, the crack tip effectively changes locations, and the crack-tip singularity, which was driving the high rates of reversed plastic strain, effectively vanishes from its original location. As a result, the development of the reversed plastic zone is arrested or at least greatly impeded.

These observations and discussions have at least three implications of major consequence for fatigue crack growth in general. First, it suggests that, at least in principle, crack closing levels (not opening levels) could be directly calculated from experimentally determined values of $\Delta r_p/r_p$ (assuming that such could be reliably measured). Second, it suggests a possible direct link between crack closure behavior and an actual crack advance mechanism. Several researchers have suggested that the range of crack tip plastic strain may be related to the rate of crack growth [46,47], and these observations point out the influence of closure behavior on those reversed crack tip strains. And third, simple estimates of reversed plastic zone size which do not take closure into account are likely to be erroneous. This may cause special difficulty for schemes which attempt to use Δr_p as a correlating parameter for fatigue crack growth rates.

2.4.4 Effect of Constitutive Model

The bilinear stress-strain curve is a useful idealization of material behavior and lends itself well to simple numerical (and analytical) schemes. Nearly all previous FEM closure research has employed this type of model, either with perfect plasticity or some nonzero hardening modulus. In several important features, however, the bilinear model does not accurately represent the constitutive response of real materials. Stresses may be overestimated at very small plastic strains and again at very large plastic strains. Observed phenomena such as cyclic ratchetting and mean stress relaxation are not simulated by simple linear hardening schemes. While these limitations may not cause problems in many analysis tasks, it is useful to consider alternative constitutive models and the possible effect of these models on crack closure behavior.

The expression for the plastic strain rate in a time-independent material may be written as

$$\dot{\varepsilon}^{P}_{ij} = \frac{1}{H} \frac{\partial f}{\partial \sigma_{ij}} \frac{\partial f}{\partial \sigma_{k\ell}} \dot{\sigma}_{k\ell} \tag{2.6}$$

where H is a scalar multiplier, σ_{ij} is the current stress, $\dot{\sigma}_{k\ell}$ its rate, and f = 0 describes a smooth yield surface. To construct the new formulation we choose

$$\frac{1}{H} = A(J_2)^N \tag{2.7}$$

and

$$f = \frac{1}{2} (S_{ij} - S^c_{ij})(S_{ij} - S^c_{ij}) - k^2 = 0 \tag{2.8}$$

where $J_2 = 1/2\ S_{ij}S_{ij}$, S_{ij} is the stress deviator, S^c_{ij} is the coordinate of the center of the yield surface in stress deviator space, k is the yield stress (maintained constant) in simple shear, and A and N are constants. These are the simplest permissible choices which satisfy the basic requirements for the accurate simulation of cyclic material response, including rounding of the stress-strain curve on each load reversal following significant plastic deformation, cyclic ratchetting with nonsymmetric stress cycling, and mean stress relaxation with nonsymmetric strain cycling [48]. The constants A and N may be easily related to the usual parameters in a simple Ramberg-Osgood power-law formulation, Eq. (2.5), by the expressions

$$N = \frac{\frac{1}{n} - 1}{2} \tag{2.9}$$

$$A = \frac{(\sqrt{3})^{(1/n)-1}}{n\ K^{1/n}} \tag{2.10}$$

Another advantage of this type of stress-strain relation is its easy adaptation to much more complex constitutive behaviors, including cyclic hardening and softening, variable relaxation and ratchetting rates, and time- or temperature-dependent properties [49,50].

The specific model parameters chosen are given in Fig. 2.21, where the power-law representation of the 1070 steel is also compared with the earlier bilinear representation. The radius of the initial yield surface is chosen to correspond to the 0.025 percent offset yield stress, which is 277 MPa. Note that the 0.2 percent offset yield stress

in the power-law formulation is approximately the same as the yield point in the bilinear model, 430 MPa. All calculations reported in this thesis based on the power-law relationship use these material properties, unless explicitly specified otherwise.

The basic results for crack opening stresses, comparing the two models, are shown in Fig. 2.22. For R = 0, the power-law hardening model gives values for S_{open}/S_{max} which are significantly higher. This is also true for low maximum stresses at R = -1, but normalized opening stresses drop off sharply with increasing maximum stress at R = -1. At S_{max}/σ_o = 0.8, for example, opening stresses are dramatically lower for power-law hardening than for linear hardening. This curve actually resembles the H/E = 0.01, R = -1 opening stress curve more than it does the curve for H/E = 0.07.

Some of the reasons for these differences are suggested by plots of the crack opening displacements in Fig. 2.23. For R = 0, residual displacements seem to be much larger in the power-law model. This is consistent with the development of plastic strains at lower stresses for power-law hardening in comparison to linear hardening, which leads to more plastic deformation at the crack tip. The same appears to be true for R = -1, S_{max}/σ_o = 0.4. At S_{max}/σ_o = 0.8, R = -1, however, the entire plate is experiencing at least limited plastic strains with a power-law model. The ensuing loss of constraint leads to the sharp decrease in opening levels. Reversed deformation at the crack tip also appears to be a significant factor in this case. The difference between stationary and fatigue COD values is much smaller and even becomes "negative" farther behind the crack-tip, due at least in part to the effect of the notch.

Another significant difference between the power-law and linear hardening models, in addition to the general shape of the stress-strain curve, is that the present power-law formulation implicitly incorporates mean stress relaxation behavior. This can be particularly important for positive mean stresses. The difference is illustrated in Fig. 2.24. Here the stresses and strains (σ_{yy} and ε_{yy}) at a single material point are tracked throughout the entire load history, as the crack tip approaches and passes that location. The chosen material point corresponds to an integration point in the element just ahead of the node at x = 100, y = 0 (i.e., when the crack tip corresponds to that node, the crack length is a = 100, and the material point is immediately ahead of the crack tip). Clearly, mean stress relaxation does not occur with the linear hardening model, but does occur with the power-law hardening model.

This mean stress relaxation phenomenon introduces a new dimension to the choice of crack advance scheme. In an earlier discussion of modeling issues, it was pointed out that some local redistribution of stress occurred if the cracked body experienced two full cycles of loading each time before the crack was advanced one element. After the second cycle, however, the stress-strain response was stable and did not change with further cycling. These observations were all based on the linear hardening model. With the power-law hardening model, however, mean stresses will continue to relax on each cycle. An extreme case is shown in Fig. 2.25. Here six loading cycles were completed at each crack length before the crack-tip was advanced one node. This figure shows the normalized stress distribution along the crack line at maximum

load for each of the six cycles at a = 100. Stresses seem to have stabilized after five or six cycles. For comparison purposes, the stress distribution corresponding to the usual crack advance scheme (one cycle per crack growth increment) is also shown. Only slight mean stress relaxation occurs in that case. The final stress distribution with full mean stress relaxation is probably not particularly realistic. Immediately ahead of the crack tip mean stresses have relaxed almost completely away, while farther in front of the crack tip the criterion for mean stress relaxation implicit in the constitutive model (yielding upon reversed loading) has not yet been satisfied. Nevertheless, an important interplay between two competing effects has been illustrated. As the crack-tip advances, stresses at a given point ahead of the crack tip will increase. On the other hand, as cycling continues, mean stresses in the region of inelastic deformation will slowly decrease. The actual stress distribution will depend both on the rate of crack advance and the rate of mean stress relaxation, neither of which is explicitly modeled by the current FEM formulation. Certainly mean stresses in a real component will fade away much more slowly than in the present constitutive model. In this context it is therefore probably reasonable to advance the crack at a fairly high rate (Δa = element size) with respect to the total number of cycles. Nevertheless, there will likely always be at least minor perturbations in the stress fields associated with the discrete and nonsynchronized jumps in crack length and mean stress.

These large changes in mean stresses are significant because they lead to large changes in crack opening stresses. Figure 2.26 presents

preliminary results for S_{open}/S_{max} values determined with different crack advance schemes. The parameter changed is the number of load cycles completed at each crack growth increment. More (cycles /Δa) bring about lower crack-tip mean stresses. Clearly there is a major effect: opening stresses drop sharply with decreasing mean stress. Apparently the drop in mean stress near the crack tip produces crack opening behavior typical of remote stress histories with lower mean stresses. Crack opening levels for R = -1 remote loading, for example, have previously been noted to be significantly lower than for R = 0 remote loading.

The presentation of two different constitutive models leaves the engineer or future researcher with an obvious question: which model is "right"? Or, which model gives the most accurate results? At first glance, the preference would seem to be for the power-law model, since it is more sophisticated. Certainly it is superior in its ability to accurately simulate real material behavior involving extensive cyclic plasticity, including realistic hysteresis loop shapes and the mean stress relaxation phenomenon. This may be particularly important under certain conditions, such as high R-ratio cycling. And yet this more advanced model is not without significant limitations. Its complexity is something of a liability. Given that mean stress relaxation can be modeled, for example, now we must be concerned with modeling the proper rate of mean stress relaxation and insuring that extremely unrealistic behaviors are not generated. The experience base of this model is much smaller, both within the current research activity and in previously published research. Modeling issues such as mesh refinement and the

effect of notches or initial defects are not yet as well characterized, and other, as yet undiscovered, pitfalls may be lurking.

The bilinear model, although incapable of simulating complex phenomena and matched to real stress-strain curves only through somewhat arbitrary choices of σ_0 and H, is well-understood and well-behaved. The stress-strain response is inherently stable and easily related to even simpler models commonly encountered in complex analyses, such as the elastic-perfectly plastic idealization.

One important issue involved in making a choice between the two models is the nature of real material response, especially in ferrous metals. Many of these alloys exhibit yield point behavior, which means that the stress-strain response is essentially purely elastic until the yield point is "broken." After this moment the constitutive response gradually approaches a stable state described by a smooth curve, changing at a rate which is related to the magnitude of the plastic deformations. The present power-law formulation is an excellent representation of a cyclically stable stress-strain relationship, and therefore is probably a better descriptor of near-tip behavior. But the bilinear form is a much better estimate of pre-yield point behavior, which probably dominates the stress-strain field remote from the crack tip at all but the highest nominal stress levels. The power-law model may tend to seriously overestimate plastic strains in material which would not yet have seen the yield point broken. This may, in turn, have serious consequences for loss of elastic constraint and therefore loss of closure. The sharp drop in S_{open}/S_{max} with high S_{max} at R = -1 in the power-law analysis may be indicative of such. The "ideal" consti-

tutive model might handle both pre-yield and post-yield behaviors with appropriate formulations, but this would introduce still further complications.

Ultimately, the question of accuracy should be resolved by an appeal to experimentally measured crack opening stresses. Unfortunately, the experimental data available exhibit even wider scatter than the competing finite element models and are accompanied by several controversial issues. Some of the most accurate measurements of S_{open} currently available are those of Davidson and Lankford [51,52], who have worked extensively with stereoimaging of scanning electron photomicrographs obtained during in-situ fatigue cycling. Their results for high maximum stresses and R = 0 cycling are closer to the simulations using the power-law scheme. More common results for R = 0 cycling, such as the well-known values originally published by Elber [4], tend to give lower S_{open} which are more in keeping with the bilinear figures, but some dependence of results on measurement location [53,54] may be involved here.

Finally, what is probably the most crucial issue in the selection of a constitutive model has not yet been mentioned here: the role of plane strain constraint. It is well known that the severe stress concentration at the crack tip leads to triaxial stress states with significant hydrostatic components. The associated constraints on deformation will vary with specimen thickness, proximity to the specimen surface, and distance from the crack tip. A full three-dimensional analysis is necessary to characterize properly this stress state. Such an analysis has been reported by Chermahini and Newman [24,25] for one

simple case, and their results confirm not only the significant variations in σ_z (out-of-plane stress) within the cracked body but also the implications for crack closure behavior. It should be pointed out here that the entire issue of crack closure under plane strain is a controversial one, and remains an unresolved question under active study.

A simple two-dimensional estimate of this effect can be achieved by modeling the entire plate as under the influence of plane strain. This type of FEM analysis has been recently reported by Fleck [22,23], who concluded that, in general, crack closure did not occur under steady-state plane strain conditions. These results are somewhat in contradiction to the earlier work of Blom and Holm [21] and perhaps even Ogura, et al. [9], both of whom reported plane strain closure levels.

Plane strain closure analyses have not yet been fully completed with the current FEM formulation, but the recent results of Lalor and Sehitoglu [28,29] and preliminary studies with the present model suggest that closure does occur under plane strain. Preliminary results are shown in Fig. 2.27 in comparison with plane stress values. The general tendency to lower S_{open} values with increasing constraint should be noted. It could be assumed that these plane stress and plane strain lines represent upper and lower bounds for an actual material response. However, significant differences in out-of-plane deformation between near-tip and far-field locations may induce quite different effects on crack-tip inelastic deformations and remote elastic constraint and hence leave the boundedness in question.

The bottom line is that an extremely accurate description of a pure plane stress response may or may not give an accurate description of experimental closure behavior, even in thin sheets. There is no particular evidence that the present plane stress analyses are significantly deficient because of their two-dimensional limitations, and certainly some experimental evidence exists that suggests their S_{open} values to be reasonably accurate. Nevertheless, the three-dimensional aspects of the problem should be explored more fully, both with full three-dimensional analyses and perhaps with pseudo three-dimensional analysis such as the two-dimensional overlay techniques used by Dodds and Read [55] in monotonic fracture studies.

In the remainder of the present thesis, the results obtained with the linear hardening model will, in general, be preferred. This is due primarily to reasons stated earlier, including greater experience and associated greater confidence with the model and fewer potentially disruptive side issues with which to deal. This choice should not be construed as a rejection or critical judgment of the power-law model. In a few situations where the power-law model was judged to capture best a significant trend, it was employed, although care was taken never to mix and match the models for the purpose of getting a better correlation.

2.4.5 Opening Levels versus Closing Levels

The "crack opening stress" identified throughout this thesis is the point during the forward loading excursion when the crack tip first becomes fully open; i.e., there are no points of contact remaining

along the crack surfaces behind the crack tip. Another characteristic stress level is also descriptive of the crack closure phenomenon: this is the "crack closing stress," the moment during the unloading excursion when some point along the crack surface first makes contact with the y = 0 line (assuming symmetry across the y-axis). Often the opening and closing levels have been assumed to be exactly the same. While the opening level is generally regarded to be more significant to the physical crack advance mechanism, several researchers have found it more convenient experimentally to measure S_{clos} rather than S_{open}. In that case the assumption about similarity is a rather attractive one.

The present finite element simulation suggests that opening and closing levels are not the same. See Fig. 2.28. Closing levels are consistently lower than corresponding opening levels. As maximum stresses become greater, this difference increases. In the limit, as maximum stresses approach and pass the level of general yielding, closing levels (not opening levels) approach the minimum stress in the cycle. This trend has been confirmed experimentally [56] and is probably associated with the large total crack opening displacements generated under these conditions, which require very extensive reversed plasticity to be reduced back to zero.

2.5 Conclusions

1. The finite element method is a powerful technique for the simulation of fatigue crack growth and the analysis of fatigue crack closure.

2. In order to preserve the reliability of the results, special attention must be given to mesh refinement along the crack line and to transient closure response as the crack moves beyond its initial position. Mesh refinement is more likely to be a problem at low stress amplitudes and high stress ratios, while opening levels will take longer to stabilize at higher stress amplitudes and lower stress ratios.
3. Crack opening stresses (normalized by the maximum stress) decrease with increasing maximum stress. This dependency on maximum stress is greater for lower stress ratios and lower hardening moduli.
4. Crack closure behavior can be understood in terms of the interaction between residual displacements behind the crack tip and the total crack opening displacements. Normalized crack opening stresses will decrease with either decreases in residual displacements or increases in total COD.
5. The size of forward and reversed crack tip plastic zones is somewhat dependent on crack closure levels.
6. The choice of a constitutive model can have a major impact on crack closure modeling. Important factors include the inelastic strain response at low stresses and the phenomenon of mean stress relaxation.
7. Crack closing levels are generally lower than crack opening levels, and the difference is greater at lower stress ratios and higher maximum stresses.

3. CORRELATION OF CRACK GROWTH RATES IN INTERMEDIATE AND LARGE SCALE YIELDING

The range of the elastic stress intensity factor, ΔK, has achieved widespread acceptance as a correlating parameter for fatigue crack growth (FCG) rate data from tests in which only small scale yielding (SSY) has occurred. As stresses and plastic strains increase and begin to violate the strict criteria for SSY, however, ΔK often fails to correlate the data, and other parameters must be adopted. In this chapter, attention is given to the engineering parameters which are specifically developed to correlate crack growth rates under conditions of intermediate and large scale yielding (ISY and LSY). First, a variety of previously suggested parameters are critically reviewed and compared from an engineering standpoint. Second, the possible role of crack closure in these parameters is discussed, and finite element analyses and experimental investigation of crack closure under ISY and LSY are presented. Third, selected parameters with and without closure considerations are used to correlate a variety of experimental crack growth rate data.

3.1 Existing Parameters for FCG under ISY and LSY

3.1.1 Background

3.1.1.1 Intermediate Scale Yielding

The inherent paradox in the use of a linear elastic parameter such as ΔK to describe the fatigue process, which is driven by plastic strains, has long been recognized. The landmark paper of Paris [1] which demonstrated the validity of a K-based parameter was rejected by the leading journals of its day for this very reason [57]. The

original use of K as a descriptor of monotonic fracture in ductile metals was also not without criticism and theoretical difficulty. For cracks under both monotonic and cyclic loading, however, it was soon generally understood that if plastic deformation (characterized by the width of the crack tip plastic zone, r_p) was confined to a very small region relative to the crack length ($r_p << a$), K-based equations were still accurate representations of the near-tip stress and strain fields and hence of the fracture event.

Practical engineering problems occasionally demanded some stretching of these boundaries, however. Could K still be used when SSY assumptions were not strictly valid? Irwin [43] considered the redistribution of stresses caused by near-tip yielding and proposed that use of a fictitious crack length a' led to a more accurate description of actual stress fields ahead of the crack. He suggested

$$a' = a + r_Y \tag{3.1}$$

where r_Y is the radius of the crack tip plastic zone, estimated for a plane stress crack as

$$r_Y = \frac{1}{2\pi} \left(\frac{K}{\sigma_{ys}}\right)^2 \tag{3.2}$$

This leads to a slight increase in K (or ΔK). To a first approximation (neglecting the iterative effect that increasing K means increasing a', which in turn further increases K, and so on), we can write for a reference center crack ($K = S\sqrt{\pi a}$) that

$$r_Y = \frac{1}{2}\left(\frac{S}{\sigma_{ys}}\right)^2 a \qquad (3.3)$$

As S approaches σ_{ys}, the Irwin type of correction factor suggests an increase in K by a factor of 1.22.

The application of these concepts to cyclic loading is straightforward, requiring only the replacement of K with K_{max} in Eq. (3.2) and S with S_{max} in Eq. (3.3). This adaptation assumes that the forward plastic zone size is of primary interest. The reversed plastic zone size upon unloading, Δr_p, could also be considered to be of greatest significance. Following the suggestion of Rice [44] that $\Delta r_p = r_p/4$, however, results in a crack length correction factor which is essentially negligible.

Equation (3.2) has typically been interpreted as representative of a elastic-perfectly plastic material. Shih [45] suggested for a power-law hardening material the more general form

$$r_Y = \frac{1}{2\pi}\left(\frac{1-n}{1+n}\right)\left(\frac{K}{\sigma_{ys}}\right)^2 \qquad (3.4)$$

where n is the strain hardening exponent in a constitutive model of the form

$$\frac{\varepsilon}{\varepsilon_o} = \alpha\left(\frac{\sigma}{\sigma_o}\right)^{1/n} \qquad (3.5)$$

Kumar and Shih [58], in a more general consideration of the J-integral as an elastic-plastic parameter, chose to use an adjusted crack length given by

$$a' = a + \phi r_Y \tag{3.6}$$

where ϕ was defined as

$$\phi = \frac{1}{1 + (P/P_o)^2} \tag{3.7}$$

Here P_o is a limit load. This form was also employed in the EPRI elastic-plastic fracture handbook [59]. Primary motivations for ϕ were considerations involving the more general form of J, especially at and above general yield, and so no conclusions about increased accuracy in K should be construed. The result of ϕ is a further reduction in the total correction factor. For the nominal case where $\sigma/\sigma_o = P/P_o$ and $\sigma = \sigma_o$, $\phi = 0.5$. Dowling [60] has correctly pointed out that the value of ϕ is somewhat arbitrary and that, in general, contributions from the ϕr_Y term are almost never significant when a complete elastic-plastic parameter is used. In the present research, ϕ contributions were neglected ($\phi = 1$).

3.1.1.2 Large Scale Yielding

Many important fatigue problems involve nominal stresses which are at or well above the yield stress, at least in local regions. Accurate description of crack growth under these conditions is not possible even with modified forms of ΔK, and so alternative parameters have been developed.

3.1.1.2.1 Strain-Based Intensity Factors

One of the first attempts to develop a LSY FCG parameter was the work of Boettner, Laird, and McEvily [61]. They successfully correlated crack growth rates at very large strains in a variety of materials with the relationship

$$\frac{da}{dN} = C(\Delta\varepsilon_p\sqrt{a})^m \tag{3.8}$$

where $\Delta\varepsilon_p$ is the plastic strain range. This is an attractive formulation conceptually because it can be interpreted as the inversion of the Coffin-Manson relationship for low cycle fatigue,

$$\frac{\Delta\varepsilon_p}{2} = \varepsilon_f' (2N_f)^c \tag{3.9}$$

A major disadvantage of this form is that during SSY, $\Delta\varepsilon_p$ goes to zero and the parameter is not functional, so it is impossible to make any comparison with ΔK-controlled FCG.

A minor modification to Eq. (3.8) which increases its generality is to replace $\Delta\varepsilon_p$ by $\Delta\varepsilon$, the total strain. At very high strains, the elastic component is negligible and so $\Delta\varepsilon_p \approx \Delta\varepsilon$. At low strains $\Delta\varepsilon$ is all elastic and hence proportional to $\Delta\sigma$. This form was first explicitly stated by McEvily [62].

Solomon [63] introduced what he called a "pseudostress" intensity factor,

$$\Delta(PK) = E\ \Delta\varepsilon\sqrt{a} \tag{3.10}$$

by including Young's modulus in the parameter. This has the advantage of reducing almost exactly to expressions for ΔK when $\Delta\epsilon_p$ is negligible. This type of strain-based intensity factor was further popularized by El Haddad [64,65] and Skelton and co-workers [66 68], generally represented (for a reference center crack) as

$$\Delta K_\epsilon = E\Delta\epsilon \sqrt{\pi a} \tag{3.11}$$

3.1.1.2.2 Crack Tip Opening Displacement

Many of the early studies of fatigue crack growth laws and mechanisms focused on the crack-tip opening displacement, δ_t, as the critical parameter both for understanding and quantifying crack advance processes. Included here is the work of Tomkins [69,70], McEvily [62,71], Lardner [72], Pelloux [73,74], and others. A variety of theoretically-based and semi-empirical formulas were proposed, and few appeared twice in the literature.

Many of these publications were attempts to describe crack growth under traditional SSY conditions. Conceptually, however, δ_t is equally valid as a characteristic parameter for LSY, and this motivated further work by McEvily [75] and Tomkins [76-78]. Both developed estimates of δ_t based on the Bilby-Cottrell-Swinden (BCS) model [32] for an idealized monotonically loaded crack. This form is

$$\delta_t = \frac{8}{\pi}\frac{\sigma_o}{E}\, a\, \ell n\left[\sec\left(\frac{\pi\sigma}{2\sigma_o}\right)\right] \tag{3.12}$$

where σ_o is a characteristic flow stress, generally taken as the yield stress. In order to extend this model into the regime of LSY, McEvily and Tomkins each replaced σ_o and E with related elastic-plastic quantities. McEvily replaced the elastic modulus E with a form of the secant modulus, while Tomkins chose a form of the tangent modulus. Both substituted the ultimate strength σ_u for σ_o.

McEvily and Tomkins each ultimately suggested some direct relationship between δ_t or its component parts and the crack growth increment Δa. While attractive from a theoretical or mechanistic point of view, this step does limit the immediate engineering usefulness of the parameter. Tanaka and Hoshide [79] have presented a more general use of δ_t in a Paris-type power law crack growth expression, determining δ_t values from the related parameter ΔJ or from experimental measurements. Others [56,80] have explored similar engineering applications.

3.1.1.2.3 "Equivalent" Stress Intensity Factor

Gowda and Topper [81] employed the theories of Neuber [82] about the relationship between stresses and strains at the crack tip to develop what they called an equivalent or modified stress intensity factor. They wrote this as

$$\Delta K' = \Delta K \left(1 + \frac{\Delta\varepsilon_N^P}{\Delta\varepsilon_N^e}\right)^{1/2} \qquad (3.13)$$

where ΔK is the usual stress intensity factor, except that the $\Delta\sigma$ factor in ΔK (and the strain terms $\Delta\varepsilon_N^P$ and $\Delta\varepsilon_N^e$) are based on net section

stresses and strains. The same basic concept has been more recently employed by Bhanderi, et al. [83], who proposed an intensity factor $K_\gamma = \sqrt{K_\sigma K_\varepsilon}$. Here K_σ and K_ε are the usual stress and strain intensity factors but calculated on the basis of the stresses σ_{yy} and ε_{yy} at the crack tip location in an uncracked body.

3.1.1.2.4 Range of the J-Integral

Dowling and Begley [84,85] were the first to propose the range of the J-integral as a correlating parameter for elastic-plastic fatigue crack growth. Working from the fundamental identity of J as an energy term, they estimated ΔJ from load-deflection curves for deeply-cracked compact tension and center crack specimens according to the approximation

$$J = \frac{2}{B(W-a)} \int P \, d\delta \qquad (3.14)$$

where P is the load, δ the load-line deflection, B the specimen thickness, and (W-a) the remaining ligament.

Considering next the smooth cylindrical specimen with much smaller crack sizes, for which no similar approximation formula was available, Dowling [86] drew on the work of Shih and Hutchinson [87] to develop an expression for ΔJ. They had suggested that J could be estimated by summing elastic and plastic components,

$$J = J_e + J_p \qquad (3.15)$$

where

$$J_e = \frac{K^2}{E} \tag{3.16}$$

for plane stress and

$$J_p = h(n)\ \sigma\ \varepsilon_p\ a \tag{3.17}$$

Here h(n) is a function of the strain hardening exponent determined from numerical analysis, and changes with specimen geometry, stress state, and crack length. This type of simple estimation scheme has been adopted by many researchers [88-93], including further studies by Dowling [94]. Other researchers [95-97] have continued to work from the more fundamental definition of Eq. (3.14). Currently ΔJ is the most commonly used elastic-plastic parameter, although serious objections have been raised by several authors (e.g., [98]) concerning its validity and theoretical suitability.

3.1.2 The Structure of Estimates for LSY FCG Parameters

Each of the proposed parameter for LSY FCG has a certain attractiveness of its own because of the particular insight it provides into the crack tip event. The crack tip opening displacement, for example, probably has some direct relationship to the mechanism of crack advance, while ΔJ may provide some direct measure of the intensity of the near-tip stress-strain field. No matter how true these concepts are in theory, however, these parameters are only useful to the engineer

when they can be easily quantified for a particular combination of geometry, material, and load history. This suggests that attention should be focused on the schemes used to estimate these parameters in practice. The paragraphs that follow will critically compare the structure of the common estimates for each of the major parameters.

We begin with the most common parameter, ΔJ. The most common estimation scheme, based on Eqs. (3.15) through (3.17), may be expanded as

$$\Delta J = \frac{F^2(\Delta\sigma)^2 \pi a}{E} + F^2 h(n) \Delta\sigma \Delta\varepsilon_p a \qquad (3.18)$$

where F is the total elastic geometry correction factor relative to a center cracked plate (CCP) and h(n) is based on the CCP. Alternate forms of h(n) have been used, but the concept is similar. This may be rewritten for discussion purposes as

$$\Delta J = F^2 \pi a \Delta\sigma [\Delta\varepsilon_e + (\frac{h(n)}{\pi}) \Delta\varepsilon_p] \qquad (3.19)$$

Estimates of δ_t typically begin with the BCS expression, Eq (3.12). Tomkins [78], for example, made the substitutions previously mentioned and then employed a series expansion of the $\ell n(\sec(x))$ term to get the form

$$\delta_t = \frac{\pi \sigma_{max}^2 a}{2\sigma_u E} + \frac{\pi \sigma_{max} \Delta\varepsilon_p a}{\sigma_u (1+n)} \qquad (3.20)$$

which can be rewritten as

$$\delta_t = \frac{\pi\ a\ \Delta\sigma}{8\sigma_u} \left[\Delta\varepsilon_e + \left(\frac{1}{1+n}\right) \Delta\varepsilon_p\right] \tag{3.21}$$

McEvily [75] chose not to carry out this type of an expansion and simplification, but working from his initial equations and assumptions it is possible to derive the form

$$\delta_t = \frac{\pi\ a\ \Delta\sigma}{4\sigma_u} \left[\Delta\varepsilon_e + 2\Delta\varepsilon_p\right] \tag{3.22}$$

Consider next the equivalent stress intensity factor of Gowda and Topper [81]. In order to compare $\Delta K'$ directly with ΔJ, it is necessary to consider the quantity $(\Delta K')^2/E$ (compare Eq. (3.16)). For the simple case of a small crack in a large unnotched plate, this gives

$$\frac{(\Delta K')^2}{E} = F^2 \pi\ a\ \Delta\sigma\ \left[\Delta\varepsilon_e + \Delta\varepsilon_p\right] \tag{3.23}$$

Finally, consider the strain intensity factor, K_ε. Here we derive

$$\frac{(\Delta K_\varepsilon)^2}{E} = F^2 \pi\ a\ \Delta\sigma\ \left[\Delta\varepsilon_e + \left(2 + \frac{\Delta\varepsilon_p}{\Delta\varepsilon_e}\right) \Delta\varepsilon_p\right] \tag{3.24}$$

The common structure of all these parameters is obvious. It may be generalized to the form

$$\Delta Z = C_t\ a\ \Delta\sigma\ \left[\Delta\varepsilon_e + C_p\ \Delta\varepsilon_p\right] \tag{3.25}$$

where ΔZ is the range of the parameter, C_t is the coefficient common to the entire expression, and C_p is the coefficient of the plastic strain term. If a power law da/dN versus ΔZ relationship is used, C_t is relatively insignificant unless there are major changes in crack or specimen geometry. The only significant difference in these parameters, then, is C_p. With the exception of the strain intensity factor, C_p is a constant dependent only on specimen geometry and the strain hardening exponent. The typical range of C_p is from 1.0 to 4.0, with an average value around 2.5.

The major parameters are compared visually in Fig. 3.1 for two specific materials, a ductile 1026 steel and a strong HY100 steel. In this figure the dependent variable is the ratio of the total parameter, ΔZ, to its elastic component, $\Delta Z_e = C_t \, a \, \Delta\sigma \, \Delta\varepsilon_e$, which reduces to $[1 + C_p(\Delta\varepsilon_p/\Delta\varepsilon_e)]$. Calculations are based on a plane stress Mode I center crack in an infinite plate of material which obeys Eq. (2.5). This figure also gives some indication of the remote plastic strain amplitude at which the plastic component of each parameter becomes numerically significant.

So what are the philosophical implications of these observations about parameter structures? First of all, no matter which of these parameters an engineer is using and what he has named it, he may be basically using a single parameter, the product of stress, crack length, and a weighted summation of strain components. Such a parameter could perhaps have been generated just as easily from an intuitive empirical process. Second, extensive analyses and debates over the validity and suitability of various parameters may be missing the point. The most

important issue often may not be whether a given parameter is "correct", but whether a particular estimation scheme bears resemblance to any significant reality. This does not mean that conceptual, mathematical, and mechanistic studies are worthless, but it does mean that their conclusions may have no practical impact on the design engineer. Third, in view of the first two implications, comparisons between two parameters for the purpose of proving that one is right and the other is wrong may have little value unless new estimation schemes are developed which characterize the unique qualities of a particular parameter.

From a more quantitative standpoint, four conclusions seem worthy of note. First, one significant difference between various parameter estimates is the value of C_p. The best choice of C_p and the factors that contribute to its determination need to be investigated from either a theoretical or empirical standpoint. Second, the C_t factor will in some cases be significant, particularly when large changes in specimen geometry occur. One criteria for the selection of the most useful parameter should be its ability to handle such changes.

The third conclusion relates back to the question of crack growth during SSY and when simple parameters such as ΔK are sufficient. Returning to Eq. (3.25), we reorganize it as

$$\Delta Z = C' \left[\frac{(\Delta K)^2}{E} + C_p \, \Delta\sigma \, \Delta\varepsilon_p \, a\right] \qquad (3.26)$$

where C' is a new constant independent of stress or strain*. This equation implies that any time the product of C_p and the remote plastic strain is small relative to the elastic strain, it is sufficient and valid to use only ΔK as a correlating parameter. Such an implication may have particular significance for ferrous metals that exhibit yield point behavior. In these materials the remote stress-strain response is essentially purely elastic (i.e., remote plastic strains are negligible) until the yield point is broken. Now, "breaking" the yield point does not necessarily require exceeding the upper yield point stress and it does occur gradually with cycling at lower stress amplitudes. Nevertheless, at low stress amplitudes the inelastic material response will probably more closely follow the elastic line than the stable cyclic stress-strain curve obtained from an incremental step test, and this is good news for ΔK.

The fourth conclusion relates to the third but points out a problem. At stresses between the yield stress and the endurance limit (assuming that one exists), the inelastic material response can be extremely history-dependent. Cyclic stress-strain curves obtained from constant amplitude tests, block tests, and incremental step tests can be quite different at these lower stresses, for example [99-101]. Several of the elastic-plastic parameters, unfortunately, have a strong dependence on $\Delta\varepsilon_p$ at relatively low values of $\Delta\varepsilon_p$. Here the uncertainty

*Actually there is a term missing which could be included, the additional contribution of a plasticity-modified ΔK based on a modified crack length a' (Eq. (3.1)). As was mentioned earlier, however, this term is rarely significant and hence may be best omitted in the interest of simplicity.

in $\Delta\varepsilon_p$ can cause great difficulty. Furthermore, it may be that large percentage changes in relatively small values of remote $\Delta\varepsilon_p$ really have considerably less effect on da/dN values than would be predicted. No solution is proposed here, only a warning.

3.2 The Role of Crack Closure

3.2.1 Background

Elber [3,4] revolutionized the study and application of fatigue crack growth concepts by his discovery of the crack closure phenomenon in the late 1960s. He proposed the replacement of ΔS by ΔS_{eff} in expressions for ΔK, now renamed ΔK_{eff}, where $\Delta S_{eff} = S_{max} - S_{open}$ and S_{open} is the remote stress at which the crack tip first fully opens. Attention was typically focused on the changes in $U = \Delta S_{eff}/\Delta S$ with changing R and with variable amplitude histories. Normalized opening levels were typically assumed to be independent of S_{max} [4].

Some preliminary attempts have been made to incorporate closure concepts into elastic-plastic FCG parameters. Dowling and Begley [84,85] and Mowbray [95], in their early work on ΔJ, estimated closure levels from the cusp in the unloading line of the load-displacement curve. Implicit in this methodology is the assumption that opening and closing levels are similar.

When cracks are small relative to overall specimen dimensions, no compliance changes in the load-displacement trace are visible and this technique fails. In this case investigators have attempted to estimate opening levels either by drawing inferences from long crack behavior [86,94] or by visual inspection of the crack surfaces at low

magnification [92]. A common result of these schemes is the assumption that $S_{open} = S_{min}$ and U = 1. Other investigators assumed a priori that only the tensile portion of the cycle was effective in propagating the crack, so that $\Delta S_{eff} = S_{max}$ and, for R = -1, U = 0.5 (e.g., [89]). Haigh and Skelton [66] reached a similar conclusion with information from potential drop measurements. Heitmann [91] took U from Schijve's modification of Elber's original expression for U as a function of R. All of these methodologies have in common the assumption that within the range of their data, U does not change with S_{max}.

3.2.2 Finite Element Modeling

The basic finite element results for normalized crack opening stresses as a function of maximum stress, presented earlier, suggest this assumption to be questionable. Returning to Fig. 2.11, we note that for R = -1 (which is characteristic of LCF), S_{open}/S_{max} changes significantly with S_{max}. Comparing, for example, S_{max}/σ_o = 0.3 to S_{max}/σ_o = 0.9, U changes from 0.32 to 0.44. This corresponds to a change in ΔK_{eff} of 1.4X, which (for a typical Paris exponent of 4) suggests a change in da/dN of 3.5X. Such a change should certainly be noticeable in a set of experimental crack growth data.

Unfortunately, the finite element model in its present form does not give stable opening stresses for applied stresses at or above general yield with the linear hardening model. The constitutive scheme still converges and stress and strain distributions are generally reasonable, but opening stresses are discontinuously higher and may change erratically with increasing crack length. Closing stresses are

stable and close to minimum load. This difficulty may be associated with the sharp change in the global stiffness at $\sigma = \sigma_o$ or may be related to numerical difficulties with the large truss stiffnesses when global stiffnesses are low. Research is continuing on this problem.

3.2.3 Experimental Measurement of Closure at High Strains

Another method to assess crack opening behavior during low cycle fatigue is direct experimental measurement. Preliminary results for S_{open}/S_{max} as a function of S_{max} were first reported by McClung in Ref. [102], with additional results later presented in [56]. In these tests, through cracks in small plate specimens of a 1026 steel were initiated at 50 μm electro-discharge machined edge notches. Ten or more acetate replicas were taken of the specimen surface during a single loading excursion, and these replicas were later processed for inspection in the scanning electron microscope at magnifications up to 4500X. Examinations and comparison of consecutive replicas in the near-tip region, which may be directly inspected at the specimen surface for this geometry, made it possible to determine a crack opening stress to within 10 percent or less. Further details are reported in Ref. [56].

The results are summarized in Fig. 3.2. Here the solid circles represent the average of several measurements at each stress or strain amplitude, while the scatterbands indicate the range of measured values. Note that the highest S_{max} value corresponds to a far-field plastic strain range about 1 percent, while at the lowest S_{max} value the plastic strains are less than 10^{-4}. In the same figure these experimental quantities are compared with the finite element simulations for

H/E = 0.07. Note that the 1070 steel on which the finite element properties are based has a cyclic strain hardening exponent similar to the 1026 steel. The two materials differ primarily in their σ_o/E values, which were shown earlier to be inconsequential for closure behavior. Superimposed also on the figure are predictions based on the modified Dugdale model of Newman [37-39]. Strictly speaking, this is a SSY elastic-perfectly model, but here we follow the suggestion of Newman that the model can approximately accommodate strain hardening by choosing the flow stress σ_o equal to the average of the yield and ultimate stresses.

Agreement between the experiments and two models is generally good. The FEM analysis may slightly underestimate the S_{max} dependence at low stresses. At still higher stresses, it is likely that the FEM opening levels will begin to drop off more sharply with increasing S_{max}, as do the results for H/E = 0.01 and the power-law model, and this would correspond to the experimental data.

These results suggest that for R = -1 cycling at stress amplitudes at or above the yield stress, U values will be in the neighborhood of 0.5. This matches the potential drop measurements of Haigh and Skelton [66]. Iyyer and Dowling [103,104] have recently published experimental closure levels for low cycle fatigue cracks in smooth cylindrical specimens which confirm the dependence of U on S_{max}. Their specific quantitative values, which are somewhat lower, may be only approximations due to experimental limitations such as low magnifications, few crack observations, and possible time-dependent contributions. Rie and Schubert [105] and Hatanaka, et al. [106,107] have also reported lower

opening levels for smooth specimens. This may be a characteristic of the specimen geometry, but another possible explanation for the difference is that in a cylindrical specimen the crack tip is embedded in the specimen and cannot be inspected directly. Measurements based on surface behavior may not be representative of interior behavior. A related factor is the dependence of apparent opening level on measurement location. Several early researchers [53,54] noted that if the measurement position was not close to the crack tip, opening stresses appeared lower.

3.2.4 Closure and the Structure of FCG Parameters

Given that opening levels can be determined, a remaining question is how properly to incorporate U into estimates of elastic-plastic parameters. The straightforward approach is illustrated in Fig. 3.3. Here $\Delta\sigma$ and the related term $\Delta\varepsilon_e$ are modified by the factor U but in general, unless U is very small, $\Delta\varepsilon_p$ remains unchanged.

For ΔJ this leads to the basic form

$$\Delta J_{eff} = F^2 \pi a \Delta\sigma U^2 \left(\Delta\varepsilon_e + \frac{h(n)}{\pi U} \Delta\varepsilon_p\right) \qquad (3.27)$$

so that while the entire parameter is reduced by some factor between U and U^2, C_p is increased by the factor 1/U. This unfortunately tends to aggravate the previously discussed problem with $\Delta\varepsilon_p$ sensitivity at low stresses, when U values are generally smaller. This formulation is conceptually consistent with the fundamental definition of J as a measure of energy (elastic and plastic strain energies are denoted in

the figure by the cross-hatched areas), and the equations reduce nicely to the customary forms for ΔK_{eff} when plastic strains are negligible.

A slightly different form occurs when this type of approach is applied to the strain intensity factor. Now the "effective strain" may be described by $(\Delta\varepsilon_p + U\Delta\varepsilon_e)$, and the parameter may be written as

$$\frac{(\Delta K_\varepsilon)_{eff}}{E} = \pi\, a\, \Delta\sigma\, U^2 \left[\Delta\varepsilon_e + \left(\frac{2}{U} + \frac{\Delta\varepsilon_p}{U^2\, \Delta\varepsilon_e}\right) \Delta\varepsilon_p\right] \qquad (3.28)$$

Again, C_p increases when closure is considered.

A second approach to incorporating closure information in FCG parameters was used by Heitmann [91] and others [108]. These researchers assumed crack closure to reduce the elastic term but not the plastic term. For a ΔJ formulation, this looks like

$$\Delta J_{eff} = F^2\, \pi\, a\, \Delta\sigma\, U^2 \left[\Delta\varepsilon_e + \frac{h(n)}{\pi\, U^2} \Delta\varepsilon_p\right] \qquad (3.29)$$

so the plastic term becomes even more dominant. In Heitmann's work, however, a new value for h(n) was developed which was smaller than the current suggestions of Dowling [60], and this tended to offset some of the U effect.

A third approach has been recently suggested by Dowling [109,110]. Responding to some criticisms of the validity of ΔJ as a parameter for cyclic loading, especially when closure occurs, he proposed that the point on the far-field hysteresis loop corresponding to the closing stress be adopted as the proper reference point. See Fig. 3.4, which is based on Fig. 3 in Ref. [109]. Here point "o"

identifies the crack opening stress and point "c" the closing stress. Dowling postulates that during a hypothetical reloading from c to b, the changes in stress and strain which occurred during b-c will be exactly reversed. The changes in δ_t for c-b and o-b should be exactly the same. But during o-b the unique hysteresis loop curve shape requirement for J is violated, while the requirement is met for c-b.

In practice, this scheme may often give effectively the same results as the straightforward approach. Figure 3.5 shows a hysteresis loop corresponding exactly to the response of a 1026 steel under fully reversed strain cycling with $\Delta\varepsilon = 0.01$. The opening stress is known from experiments to be roughly zero. In order for the product (ΔS_{eff}^{open}) $(\Delta\varepsilon_p)_{eff}^{open}$ to be equal to the product (ΔS_{eff}^{clos}) $(\Delta e_p)_{eff}^{clos}$ and hence for the two plastic ΔJ terms to be the same, the closing stress would need to correspond to S_{clos}/S_{max} around -0.95. This is a typical closing level, as suggested by the experiments of McClung [56] and Dowling [103] and the present FEM model. There will still be some changes in the elastic ΔJ term, but at such large strains the elastic term is relatively insignificant.

One issue of potential concern with this new scheme is that in the limit as far-field plastic strains go to zero, an effective stress range based on the closing stress may be different from the ΔS_{eff} based on the opening stress, which is customarily used for ΔK_{eff}. The present FEM results for opening and closing levels (Fig. 2.28) suggests that the numerical difference may not be trivial.

The bottom line about crack closure and elastic-plastic FCG parameters, from a pragmatic standpoint, is that the value of C_p increases

when closure is considered. Typical values of closure-modified C_p range from 2 to 9, roughly a factor of 2 higher than C_p values which do not consider closure.

3.3 Crack Growth Data and Correlations

Fatigue crack growth data from double edge notched specimens of a 1070 steel have been previously reported by Sehitoglu [41,111]. The material corresponds exactly to the finite element model described earlier. In terms of the stable cyclic stress-strain curve as described by Eq. (2.5), the material is characterized by the constants K' = 1472 MPa and n' = 0.192. Further details of the material, specimen geometry, and test procedures are given in [41,111]. For the present research, the original replicas of the specimen surface were re-measured in order to extract all possible crack length data; only a portion of the data was processed previously.

These data correspond to the regime of small and intermediate scale yielding. Maximum stresses range from about one-third of the yield stress up to the yield stress. All tests were conducted at R = -1. Cracks are long compared to the microstructure and notch size but moderately short compared to the specimen width.

The ability of various ΔK-based parameters to correlate the data is examined in Fig. 3.6. Here ΔK is calculated as

$$\Delta K = 1.12\ \Delta S\ \sqrt{\pi a}\ \left[\sec\left(\frac{\pi a}{2W}\right)\right]^{1/2} \qquad (3.30)$$

Observe first that ΔK alone is not successful in correlating the data (upper left). The "layering" effect associated with noncorrelation is more easily visualized in the lower left graph, where each set of data corresponding to a particular S_{max} is replaced by its linear least-squares regression line.

The second attempt to correlate the data is based on a plasticity-modified ΔK, where the crack length is replaced by its modified value according to Eq. (3.1). See the middle plots. The correlation is only slightly better, and still unacceptable.

The final attempt to correlate the data employs the crack closure information obtained from finite element analysis, Fig. 2.11. The plasticity-modified ΔK_{mod} is multiplied by U to give ΔK_{eff}. This parameter is generally successful in correlating the data, as exhibited by the rightmost graphs. The crack growth data corresponding to the highest stress level may still lie slightly above the central tendency of the other data, but this should not be surprising. Remember that ΔK can be understood as the elastic term in a general elastic-plastic parameter. As maximum remote stresses approach the yield stress, some inelastic deformation will occur throughout the cracked body and the missing plastic term is no longer negligible.

A wider range of crack growth data is available for a hot-rolled 1026 steel characterized by a 0.2 percent offset yield strength of 322 MPa and a cyclic strain hardening exponent of 0.215. A first series of tests were conducted on small flat specimens with a rectangular cross-section measuring 0.1" x 0.5" (2.54 mm x 12.7 mm). Small cracks (typically 0.1 mm - 1.0 mm) initiated at 50 μm notches were grown under

constant amplitude strain cycling at strain amplitudes ranging from $\Delta\varepsilon/2 = 0.001$ to 0.007. The lowest strain tests correspond to S_{max} roughly 60 percent of the yield strength and $\Delta\varepsilon_p$ values on the order of 10^{-4}, while the highest strain tests correspond to S_{max} values 20 percent above yield and $\Delta\varepsilon_p$ values about 0.01. These are the same specimens, and in some cases the same tests, used to determine crack opening stresses, as described earlier. Here all tests were R = -1, except for one low strain test at R = -0.25. Further details are given in Ref. [56].

These crack growth data are correlated in Fig. 3.7 (top) with the range of the J-integral, where ΔJ takes the traditional form [60]

$$\Delta J = 1.25\,\pi\,a\left[\frac{(\Delta\sigma)^2}{E} + \sqrt{1/n}\,\Delta\sigma\,\Delta\varepsilon_p\right] \qquad (3.31)$$

Clearly the quality of the correlation is low. A much better correlation is accomplished with ΔJ_{eff}, however (see bottom figure). Here opening stresses are estimated from finite element results at low strains (for consistency with other data sets to be introduced). At high strains where FEM results are not available, opening stresses are taken directly from experimental measurements. Closure information is applied to Eq. (3.31) in the straightforward manner, by replacing $\Delta\sigma$ with $\Delta\sigma_{eff}$.

Another set of crack growth data for the same material has been previously published, in part, by Sehitoglu [93]. Here the specimens were rectangular bars nominally 2 in. wide by 0.225 in. thick (50 mm x 5.7 mm). Cracks were initiated as a center slot notch of total width 2c

= 0.3 in (7.6 mm). All tests were load controlled at a load ratio of R = -1. Maximum stresses ranged from S_{max}/σ_o = 0.30 to 0.51. Crack lengths considered in this thesis were beyond the region of significant notch influence but still within the limits of a/W < 0.4. The data are presented graphically in Fig. 3.8 as a function of ΔJ_{eff}. Here ΔJ_{eff} has been calculated from ΔK_{eff} according to Eq. (3.16), where closure information was based on finite element results and the original ΔK was calculated from the usual expression, including finite width effects. Remote plastic strains were entirely negligible. This particular data set would have been correlated equally well by an ordinary ΔJ or ΔK, because U does not vary widely within the range of maximum stresses considered.

A comparison of the high stress, short crack length data (Fig. 3.7) with the low stress, long crack length data (Fig. 3.8) demonstrates even more vividly the need to consider closure information. See Fig. 3.9. Here only data for R = -1 are shown for clarity. The correlation with ΔJ (top) is clearly inadequate. When crack opening stresses are taken into account (bottom), the correlation is remarkably strong.

A third data set from the same material is based on the growth of small cracks in smooth, cylindrical specimens at fully reversed large strains. These data are shown in Fig. 3.10, where the calculation for ΔJ_{eff} is based on the suggestion of Dowling [60] according to

$$\Delta J = C_o \pi a \left[\frac{(\Delta\sigma)^2}{E'} + h_o \Delta\sigma \Delta\varepsilon_p\right] \qquad (3.32)$$

Here C_o = 0.434, $E' = E/(1-\nu^2)$, and $h_o = 0.75\sqrt{1/n}$. The crack depth, a, is based on the measurement of surface crack lengths ℓ and the assumption of semicircular crack shapes ($2a = \ell$). Crack opening stresses were taken from the earlier experimental measurements on flat specimens. Again, the difference between ΔJ and ΔJ_{eff} correlations within this data set was small, because U varied little between $\Delta\varepsilon/2$ = 0.003 and 0.005. The scatter of these data is generally greater, probably because of irregularly shaped cracks, crack linking and branching, and other phenomena associated with naturally occurring three-dimensional cracks.

A comparison of these data with all previous data from the same material reveals, again, a strong correlation (Fig. 3.11). Note that this figure includes data from three different specimen geometries, crack lengths ranging from a = 0.075 mm to 2a = 20 mm, maximum stresses ranging from 0.30 σ_o to 1.2 σ_o, and plastic strains ranging from essentially zero up to $\Delta\varepsilon_p$ = 0.01.

3.4 Conclusions

1. Engineering estimates for the four most common elastic-plastic fatigue crack growth parameters have essentially the same structure and are numerically similar, despite their widely differing theoretical backgrounds.
2. Normalized crack opening stresses change significantly between small-scale and large-scale yielding conditions. Changes in closure behavior have further implications for the numerical structure of estimates for crack growth parameters.

3. Crack closure information must be considered in order to construct successful correlations of experimental fatigue crack propagation data at a wide range of maximum stresses.

4. CLOSURE AND GROWTH OF MODE I CRACKS IN BIAXIAL FATIGUE

4.1 Background

The effect of biaxial stressing on fatigue growth rates has been the subject of numerous investigations. Early experimental studies [112-116], which often were based on nontraditional, complex specimen designs and test methods, did not give conclusive results. More recent investigators [117-128], typically testing cruciform specimens, observed a general tendency for faster crack growth when remote stresses parallel to the crack are of opposite sign to normal stresses ($\lambda = -1$, where $\lambda = S_x/S_y$), and slower crack growth when S_x is of the same sign as S_y. Nomenclature is illustrated further in Fig. 4.1. Other researchers [129-130] reported no significant change in fatigue crack growth rates with biaxiality. A more detailed review of some of this data is given by Smith and Pascoe [131]. Note that in this thesis, discussion will be limited to Mode I cracks under loading which is proportional, either fully in-phase (e.g., $\lambda = +1$) or 180° out-of-phase ($\lambda = -1$).

Several explanations have been proposed for these effects. Kitawaga, et al. [125] claimed that the effect was only apparent, and could be rationalized with an exact calculation of K which accounted for load biaxiality. In general, however, they found relatively little change in crack growth rates with λ, and so the required corrections were minor.*

*At higher stresses, higher R-ratios, and shorter cracks, Kitawaga, et al. [126] found larger biaxiality effects which were not similarly explained. In those tests the effect was actually reversed: slower crack growth with decreasing λ. Hoshide, et al. [124] found a similar anomalous behavior for $R = 0$, $\lambda = -1$, and they explained it in terms of a pre-strain effect. These two results are exceptions to the general trend.

A number of investigators have suspected that changes in crack-tip plasticity, perhaps characterized by the plastic zone size and shape, are a crucial factor influencing biaxial crack growth rates. Brown and Miller [80,117,118,128], in particular, have attempted to explain and correlate fatigue crack growth data with simple estimates of forward or reversed plastic zone sizes or "severe-strain" zone sizes for various loading conditions. As engineering estimates, these have been moderately successful.

The possible role of crack closure has received some attention. Tanaka, et al. [123], and Hoshide, et al. [124], attempted to determine opening stresses experimentally from crack opening displacement measurements taken either along the crack centerline or 250 μm behind the crack tip. They found U, in general, to be largest for $\lambda = -1$ and smallest for $\lambda = +1$, although the difference was sometimes small and U values were all quite large, ranging from 0.52 to 0.87. Kitawaga, et al. [126] reported essentially no change in crack opening stresses with biaxiality from their experimental measurements. Brown, et al. [80], developed a simple analytical model for plane strain closure, based on the Dugdale crack, which considered biaxial stressing. They predicted U values from 0.61 to 0.67 for $R = -1$ with a moderate dependence on both biaxiality ratio and maximum stress.

Ogura, et al. [7] applied their early finite element simulation of fatigue crack closure to the problem of biaxial stressing. For a plane stress crack growing from a sharp notch at $S_{max}/\sigma_o = 0.40$, they reported no effect of biaxiality on crack opening levels at $R = 0$. At $R = -1$, they showed lowest opening levels for $\lambda = -1$ cycling, while $\lambda = 0$

and λ = +1 levels were similar. Their results may be suspect, however, because of several possible problems with the model which have been discussed in detail in Chapter 2. First of all, their mesh refinement for these stresses and crack lengths may have been insufficient. Second, the cracks were initiated at the notch root and apparently grown only to a length five percent of the notch depth. At this location there will still be a significant notch effect on opening behavior, and in fact the opening stresses shown in Fig. 2-3 of Ref.[7] do not appear to have reached stable levels.

4.2 Finite Element Analysis of Closure

The present finite element model, described in detail in previous chapters, was used to study crack closure under biaxial stressing. Stresses parallel to the crack were applied simply by specifying additional traction loading of appropriate magnitude and sign along the right boundary of the mesh. The results for R = -1 cycling of H/E = 0.07 plane stress material at λ = -1, 0, and 1 are summarized in Fig. 4.2. In general, stabilized S_{open}/S_{max} values are highest for equibiaxial loading and lowest for shear loading, with uniaxial loading an intermediate case. Below S_{max}/σ_o = 0.4, opening levels may be roughly the same for all three biaxiality ratios, although this stress amplitude represents the limit of reliable results for the present formulation and particular mesh used, and so no solid conclusions can be reached. Above S_{max}/σ_o = 0.4, equibiaxial opening stresses are higher than uniaxial opening stresses by a constant fraction of the maximum stress, while opening stresses for λ = -1 drop off more sharply with

increasing S_{max}. Note that no values of S_{open}/S_{max} were obtained for $\lambda = -1$ above $S_{max} = 0.5//$, because of previously discussed limitations of the current formulation associated with general yielding.

More insight into this closure behavior can be obtained from Fig. 4.3, which shows crack opening displacements at maximum load for both stationary and fatigue cracks at the three biaxiality ratios. As discussed earlier, the difference between stationary and fatigue COD values is a first approximation to the residual displacements which cause closure. Note that these estimates of residual displacement magnitudes are relatively similar for all three λ values. The primary reason for the differences in closure behavior, then, seems to be the differences in total COD. Crack opening displacements are clearly largest for $\lambda = -1$, and slightly lower for $\lambda = +1$ in comparison to $\lambda = 0$, as has been observed previously for stationary cracks [132]. The residual displacement as a fraction of the total COD, which is a predictor of closure behavior, is smallest for $\lambda = -1$ and largest for $\lambda = +1$.

Plastic zone size and shape information is also available from the finite element model and is worthy of note. Active plastic zones at maximum load for the three biaxiality ratios are shown in Fig. 4.4. Plastic zones for $\lambda = 0$ and $\lambda = +1$ are similar, of equal width along the crack line. The uniaxial plastic zone, $\lambda = 0$,is slightly larger along a 45° ray from the crack tip. The plastic zone for $\lambda = -1$, while actually narrower along the crack line, is much, much larger overall. Reversed plastic zones, or active plastic zones at minimum load, are shown in comparison to forward plastic zones in Fig. 4.5. Note that reversed

plastic zones for $\lambda = 0$ and $\lambda = +1$ are essentially identical, but still much larger for $\lambda = -1$. Similar trends have been shown by other researchers [9,132].

4.3 Crack Growth Data and Correlations

Several reliable sets of fatigue crack growth data for biaxial stressing are available in the open literature, each presented graphically in terms of ΔK. It is interesting to use the finite element model to predict crack opening levels for each set of test conditions, make a first-order modification of ΔK to ΔK_{eff} based only on U, and replot the data.

4.3.1 Brown and Miller (1985)

Brown and Miller [128] tested cruciform specimens of an AISI 316 austenitic stainless steel at three biaxial stress ratios and two temperatures. Here for simplicity we consider only the room temperature data, which include three maximum stress levels and two stress ratios. The monotonic 0.2 percent yield stress for this material is given as 395 MPa. At the stress levels encountered in testing, however, the cyclic (rather than monotonic) stress-strain properties are probably more appropriate. These were determined from information graciously supplied by Dr. Brown* to be an 0.2 percent offset yield stress of 315 MPa and a cyclic strain hardening exponent about $n' = 0.25$ (for $\Delta\varepsilon_p/2 \geq 0.0015$).

* Private communication, September 1987.

The data for R = -1 cycling are reproduced in Fig. 4.6 (top) as a function of the original ΔK, where

$$\Delta K = \Delta\sigma_y \sqrt{(\pi a)\ \sec(\pi a/W^*)} \qquad (4.1)$$

Here $\Delta\sigma_y$ is the stress normal to the crack, including the compressive portion, and W* is the equivalent width of the cruciform specimen. Data for cracks very close to the original notch root have been removed for clarity. Two different types of noncorrelation are observed in the data; not only is there a biaxial effect, but there is also an apparent layering of the data due to maximum stress.

Crack opening stresses were estimated from the finite element results of Fig. 4.2. The modulus ratio H/E = 0.07 was judged to be an adequate description of the appreciable hardening observed in the 316 stainless steel. Changes in the σ_o/E ratio have been shown to be insignificant for the finite element modeling. The model parameter σ_o was interpreted as the 0.2 percent offset yield stress for normalization purposes. When test conditions fell just outside the range of finite element results, simple linear extrapolations were used to estimate the opening stress. A first-order correction to ΔK was carried out as $\Delta K_{eff} = U\Delta K$, and the data were replotted in Fig. 4.6 (bottom). The improvement in the correlation is obvious.

4.3.2 Hoshide, Tanaka, and Yamada (1981)

Hoshide, et al. [124], have published crack growth data from cruciform specimens of a structural low-carbon steel. Three biaxiality

ratios (λ = -1, 0, +1) were considered at both R = 0 and R = -1. In all tests the maximum stress was 67.1 percent of the yield stress (σ_{ys} = 228 MPa). The original data are shown in Fig. 4.7 (top) in terms of the elastic ΔK determined analytically by the original authors for the particular specimen geometry. Omitted from consideration here are the data for λ = -1, R = 0, which were noted by the original authors to be unduly influenced by pre-strain effects.

Again, crack opening stresses for this high hardening material were estimated from finite element results for H/E = 0.07. Trends in crack opening levels with biaxiality for R = 0, not shown here, were qualitatively similar to Fig. 4.2. A first estimate of the effective stress intensity factor range was taken as $\Delta K_{eff} = U\Delta K$. The resulting correlation of da/dN values is given in Fig. 4.7 (bottom). The scatterband is wider than for the Brown and Miller data, but some of the scatter is due to variations in the original data. For example, the Paris exponent (slope) changes from data set to data set, and this could not be explained by a simple closure argument.

4.3.3 Smith and Pascoe (1985)

Smith and Pascoe [127] have reported biaxial fatigue crack growth data obtained under slightly different test conditions. They conducted three tests on cruciform specimens of an HY100 high yield-strength weldable steel which resulted in Mode I crack growth. All tests maintained about the same positive mean stress, but normal and transverse stress ratios and maximum stresses were different in each case. Loads were chosen in order to maintain the same strain range and

mean strain across the working section. A brief summary of test conditions is given in Fig. 4.8, adapted from the original references [127,133]. Note that Smith and Pascoe defined a new λ for their purposes as $\lambda = \Delta S_x/\Delta S_y$. A positive λ denotes in-phase cycling, a negative λ 180° out-of-phase cycling. The original crack growth data appear in Fig. 4.9 (top) as a function of ΔK.

New finite element analyses of closure were conducted in order to model these tests as nearly as possible. A power-law constitutive model was chosen in order to include the effects of possible mean stress relaxation, which may be significant at these positive stress ratios. Model constants corresponded to material properties of 0.2 percent offset yield stress σ_{ys} = 733 MPa, strain hardening exponent* n = 0.05, and strength coefficient* K = 1000 MPa, as determined from stress-strain information in reference [133]. Maximum and mean stresses matched experimental conditions closely. The following effective stress range ratios were determined: U = 1.0 for λ = -1, U = 0.55 for $\lambda = +\nu$, and U = 0.39 for λ = +1. The resulting correlation of da/dN values by ΔK_{eff} is shown in Fig. 4.9 (bottom). The quality of this closure-modified correlation is again much improved.

4.4 Discussion

4.4.1 Limitations and Purpose of this Analysis

It is important to point out immediately that we have been stretching ΔK beyond its limits of strict validity. When maximum

* as defined by the stress-plastic strain relationship $\sigma = K\varepsilon_p^n$

stresses are two-thirds of the yield under $\lambda = -1$ configurations, for example, significant plastic deformation will be occurring. Nevertheless, it is convenient to use ΔK, much as did Brown and Miller [128], as a simple parameter which provides suitable correction factors for specimen geometry effects and as a useful framework to compare relative crack growth rates under different conditions.

A second important confession is that, clearly, the issue of biaxial crack growth effects is more complicated than closure-modified ΔK values based only on stresses normal to the crack. An exact analysis would likely require consideration of near-tip stress and strain fields as well as microstructural issues such as crack path bifurcation or cleavage contributions to crack advance.

The point of the present chapter is that changes in crack closure behavior with biaxiality may be the single most significant reason for changes in crack growth rates. Furthermore, first-order corrections to simple crack growth parameters considering only changes in crack opening stresses may be entirely sufficient for many engineering design purposes. Descriptions of crack closure behavior provide a convenient way of simultaneously considering not only biaxial effects but also the effect of maximum stress, stress ratio, etc.

4.4.2 The Issue of Out-of-Plane Constraint

One modeling decision which was quietly made at the beginning of this analysis was the specification of out-of-plane constraint. Simple two-dimensional finite element analyses can be plane stress or plane strain, and in this chapter only plane stress results have been

used to correlate experimental data. Is this an accurate representation of actual experimental conditions?

The question of stress state near the tips of three-dimensional fatigue cracks is a complex one. Clearly there will always be some plane strain constraint at the crack tip in the midsection of a thick component. That constraint will gradually decrease with increasing distance from the crack tip or with proximity to the specimen surface. The ideas of plane stress or plane strain are actually only limiting extremes of constraint between which most of reality actually occurs.

In practice, however, it is often convenient to choose one or the other of these two extremes as a simple description of stress state. For crack problems, it has been common to make this choice on the basis of a comparison between specimen thickness and estimates of the crack tip plastic zone size. Full plane strain constraint is frequently assumed to exist [134-136] whenever a criterion similar to that specified in ASTM Standard E399-83 is satisfied,

$$B \geq 2.5 \left(\frac{K_{max}}{\sigma_{ys}}\right)^2 \qquad (4.2)$$

where B is specimen thickness.

Full plane stress conditions are typically assumed when the crack tip plastic zone width is on the order of one-half the specimen thickness [136-138], or

$$B \leq \frac{2}{\pi} \left(\frac{K_{max}}{\sigma_{ys}}\right)^2 \qquad (4.3)$$

When neither of these criteria is satisfied, partial constraint is assumed.

Application of these criteria to the three sets of data considered earlier in this chapter results in the conclusion that "full" plane strain constraint is almost never achieved, since maximum stresses are generally high and specimen thicknesses are usually small. A portion of the data falls into the "partial" constraint region, while a majority of the data satisfies the "full" plane stress criterion. In reality, of course, all of the cracks are under partial constraint, but a plane stress representation was judged to be a better choice than plane strain.

4.4.3 When are Biaxial Closure Effects Significant?

The present finite element analysis suggests that above $S_{max}/\sigma_o = 0.4$ for $R = -1$ and above $S_{max}/\sigma_o = 0.5$ for $R = 0$ there will be a clear effect of biaxiality on crack opening stresses. This appears to be confirmed by the experimental crack growth data presented in 4.3. At lower maximum stresses the finite element results are not conclusive, since we are at the limits of acceptable mesh refinement, but it appears that closure behavior does not differ significantly with biaxiality.

This absence of an effect also seems to be confirmed by the available data. Miller [118], for example, reported results for biaxial stressing of a high-strength aluminum alloy at S_{max}/σ_o values in the vicinity of 0.2 or 0.3 for $R = 0$ and above. His data showed a definite preference for faster growth at $\lambda = -1$ and slower growth at $\lambda = +1$, but the total variation in crack growth rates was always less than a factor

of two. Liu, et al. [129], conducted a wide range of tests on cruciform specimens of 7075-T7351 and 2024-T351 aluminum alloys, varying both the biaxial stress ratio and the maximum stress. They concluded that the effect of biaxiality on propagation rates was negligible. A majority of their tests were conducted at S_{max}/σ_o values less than 0.3. The few tests that were carried out at S_{max}/σ_o values around 0.5 only saw biaxiality ratios of $\lambda = \pm 0.5$. Kitawaga, et al. [125], conducted tests on a weldable structural steel at $S_{max}/\sigma_o = 0.165$ and $R = 0.1$ and found very little variation with λ. The stainless steel data of Brown and Miller [128] at $R = 0$, $S_{max}/\sigma_o = 0.2$ and $R = -1$, $S_{max}/\sigma_o = 0.3$ also show little effect.

A good rule of thumb, then, seems to be that if maximum stresses are on the order of $\sigma_{ys}/3$ (such that small scale yielding criteria are met rigorously), biaxial stressing will have no significant effect on crack growth rates (changes in da/dN less than 2X). As S_{max}/σ_o values approach 0.5 and higher, however, significant changes in crack growth rates (perhaps 5X - 10X) can occur between $\lambda = -1$ and $\lambda = +1$. These observed trends can be explained by crack closure behavior.

4.4.4 Alternative Explanations

As mentioned previously, other factors have been suggested as explanations for biaxial effects and other factors, no doubt, are active. Of particular interest are changes in plastic zone sizes, which have been frequently discussed in the literature and which have been shown by the present finite element analysis (Figs. 4.4 and 4.5). There appear to be some difficulties, however, with correlations based on

forward or reversed plastic zone sizes. First of all, these plastic zone sizes are typically estimated from simple idealized models such as the elastic near-tip stress fields or a Dugdale crack. While these estimates are useful and easily accessible engineering tools, they may bear little resemblance to actual plastic zone shapes and sizes, as depicted more accurately by a finite element analysis. Second, as has been suggested for uniaxial loading in an earlier chapter, the actual size of a forward or reversed plastic zone may itself be influenced by crack closure behavior. Obtaining accurate estimates of $\Delta r_p/r_p$ values without some closure information may be difficult. Third, the plastic zone information obtained from finite element analysis is not entirely consistent with observed crack growth rates. At R = -1, for example, forward and reversed plastic zone sizes and shapes for λ = +1 and λ = 0 are nearly identical, while sizes and shapes for λ = -1 are much larger (e.g., Figs. 4.4 and 4.5; this was also observed to be true at other S_{max} values). Correlations based on r_p and Δr_p, then, would predict crack growth rates to be quite similar at λ = +1 and λ = 0 but much faster at λ = -1. In practice, however, the difference between λ = +1 and λ = 0 is on the same order as the difference between λ = 0 and λ = -1, perhaps slightly less, and this is more in keeping with crack closure behavior.

Another attractive feature of closure-based correlations is that the single parameter U is capable of simultaneously describing not only biaxial effects but also the effects of maximum stress, stress ratio, out-of-plane constraint, notches, and so on. The stress-ratio effect in the data of Smith and Pascoe may be greater than the biaxiality effect,

for example. The Brown and Miller data contains a significant maximum stress effect as well as a λ effect. Yet all of these data were correlated reasonably well by a first approximation of closure levels. A similar robustness does not seem to have been demonstrated for other crack growth parameters.

4.5 Conclusions

1. Biaxial stressing can have a significant impact on crack closure behavior. In general, opening stresses are highest for equibiaxial loading and lowest for pure shear loading (considering only mode I cracks).
2. Experimental crack growth data for biaxial cycling is quantitatively consistent with these trends in crack opening levels. Correlations of the experimental data with simple closure-modified ΔK_{eff} were successful as first-order engineering estimates.
3. Changes in forward and reversed plastic zone sizes with biaxiality are not entirely consistent with trends in crack growth rates.
4. These changes in closure levels with biaxiality are apparently significant only for intermediate and large scale yielding. At low stresses, closure levels and crack propagation rates do not seem to change appreciably as biaxial stress contributions change.

5. CLOSURE AND GROWTH OF CRACKS AT NOTCHES

5.1 Background

5.1.1 The "Short Crack" Effect

A common site for the initiation and subsequent propagation of fatigue cracks in an engineering component is a local stress concentration, such as a hole or the root of a sharp notch. When the crack has grown sufficiently far beyond its initiation site, its growth may be easily modeled by traditional concepts of fatigue crack propagation, neglecting the hole or notch altogether except as a contributor to the total crack length. When the crack is still very short relative to characteristic notch dimensions, however, the problem is more complex. Broek [139] was one of the first to point out clearly the anomalous behavior of these small cracks at notch roots. Others [41,64,93,140-149] have since confirmed that such a crack will tend to grow more quickly than would be expected from the usual ΔK-based analysis.

At first glance this behavior should not be surprising. The constitutive response at the notch root of the uncracked body is likely to include some significant plastic strains, and these will both accelerate crack growth rates and invalidate K-based parameters. Even in the absence of large plastic deformations, other factors are involved which include microstructurally-based short crack effects and the nonlinear form of the exact K-solution for short cracks near notches. All of these issues will tend to be most significant when crack lengths are extremely short relative to notch dimensions. And yet anomalous behavior has also been reported for cracks which are somewhat longer relative to notch sizes [41,93].

The total picture may be better organized in terms of Fig. 5.1, a schematic which is adapted from the ideas of Leis [44] and Hammouda, et al. [150,151]. Cracks growing from notches can be classified into three groups as a loose function of the crack tip location with respect to the original notch stress-strain fields in an uncracked body. Very long cracks fall in region (1), in which case the original notch has no influence on the local stress-strain fields and hence can be neglected except as a component of total crack length. Very short cracks fall into region (3), where the crack tip lies within material which experienced plastic strains prior to the formation of any significant crack. Cracks of intermediate length are in region (2). Here there is no inelastic deformation which can be attributed to the notch alone, but the notch does cause perturbations in the elastic stress-strain field within which the crack tip and associated near-tip plastic zones are contained.

Many investigators have assumed that only two regions exist, a notch field and a region beyond the notch field. Smith and Miller, [152], for example, considered analytical K solutions and experimental crack growth data for cracks near notches. They suggested that the notch field was of approximate length $0.13\sqrt{c\rho}$, where 2c is the total width of a center notch and ρ is the root radius. Beyond this distance, K was assumed to be independent of the notch, while within this distance, K was estimated as a simple function of $\sqrt{c/\rho}$. Dowling [153] separated the crack growth problem into two smaller problems: first, an edge crack growing totally in the notch field, and second, a center crack growing independent of the notch. By setting K solutions for the

two problems equal to each other, he derived a transition crack length as

$$\ell_t = c/[(1.12\ K_t)^2 + 1] \qquad (5.1)$$

where K_t is the stress concentration factor for a center notch in a wide plate*. Values for ℓ_t generally range from $\rho/20$ to $\rho/4$ for moderate to sharp notches. Note that neither the Smith and Miller nor the Dowling model considers plastic deformation or any stress amplitude effects. Hammouda and Miller [150,151] analyzed the inelastic deformation in both cracked and uncracked notch roots. They concluded that cracks would grow at abnormally high rates within the notch plastic zone, but that this effect would die away (and crack growth rates perhaps decrease) until the crack reached the elastic-plastic boundary. Beyond this distance, normal linear elastic fracture mechanics would be sufficient to characterize crack growth. Leis [144] has also concluded from an analysis of his experimental data that the transition to normal long crack behavior from anomalous short crack behavior occurs when the length of the crack approaches or equals the length of the inelastic notch field.

Other data is available, however, which demonstrates accelerated crack growth rates at crack lengths well beyond the original notch plastic zone. Sehitoglu [93] has presented such data for cracks growing from a center slot notch in a low-carbon structural steel. Some of the

*For different geometries, more general forms of Eq. (5.1) can be developed.

data of El Haddad, et al. [64], exhibit a similar behavior. In both cases, cracks are also long with respect to the microstructure. Clearly, some effect other than notch plasticity is also significant.

5.1.2 The Role of Crack Closure

Another possible contributor to this "short crack effect" is crack closure. Closure (or, more properly, the absence of closure) has been frequently suggested as a reason for the accelerated growth of very short cracks in unnotched members [154]. Since closure is primarily a wake effect, a microcrack which has not yet developed a significant wake may, in theory, open at the minimum load in the cycle. Leis [144] assumed that S_{open} was equal to S_{min} at the notch root, and he then allowed S_{open} to increase linearly up to the far-field value (dependent only on R) over a distance equal to the width of the inelastic notch field. Tanaka and Nakai [147], Sehitoglu [41], Ogura, et al. [145], and Shih and Smith [148] all made some experimental determination of crack opening levels for cracks growing out of notches. All determined that S_{open} did change significantly with crack length, and all were able to relate this change to perturbations in crack growth rates. While the greatest changes in S_{open} occurred within the inelastic notch zone, some further variations occurred beyond this region. Ogura, et al. [8], in early work, and Lalor, et al. [27-29], in recent research related to the present thesis, have employed elastic-plastic finite element analyses to show that crack opening levels change as cracks grow away from the notch root. Similar results were obtained by Newman [38] and Sehitoglu [40] using simpler analytical models based on a Dugdale crack.

5.2 Finite Element Analysis of Closure

The finite element simulation of fatigue crack growth and closure presented previously in this thesis was specifically applied to the problem of cracks growing from notches. The notched meshes used throughout the thesis were appropriate geometries for detailed study here. The transient crack opening behavior which was viewed largely as an inconvenience in Chapter 2 now becomes the focus of attention.

The basic results are reviewed in Fig. 5.2 (bottom). Normalized opening stresses are low for very short cracks and then rise to stable levels as the crack extends. The rate of increase of S_{open} and the final stable value are both lower at higher remote maximum stresses.

It is particularly interesting to compare these opening curves with stress distributions in an uncracked body at corresponding maximum stresses (see top figure). Since a bilinear stress-strain curve is being used, the boundaries of the notch plastic zones are clearly indicated by the sharp corners in the stress distributions. As the maximum stress increases, of course, the width of the plastic zone increases. Note, however, that the crack opening levels have not yet stabilized when the crack tip reaches the original inelastic notch field boundary. Further changes in S_{open} occur in the elastic field of the notch.

Why does S_{open} change as the crack grows away from the notch root? One factor is crack length. A freshly initiated crack has no previous history and no wake, and therefore has no residual displacements which induce closure. As the crack moves beyond the notch

field (as defined by Dowling [153], for example), the crack tip sees a stress intensity at maximum load which is nearly identical to a notch-free center crack. Upon unloading, however, all of the reversed deformation is concentrated in a very small distance between notch root and crack tip, instead of being distributed over the full crack length 2a. Sehitoglu's simple analytical model based on the Dugdale crack captures some of these effects.

Another factor is stress magnitude. A crack tip near the notch effectively sees a "remote" stress which is larger than the true far-field stress, magnified by the notch stress concentration. Even though the crack tip significantly perturbs the exact form of the stress and strain distributions around the notch, the notch is still a factor in the total stress redistribution problem. The previous finite element results, (e.g., Fig. 2.11) clearly showed that opening stresses were lower when far-field stresses were higher. This logic is consistent with lower opening levels closer to the notch root.

It is interesting and relatively easy to explore some of the implications of this second factor. A simple model is constructed as follows. Each point along the crack line corresponds to a local stress σ_{yy}^{max} in a corresponding uncracked body (Fig. 5.2, top). This local stress σ_{yy}^{max}, interpreted as a remote stress S_y^{max}, corresponds to a stable crack opening stress, S_{open} (Fig. 2.11). Therefore for each point along the crack line, we can "predict" a corresponding opening stress. The results of this simple model are given in Fig. 5.3, in comparison to the crack opening curves obtained from a full finite element simulation. The match is reasonably good. There is a general

tendency to estimate crack opening levels too high, especially at very short crack lengths. This may be consistent with the fact that we are not considering crack length effects. It may also reflect some limitations of the finite element simulation associated with mesh discretization: residual deformations associated with a given crack tip location will not become effective until the crack has grown at least a full Δa jump. At the highest stress level, the quality of the correlation suffers at least in part because reliable finite element closure information is not available near or above general yield.

These figures represent a circular notch ($K_t = 3$). The same simple model was applied to an elliptical notch ($K_t = 7$), and the results are summarized in Fig. 5.4. The correlation is again strong. While the difference in opening behavior between the circular and elliptical notches is not great (compare Fig. 2.6), the simple model correctly describes the lower opening stresses at very short crack lengths and more rapid stabilization associated with the sharper notch.

5.3 Crack Growth Data and Correlations

This information about closure is useful only if it can be related to changes in observed crack growth rates. Since it is not practical to conduct a full finite element simulation of every exact problem we wish to solve, we consider instead the application of our simple model to correlate experimental data. In order to do this, we must (1) estimate ΔK for a given notch and crack length; (2) estimate the local stresses for a given crack tip location in the corresponding uncracked body; and (3) estimate the opening stresses corresponding to a given maximum

stress. Task (3) was solved in the preceding paragraphs, and is based on information such as Fig. 2.11. We turn our attention briefly now to the first two tasks.

Determination of the pure elastic K for an arbitrary notch geometry and crack length is not a trivial task. Newman [155] has published K solutions for a limited number of notch shapes based on a boundary collocation technique. No general closed-form solution is available, however.

An empirical formula which provides a good fit to Newman's results was found by trial-and-error to be given by

$$K = 1.12 \left[0.77\ \sigma_{yy}(\ell) + (0.23/\ell) \int_0^{\ell} \sigma_{yy}(x)\ dx\right] \sqrt{\pi\ell} \qquad (5.2)$$

where ℓ describes the current crack tip location, $\sigma_{yy}(\ell)$ is the stress at that position in an uncracked elastic body, and the integral term describes the average stress (also in an uncracked body) behind the crack tip location. These quantities are further illustrated in Fig. 5.5.

The simple model of Eq. (5.2) is compared with Newman's results for a circular notch and on elliptical notch in Fig. 5.6. The match is good within a few percent out to ℓ/c values of 0.5 and greater. At large ℓ/c, Eq. (5.2) tends to overestimate K (ultimately by 1.12X). The advantage of the simple equation, of course, is that K can be quickly determined for any notch geometry for which an elastic stress distribution is calculable (preferably in closed form).

The second task, that of determining the elastic-plastic stress-strain distribution in an uncracked, notched body, can be easily solved by employing the well-known Neuber relationship,

$$K_t = (K^\sigma K^\varepsilon)^{0.5} \tag{5.3}$$

where K_t is the theoretical elastic stress concentration factor at a given location, and K^σ and K^ε are the corresponding concentration factors for local stress and strain, respectively. While this is only an approximate method and does not consider, for example, stress redistribution due to yielding, its accuracy was judged to be sufficient for present purposes.

Original experimental data for crack growth from notches was available for the same hot-rolled 1026 steel considered in previous chapters. Specimens with a rectangular cross-section of 0.1" x 1.5" (2.54 mm x 38.1 mm) and a length (between the grips) of 4" (101.6 mm) were cycled in load control. Central circular and slot-notched holes of varying size and shape were machined in different specimens. All tests were conducted at $S_{max}/\sigma_o = 0.54$ and $R = -1$. Crack lengths were measured by a replica technique.

The nomenclature associated with the slot notches is illustrated in Fig. 5.7. The stress distribution for the notch is essentially identical to that of its "equivalent ellipse" [156], an imaginary ellipse with corresponding total width 2c and root radius ρ. The elastic stress distribution for the ellipse (also required in order to calculate K from Eq. (5.2)) was determined from the original equations of Inglis [157].

Crack growth data from four specimens are shown in Fig. 5.8. The solid line represents the predictions of the simple model. Crack growth rates were obtained from

$$\frac{da}{dN} = C(\Delta K_{eff})^m \qquad (5.4)$$

where the empirical constants C and m were determined from a fit of long crack data, independent of notch effects. The dashed line represents a crack growth rate prediction based on a "long crack" model [153], which includes the notch only as a length contribution to a center crack and neglects any local stress concentration: $\Delta K_{eff} = (U_{stable})\Delta S\sqrt{\pi(\ell+c)}$.

The correlation of the simple model with the data is, in general, quite good, considering the simplicity of the model. There is a general tendency to underestimate crack growth at the shortest crack lengths, but this should not be surprising. The simple model does not explicitly consider any effects of yielding, since linear-elastic ΔK is used. At the shortest crack lengths, the crack tip is still embedded in the original notch plastic zone. It is important to point out, however, that accelerated crack growth is taking place far beyond the original notch plastic zone. For these stress levels and notch shapes, the boundary of the inelastic notch field, determined from finite element analyses which account for stress redistribution, generally falls between $\ell/c = 0.1$ and $\ell/c = 0.25$. The correlation appears to be poorest for the circular notch (lower right), but this is influenced by considerably greater scatter in the data. The increased scatter is due to nonsymmetric growth of very short cracks, including the development of corner cracks at the notch root.

5.4 Discussion

5.4.1 Stress Ratio Effects

All of the analyses and data discussed so far have corresponded to a remote stress ratio of R = -1. A key factor in the simple model has been the strong dependence of S_{open}/S_{max} on S_{max} for R = -1. What happens when the remote stress ratio is R = 0? In that case the S_{open}/S_{max} values change only slightly with S_{max}, and therefore if the simple model is accurate, the short crack effect will be much less pronounced at R = 0.

In fact, this is apparently true. Finite element simulations of closure for cracks growing out of notches at R = 0, Fig. 2.7, show much less change in S_{open} with changes in crack length. Experimental data is also consistent with this trend. Broek [139], who considered only R = 0.1 cycling, found only a slight short crack effect at notches. Usami [146] observed a strong short crack effect at R = -1 but much less effect at R = 0. Some of the clearest data is that of Truyens [149], who conducted four-point bend tests on rectangular beams 75 mm deep with a saw-cut edge notch 10 mm deep. Data from his unpublished Ph.D. Thesis are reproduced here as Fig. 5.9.* Calculated K_{max} or ΔK values were based entirely on long crack relationships, ignoring any short crack effects. For various stress ratios all greater than or equal to zero, top figure, no accelerated short crack growth is observed. Very short cracks grow at rates slower than long crack trends, as expected from

*By written permission of Dr. Truyens, November 1987.

Fig. 5.6. For R = -1 cycling, bottom figure, a strong acceleration effect appears at a wide range of maximum stresses.

5.4.2 Influence of the Notch Plastic Zone

The simple models developed in this chapter have essentially ignored any influence of the notch plastic zone. Clearly, however, the inelastic deformation will have some impact on crack growth behavior. It is worthwhile to briefly consider these contributions.

First of all, when a crack is growing in an inelastic field, a linear elastic parameter will obviously not be an accurate representation of the crack tip fields. An elastic-plastic crack growth parameter similar to ΔJ or ΔK_ε should be employed instead.

On the other hand, it should be realized that notch plastic zones are typically very small. Even when remote stresses are half of the yield stress, the plastic zone at the root of a circular hole will have a width typically less than 0.125 of the hole diameter. At lower stresses and for smaller holes, the notch plastic zone width may be on the order of the microstructure. Cracks that are this short will be influenced not only by notch plasticity but also by microstructural short crack effects. Often crack lengths in this range are simply assumed to be included in a crack "initiation" portion of the life, where crack growth is not tracked at all.

Furthermore, even when crack tips are contained within the original notch plastic zone, this does not mean that the notch zone dominates or engulfs the crack tip events, as might be suggested by Fig. 3 of Ref. [150]. Figure 5.10 shows finite element results for plastic zones

corresponding to an uncracked body and very short cracks at a notch root. By the time the crack has grown only halfway through the original inelastic notch field, the crack tip plastic zone at maximum load takes a form which is relatively independent of the notch. The shape of the crack tip plastic zone is typical of a crack in an unnotched body, and the crack tip zone extends far beyond the original notch plastic zone. Certainly the notch still has some effect on the size and shape of the crack tip plastic zone, but the effect is not a dominating one.

The short crack effect at notches can not be explained entirely in terms of notch root plasticity, or region (3) behavior as illustrated in Fig. 5.1. Finite element analyses and experimental data both show that under certain conditions, crack opening levels and crack growth rates exhibit a short crack effect in the notch elastic field, region (2) in Fig. 5.1.

5.4.3 Significance of the Short Crack Effect

Demonstrating cleverness in modeling unusual crack growth behaviors may be great fun for the researcher, but the designer has a different perspective. His primary concern here is probably life prediction, and his question is whether this effect is really significant for total life.

Socie, et al. [158] have shown that for a number of design problems involving the initiation and propagation of fatigue cracks at notches, it is possible to totally ignore any sort of short crack behavior, go directly from initiation to a long crack model, and still make good life predictions. This will especially be the case, for example, when

notches are small and total component sizes large. On the other hand, if notches are large and component sizes smaller, a much larger percentage of the total life may be spent in the short crack stage. In this case, an acceleration in da/dN of 4X may be a very damaging event. Furthermore, this closure behavior may also be significant at lower stresses, when fatigue thresholds and nonpropagating cracks become issues.

In a larger perspective, the analysis presented in this chapter may have significance beyond the notch life prediction problem. The principles involved in the simple model, relating crack opening levels to local stresses in corresponding uncracked bodies, may have application to a broader class of problems involving crack propagation in nonuniform stress fields. While these simple models do not consider all effects, their very simplicity makes them attractive to the engineering analyst.

5.5 Conclusions

1. Crack opening levels change significantly as small cracks grow from notches. Opening levels are low at first and then gradually rise to steady-state values as the crack tip moves away from the notch field.
2. Transient changes in crack opening levels are not limited to the region of the original inelastic notch field. Further changes occur in the elastic notch field.
3. The rate of change of opening levels with increasing crack length is a function of both far-field maximum stress and far-field stress ratio. Steady-state levels are reached more quickly at higher stress ratios and lower maximum stresses.

4. These transient changes in S_{open} can be emulated with a simple model which considers only changes in S_{open} due to changes in the local stress field.
5. These transient changes in S_{open} are quantitatively consistent with observed trends in experimental crack growth data.
6. Numerical crack closure studies and experimental propagation data both suggest that the "short crack effect" (i.e., accelerated crack growth) for cracks at notches will be much less pronounced at higher stress ratios, such as R = 0, than at lower ratios, such at R = -1.
7. The "short crack effect" can occur beyond the original inelastic notch field boundary.

6. SUMMARY

There is little purpose at this point in simply repeating the detailed technical conclusions that have emerged in the previous four chapters. There is value, however, in pausing for a moment to reflect on the underlying themes and concepts which connect and motivate the diverse findings and applications. A few words on the engineering significance of these results are also in order.

A first basic concept is that nearly any phenomenon which brings about significant changes in crack tip plasticity will bring about changes in closure behavior. These phenomena include, for example, the basic constitutive response of the material, large changes in far-field stress, out of plane constraint, biaxial loading, and variations in local stress fields. As these phenomena induce changes in crack opening displacements, crack tip plastic zones, etc., they also influence closure.

A second basic concept is the converse of the first: changes in closure behavior can be thought of as leading to changes in other behaviors. Closure levels, for example, were associated with changes in the size of the reversed plastic zones. Closure clearly leads to changes in crack opening displacements. Accurate estimates of these other quantities will depend on some knowledge of the closure event.

A third basic concept is the sum of the first two. Closure behavior can be thought of, along with plastic zone sizes and crack opening displacements, as simply another evidence of more fundamental changes in crack tip plasticity. This thesis, as well as much other previous and current research in fatigue crack growth, has sometimes

seemed to treat closure as the "Answer," the once hidden and now revealed key to the mystery of why fatigue cracks grow at certain rates. Rather than being the end of the search for answers, however, closure may provide instead a clearer road map to more fundamental answers. The real mechanisms of crack advance probably have little to do with the precise moment at which a crack tip first becomes fully open. But those mechanisms may be closely related to the cyclic plastic strains at the crack tip, and closure may need to be considered in order to accurately characterize or predict those strains.

So if closure is not really the fundamental issue, why give it so much attention? One answer to that question, and the fourth basic concept in our list, is that closure is one of the simplest and most accessible factors in fatigue crack growth. Closure information can be conveyed with a single scalar value and can be easily combined with simple field parameters such as ΔK or one of the several similar elastic-plastic parameters. This is much easier, at the present time, than attempting to directly describe the crack tip plastic strain range, and also easier than characterizing the size and shape of the crack opening displacement or crack tip plastic zone. This is particularly important for engineering applications.

A fifth basic concept is also related to engineering applications. Crack closure is an attractive framework within which to consider many different effects simultaneously. Each of the individual problems which has been addressed in this thesis has certainly been addressed before, and in many cases successful engineering solutions have been proposed. There are parameters to handle mean stress effects,

parameters for high strain effects, parameters for short crack effects, parameters for biaxial effects, parameters for variable amplitude effects, and so on. In most cases these are different parameters for different effects. And on occasion a parameter which is entirely successful in characterizing one effect will give precisely the wrong indication for another effect. For example, plastic zone sizes are a generally good predictor of biaxial crack growth rates (the two increase together), but in thicker sections, when plane strain constraint decreases the size of the plastic zone, crack growth rates generally increase. And what happens when two or more effects occur simultaneously? Current elastic-plastic parameters do not accommodate mean stress effects, for example. But crack closure provides a unified approach, a single parameter which can account for a wide range of effects.

A sixth basic concept is that crack closure information need not always be considered. This is evidenced, of course, by the many years of successful fatigue research and design conducted in ignorance of closure behavior. Fatigue crack closure always occurs, but it must be considered explicitly only when there is a significant change in closure levels from case to case. Closure levels tend to change relatively little at higher stress ratios, lower maximum stresses, and greater out-of-plane constraint, and so in these cases can often be ignored without consequence. With lower stress ratios, higher maximum stresses, and lesser out-of-plane constraint, however, crack opening stresses can vary widely, and typically must be considered to correlate data successfully. Another way of saying this is that crack closure is particularly

an issue in problems which involve intermediate and large scale yielding. In some (but not all) problems in small scale yielding, closure is not a significant issue.

An obvious limitation of detailed closure analysis is the computational expense and difficulty involved. The average engineering analyst will neither have access to a CRAY nor the time for detailed modeling studies. But (this is the seventh basic concept) the basic results of a closure analysis are very accessible. The majority of the applications to experimental data reported in this thesis were based on a single line in a single figure, Fig. 2.11. While a great many parameters do have some bearing on closure levels, the changes in S_{open} are generally smooth and continuous. It would be possible, for example, to develop a set of master curves for S_{open} as a function of basic parameters at chosen values of the parameters. Intermediate values could be easily interpolated. A similar scheme has been developed by Newman [39] for his modified Dugdale closure model; he has developed a single empirical formula which gives an estimate of S_{open} as a function of S_{max}, R, and constraint level. These simple analytical models also remain a powerful tool for the engineer. They are generally much simpler numerically, much less expensive computationally, and, with calibration by a more sophisticated analysis, can provide reliable results.

In conclusion, the study of crack closure by the finite element method has provided a great many insights into the phenomenon of fatigue crack growth. Further studies in the area appear to hold great promise for even more significant progress.

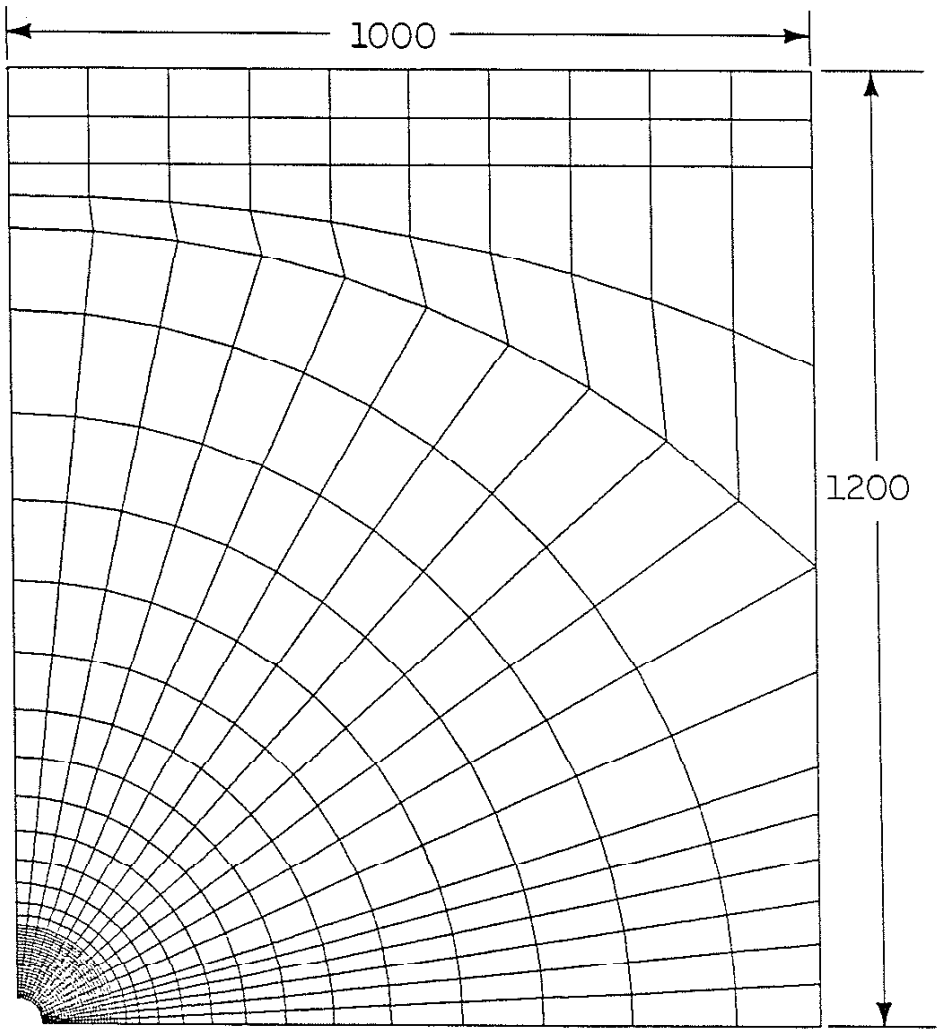

Figure 2.1 Typical mesh used in present research.

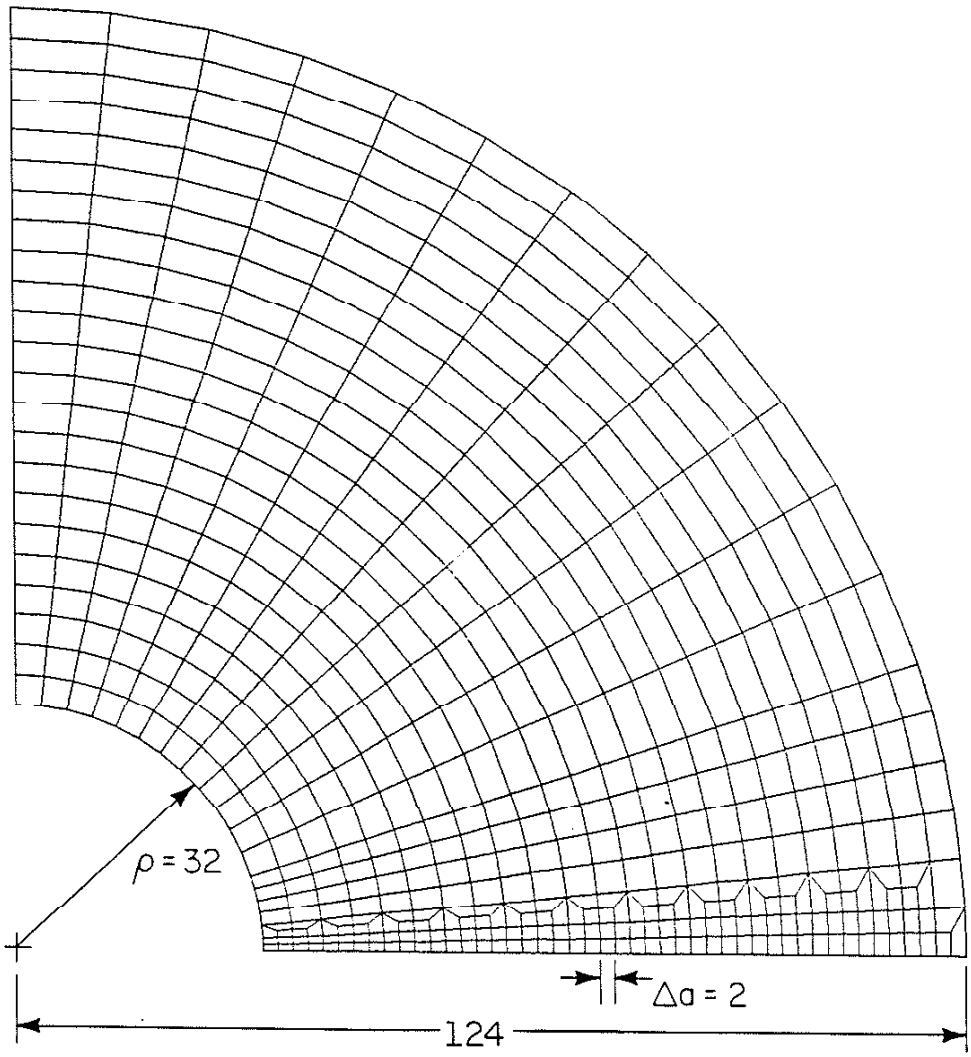

Figure 2.2 Typical fine mesh region used in present research.

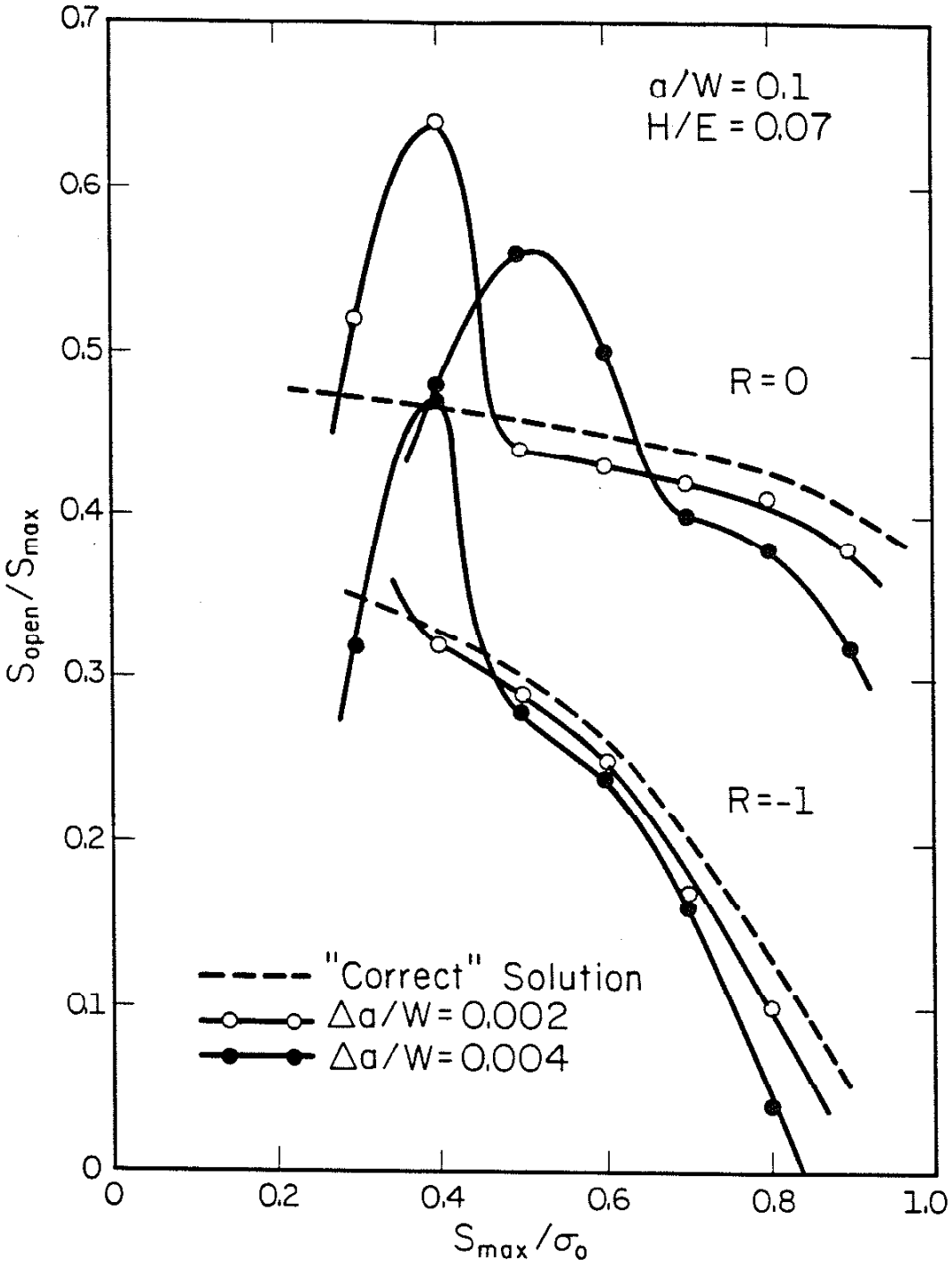

Figure 2.3 Normalized crack opening stresses as a function of maximum stress for different mesh spacings.

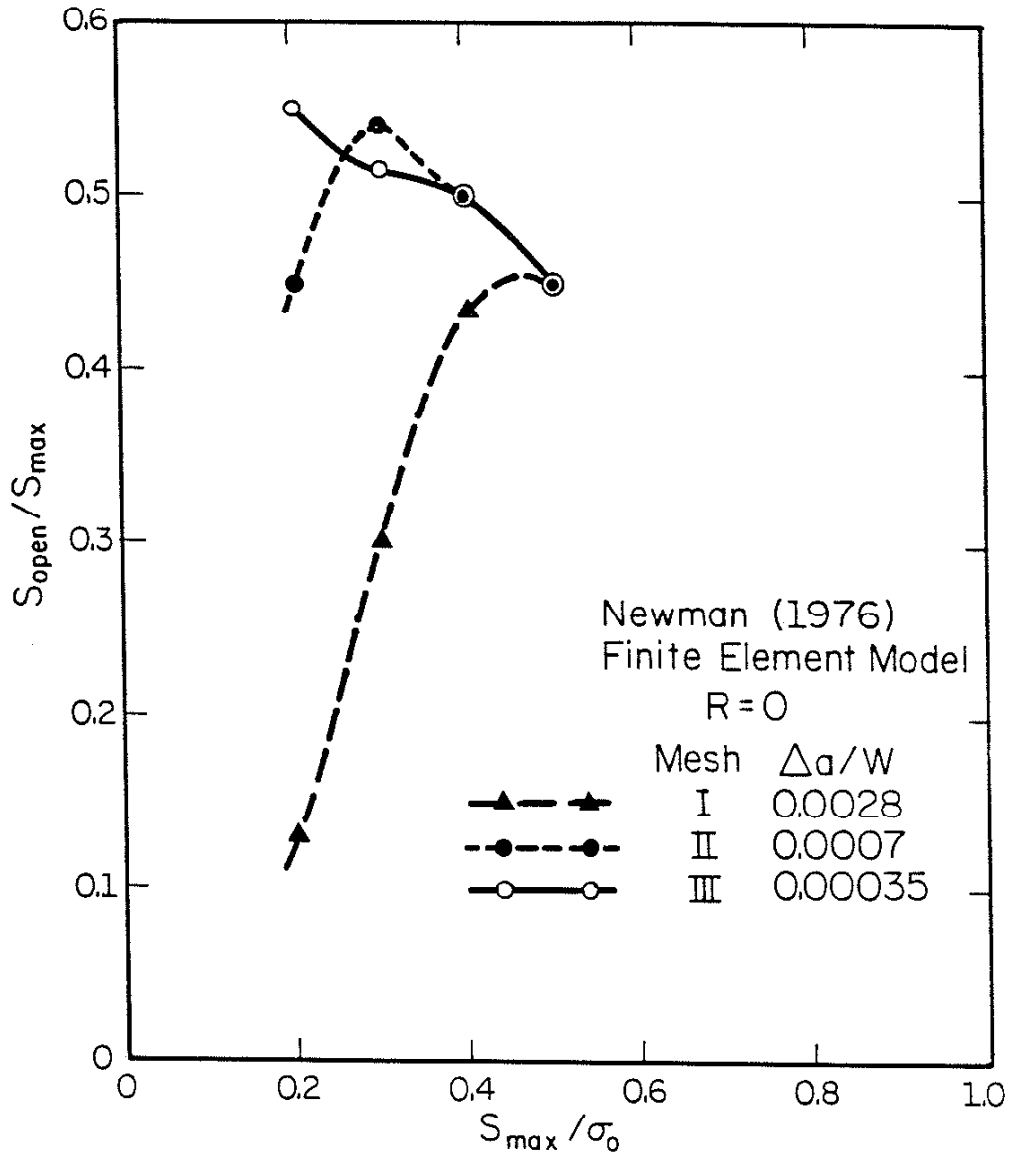

Figure 2.4 Normalized crack opening stresses as a function of maximum stress for different mesh spacings, as determined by Newman [13].

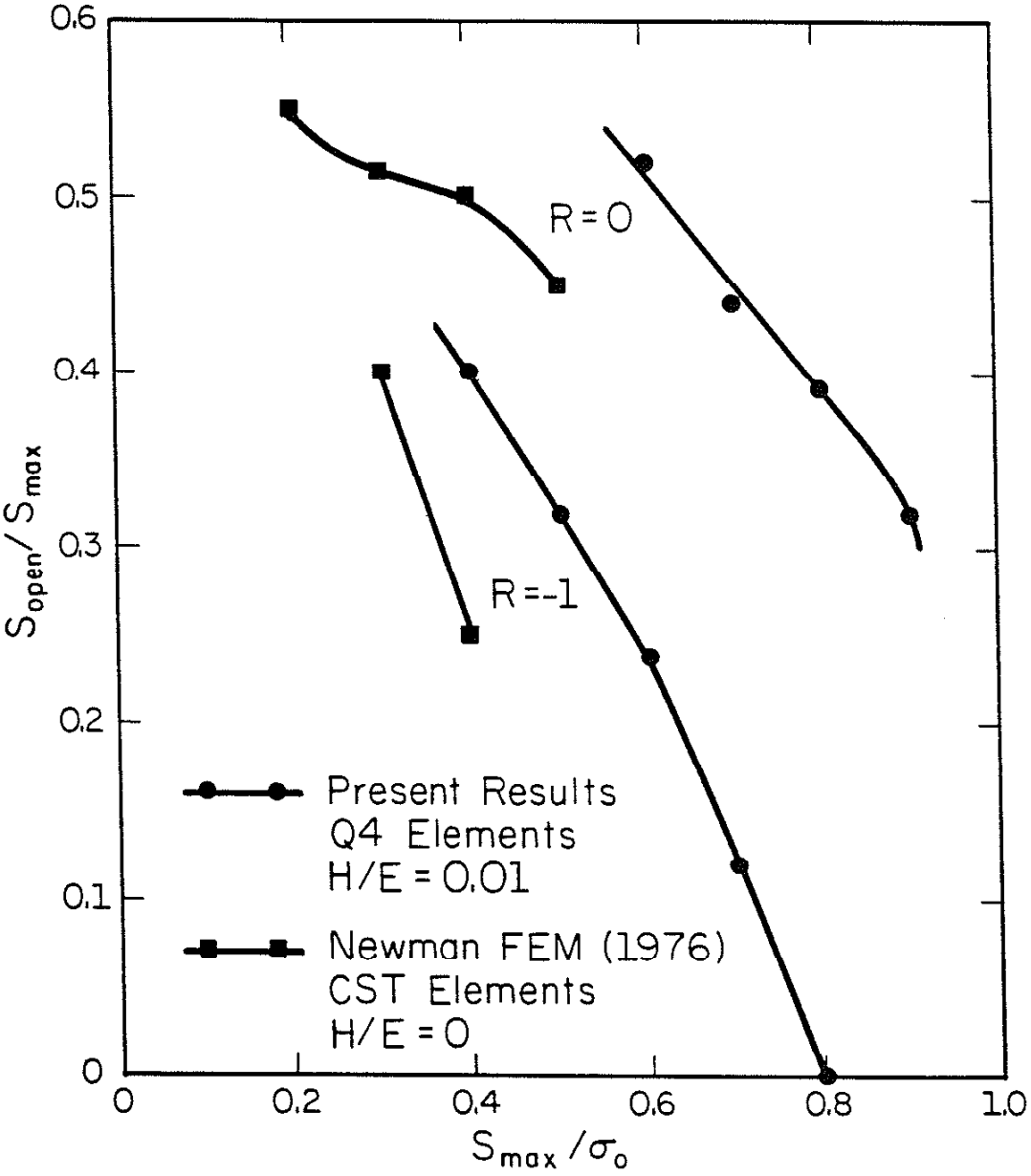

Figure 2.5 Comparison of crack opening stresses as determined by Newman [13] and the present research.

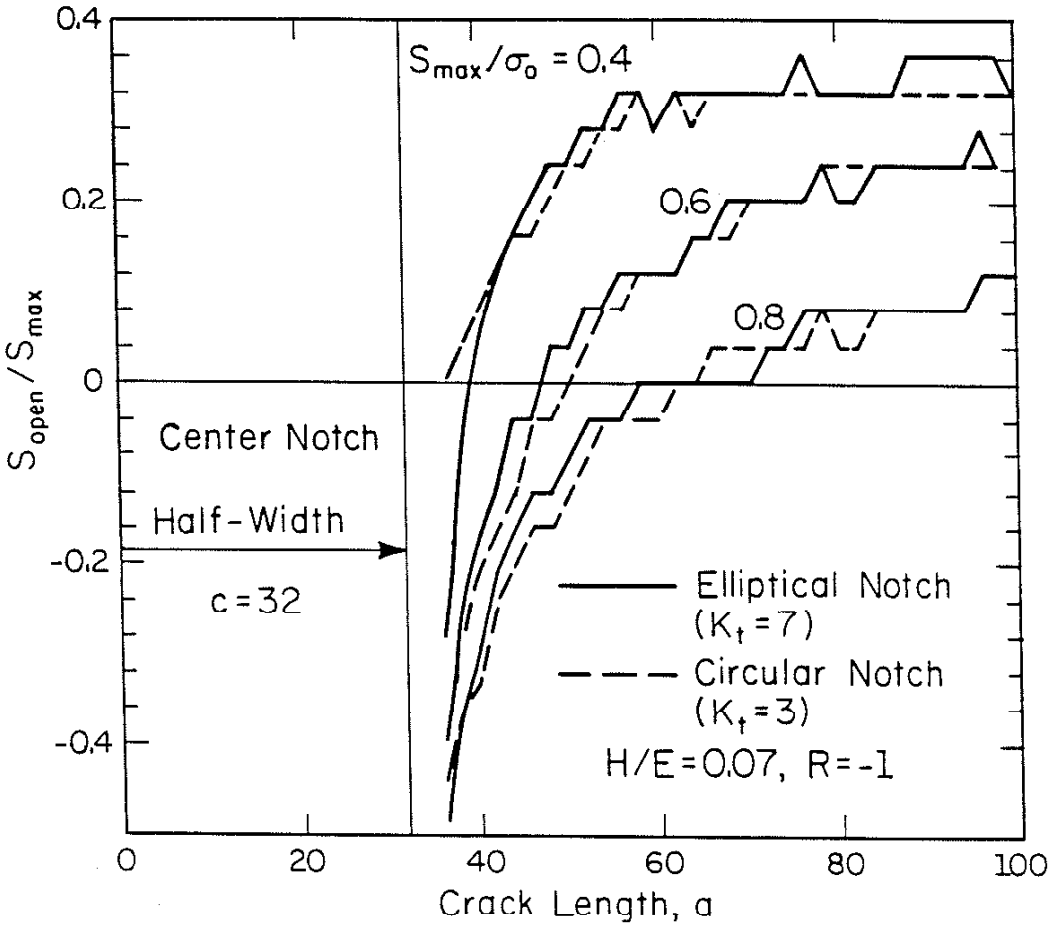

Figure 2.6 Opening stresses for cracks growing out of notches at R = -1.

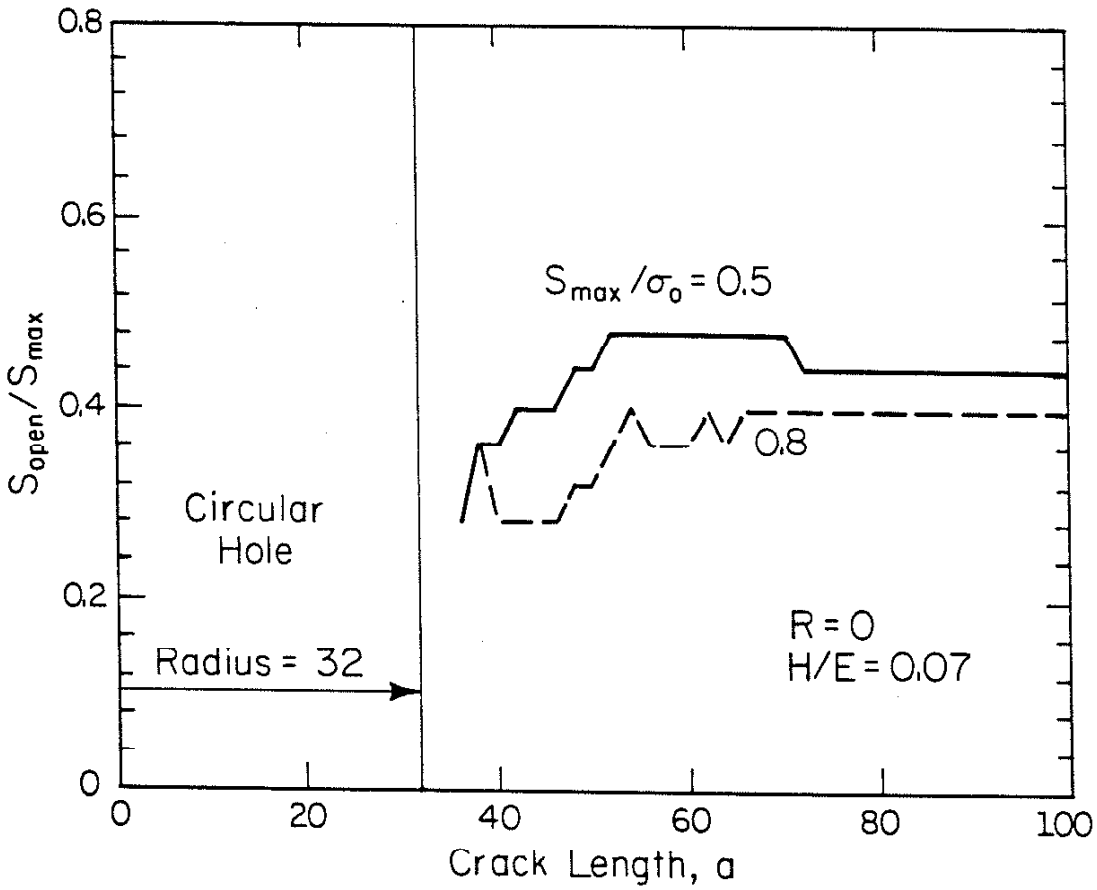

Figure 2.7 Opening stresses for cracks growing out of notches at R = 0.

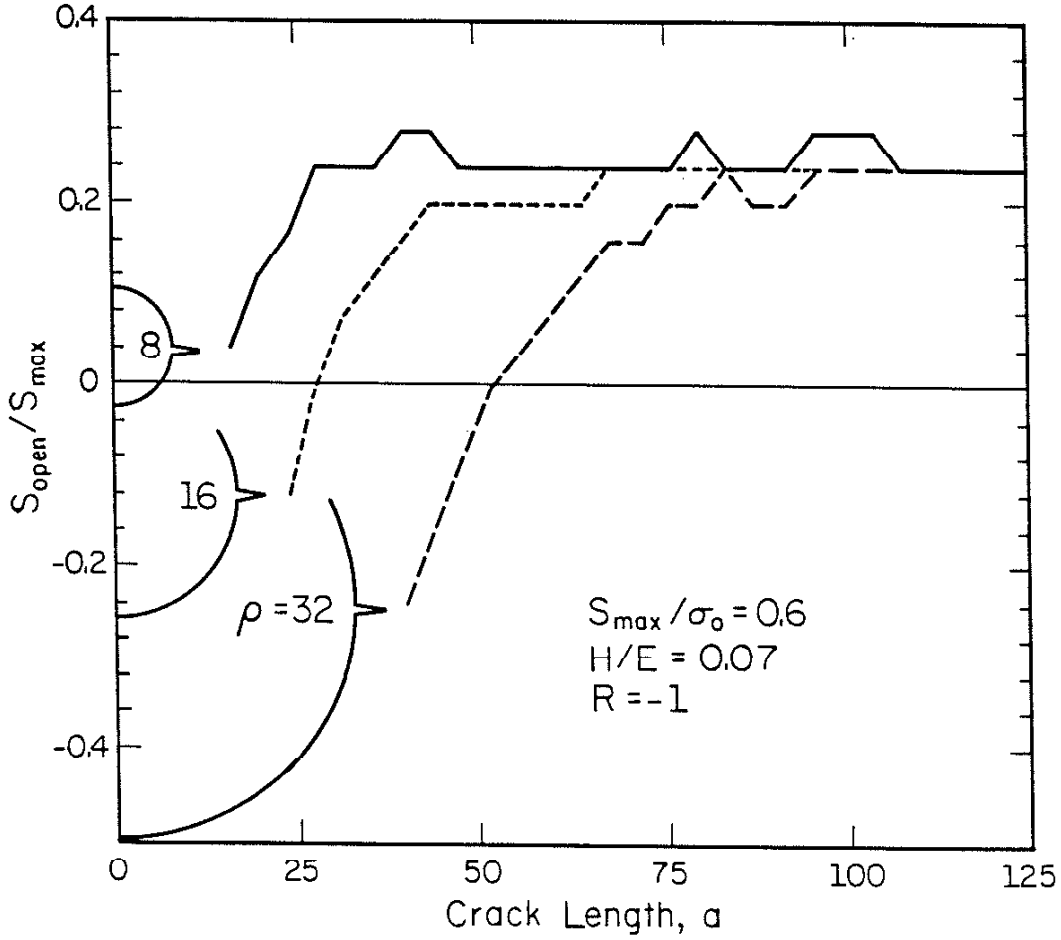

Figure 2.8 Opening stresses for cracks growing out of variously sized circular holes.

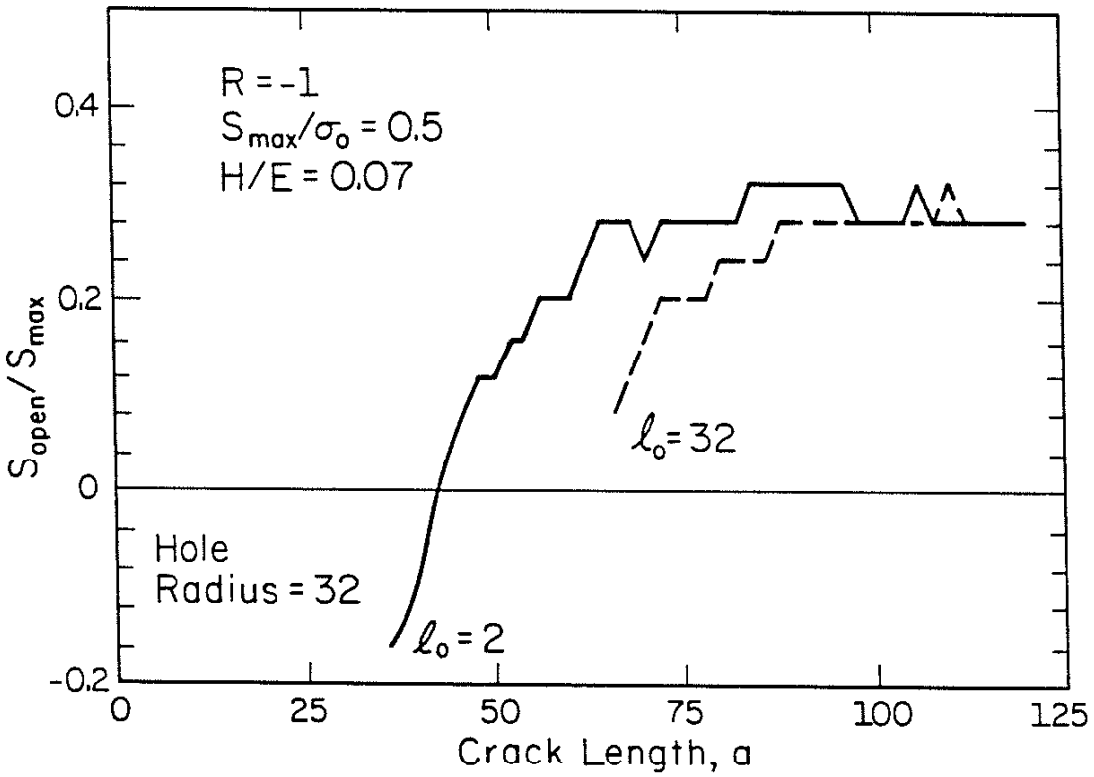

Figure 2.9 An example of the transient changes in opening stresses for a crack grown from some nonzero initial length.

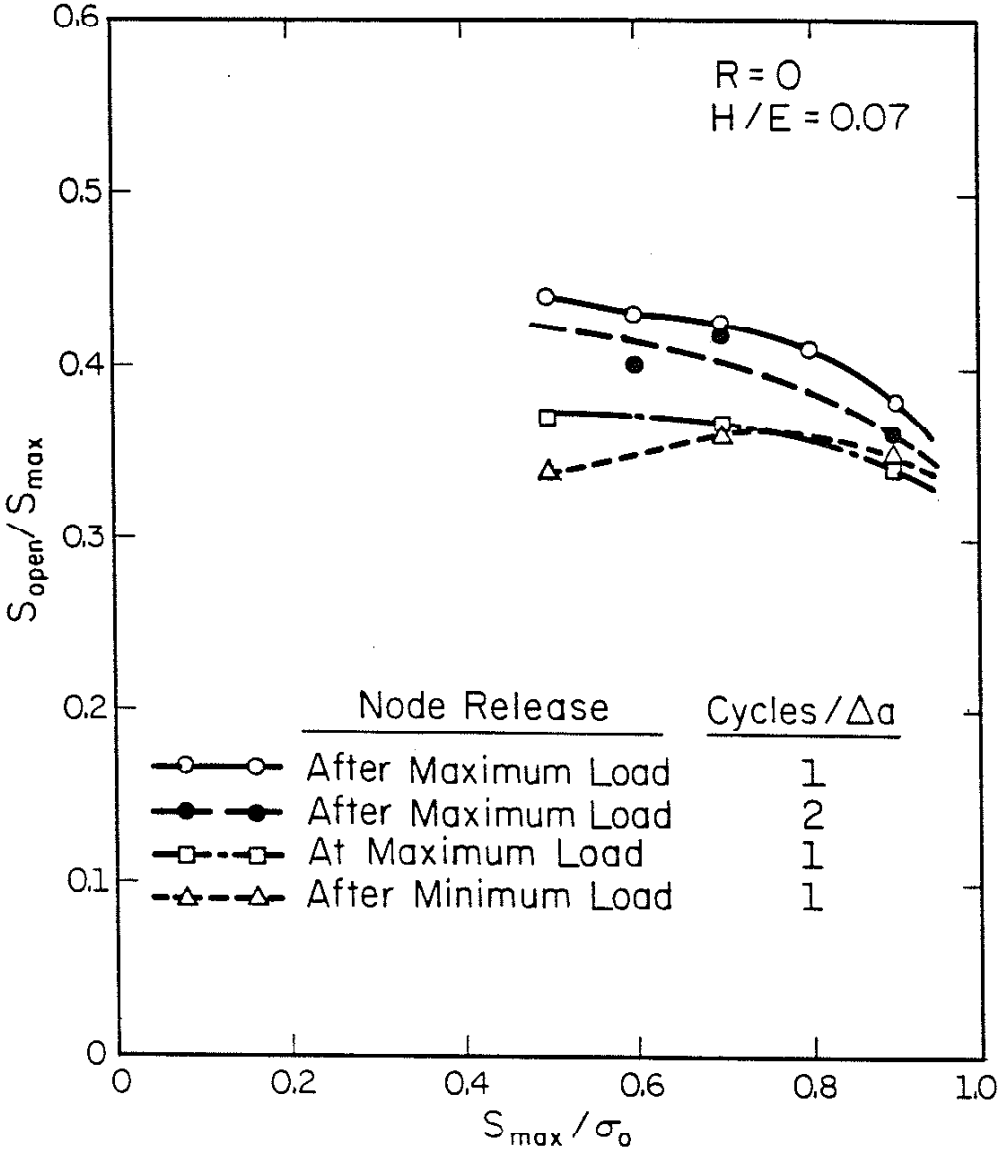

Figure 2.10 Normalized crack opening stresses for different crack advance schemes.

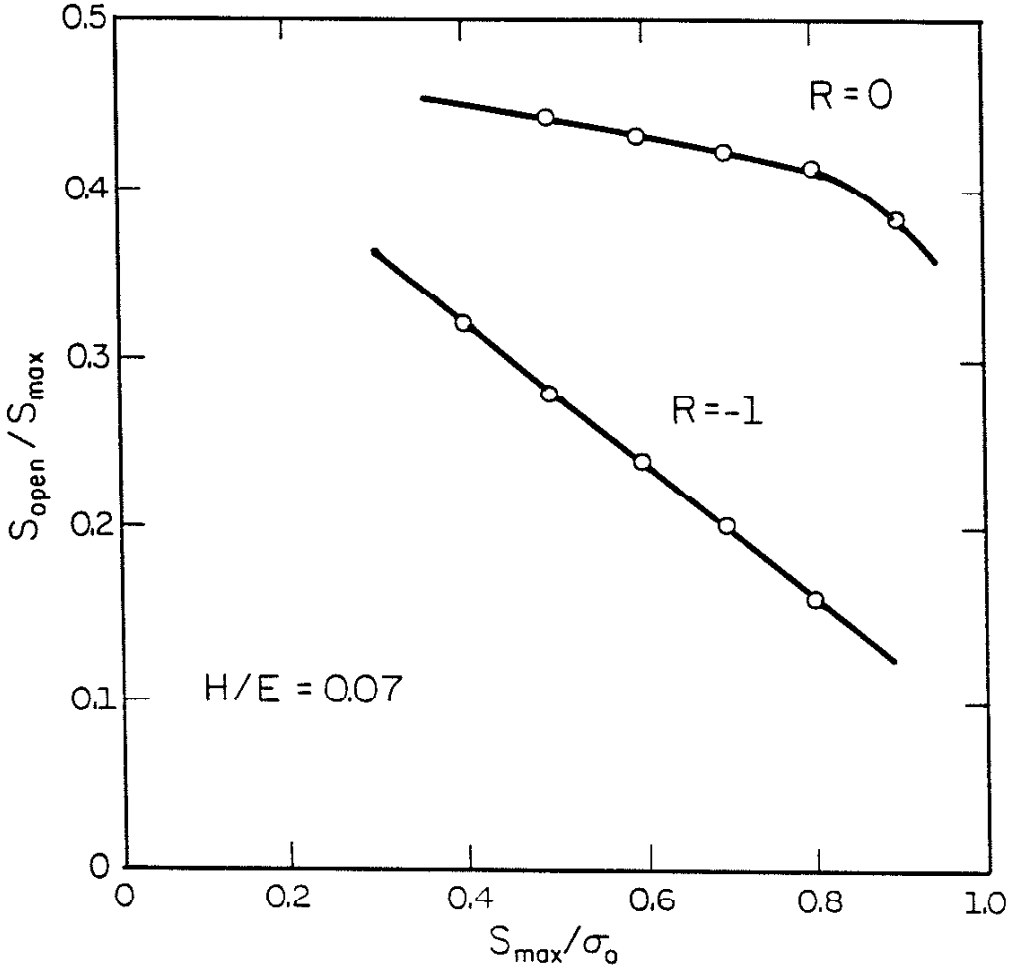

Figure 2.11 Normalized crack opening stresses as a function of maximum stress for two stress ratios.

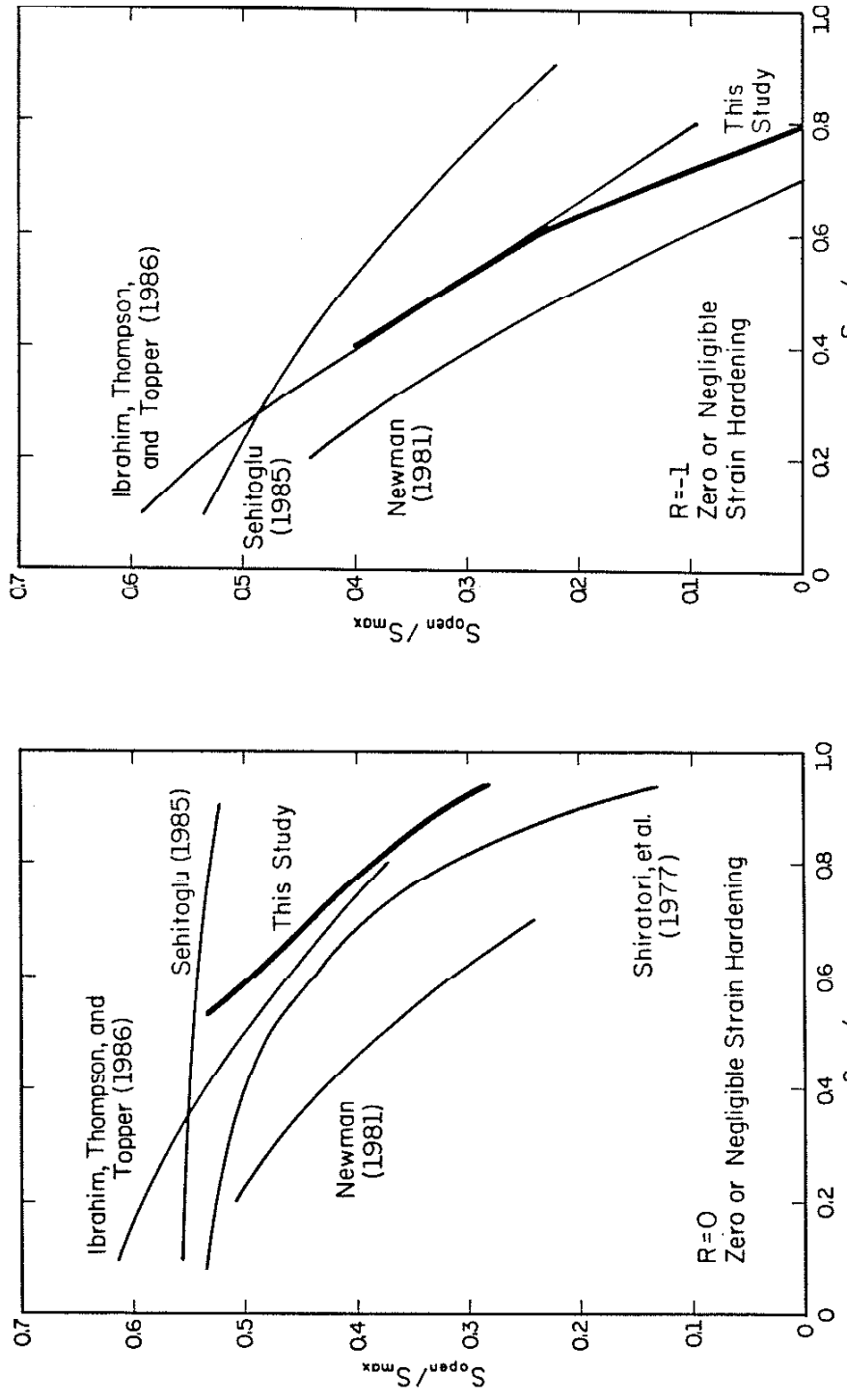

Figure 2.12 Comparison of the present finite element results with simple analytical models based on a modified Dugdale crack. (left) R = 0 (right) R = -1

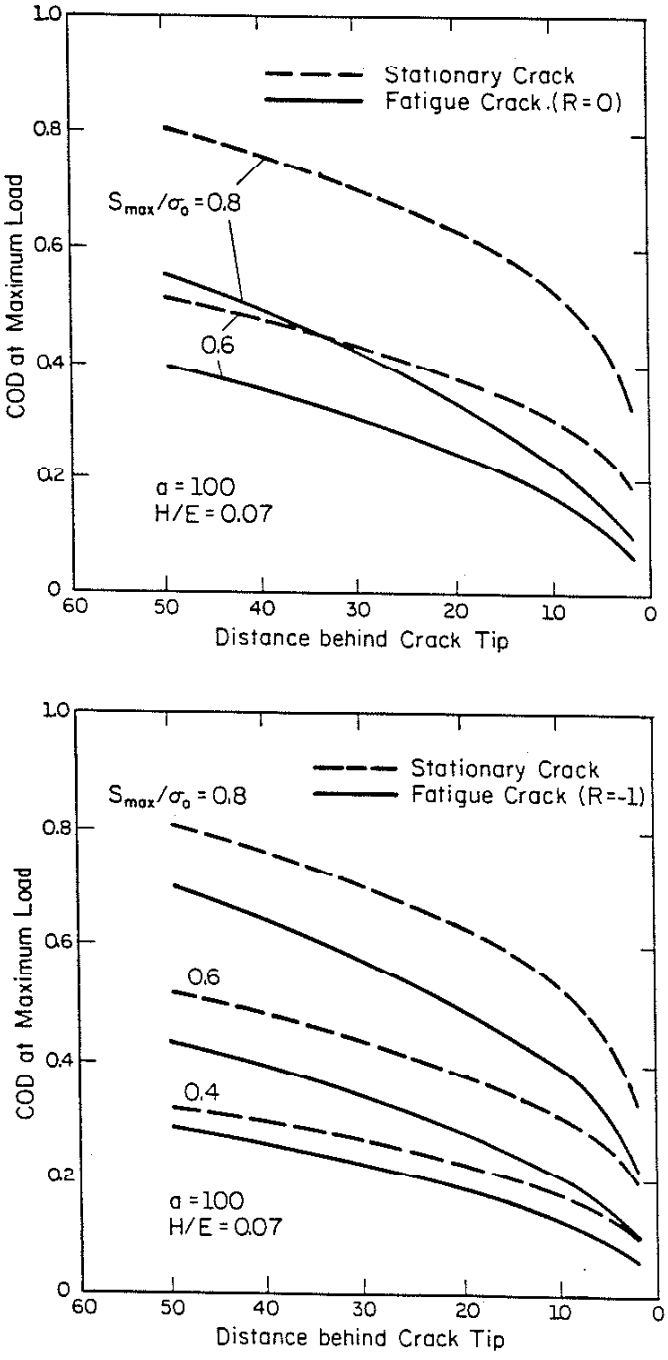

Figure 2.13 Crack opening displacements at maximum load for stationary and fatigue cracks at different maximum stresses.
(top) R = 0 (bottom) R = -1.

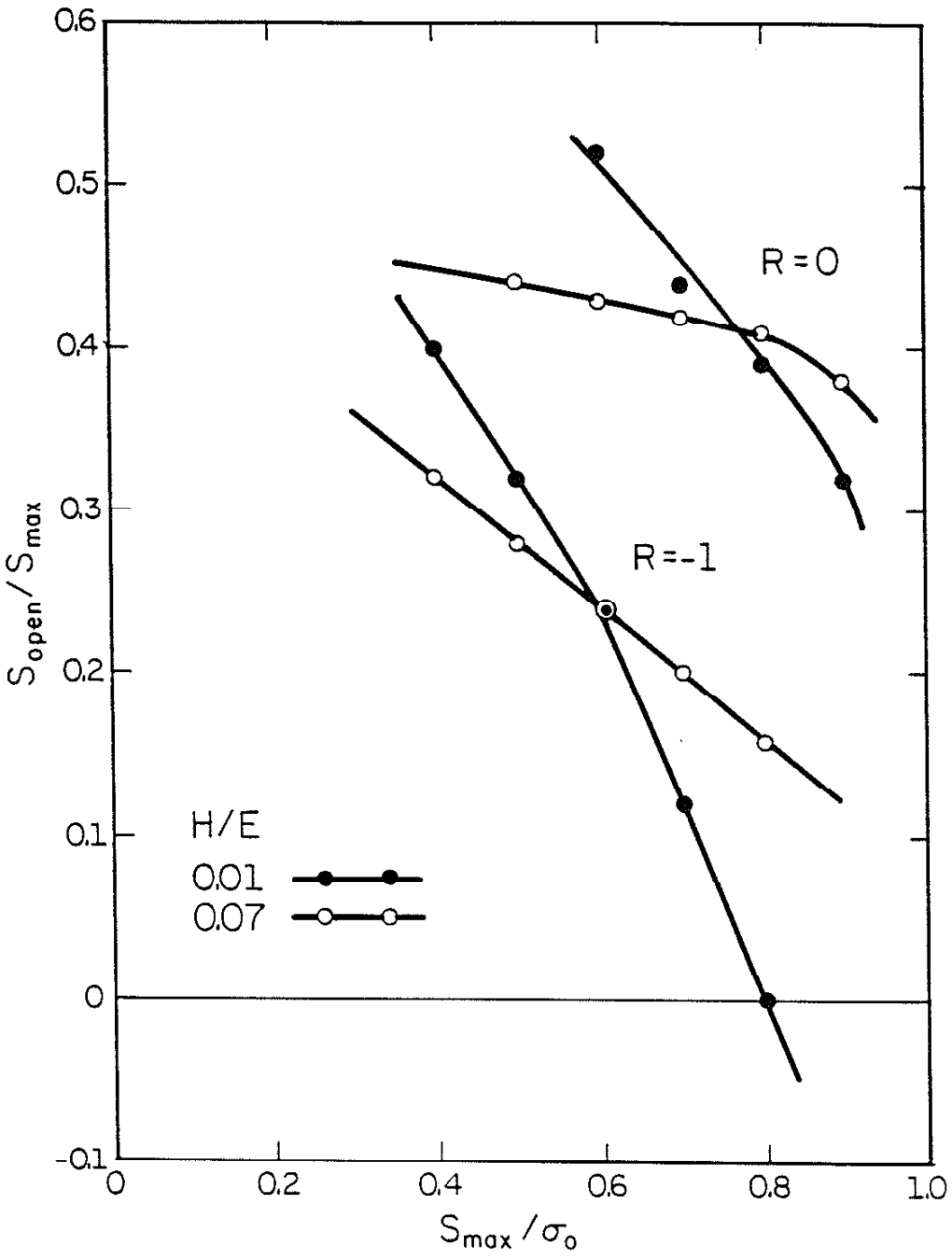

Figure 2.14 Normalized opening stresses as a function of maximum stress for different hardening moduli.

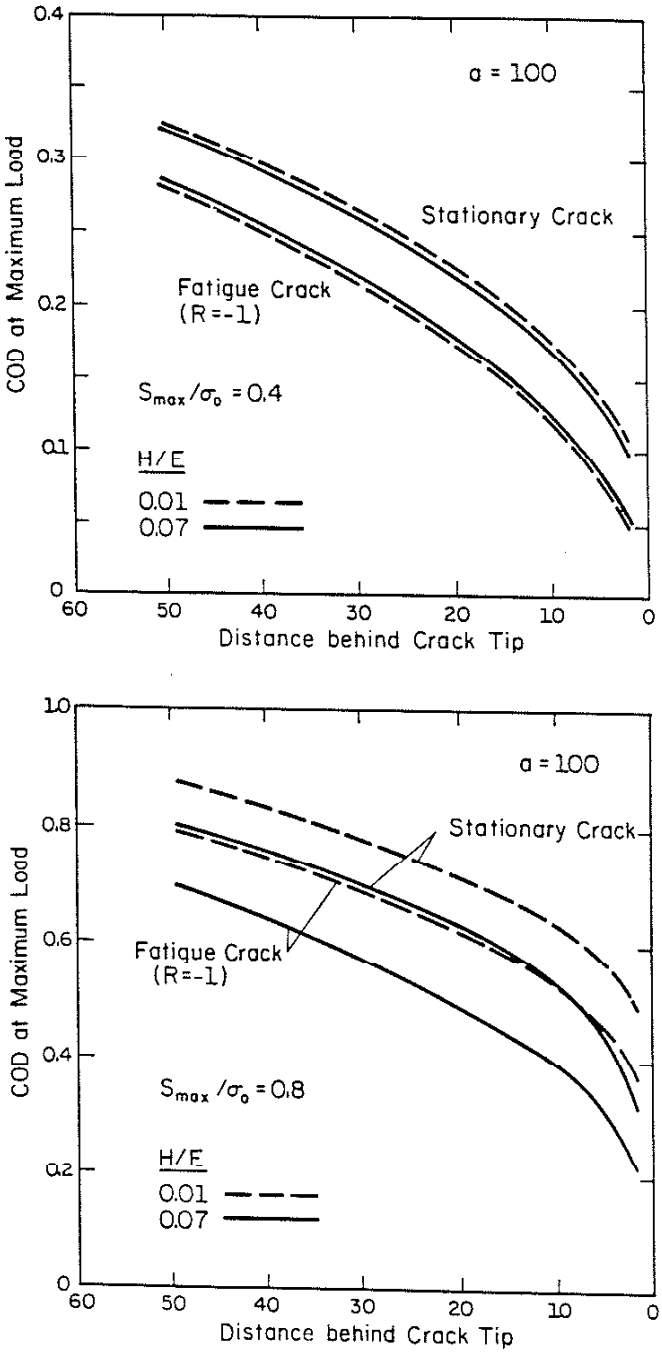

Figure 2.15 Crack opening displacements at maximum load for stationary and fatigue cracks (R = -1) with different hardening moduli.
(top) $S_{max}/\sigma_o = 0.4$ (bottom) $S_{max}/\sigma_o = 0.8$

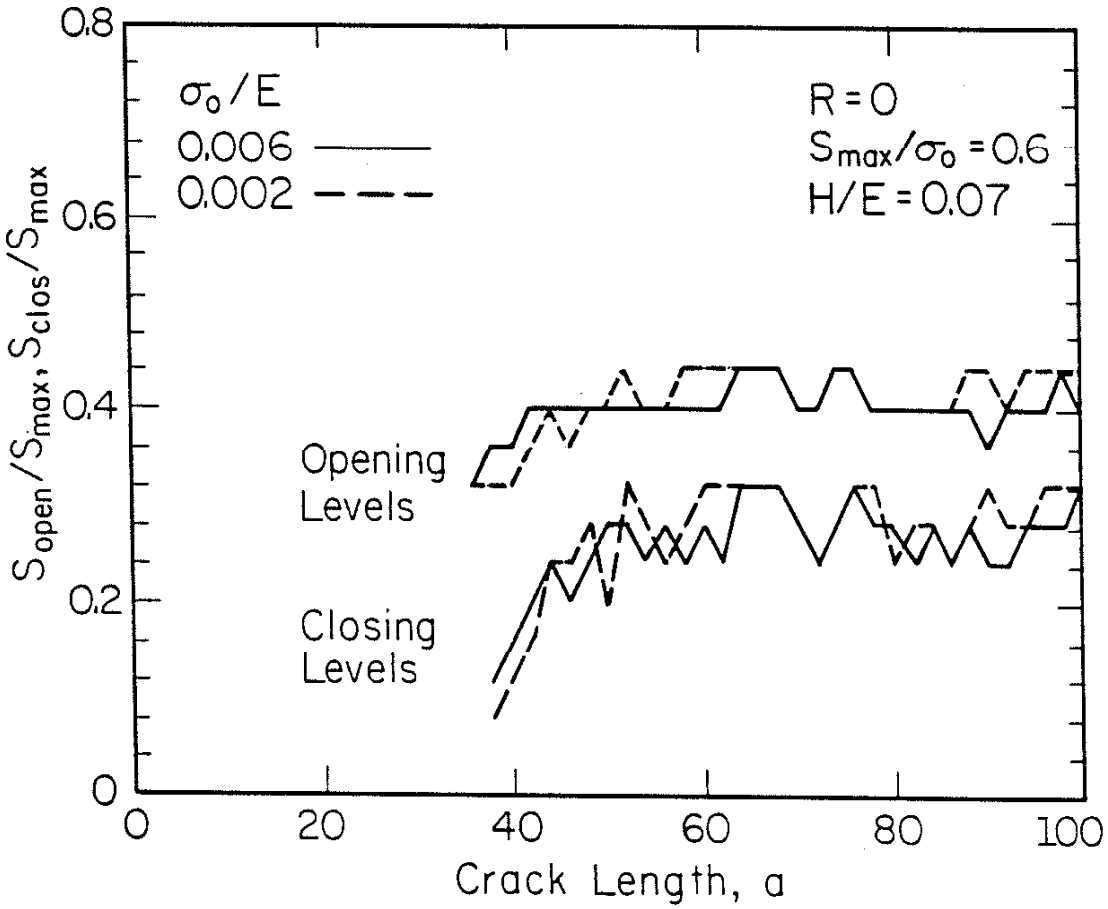

Figure 2.16 Opening and closing stresses for two different σ_o/E values.

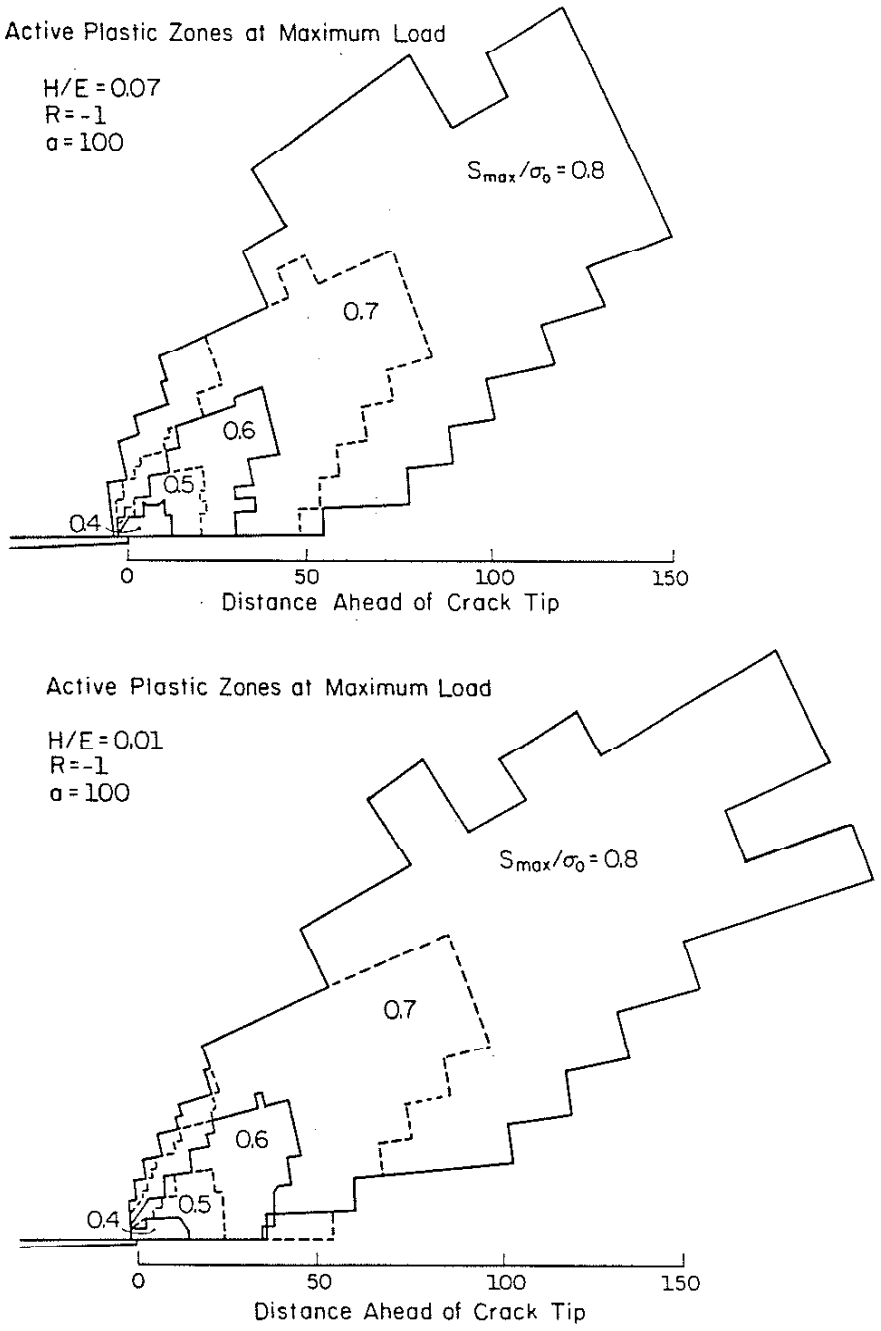

Figure 2.17 Active plastic zone shapes at maximum load for different maximum stresses.
(top) H/E = 0.07 (bottom) H/E = 0.01

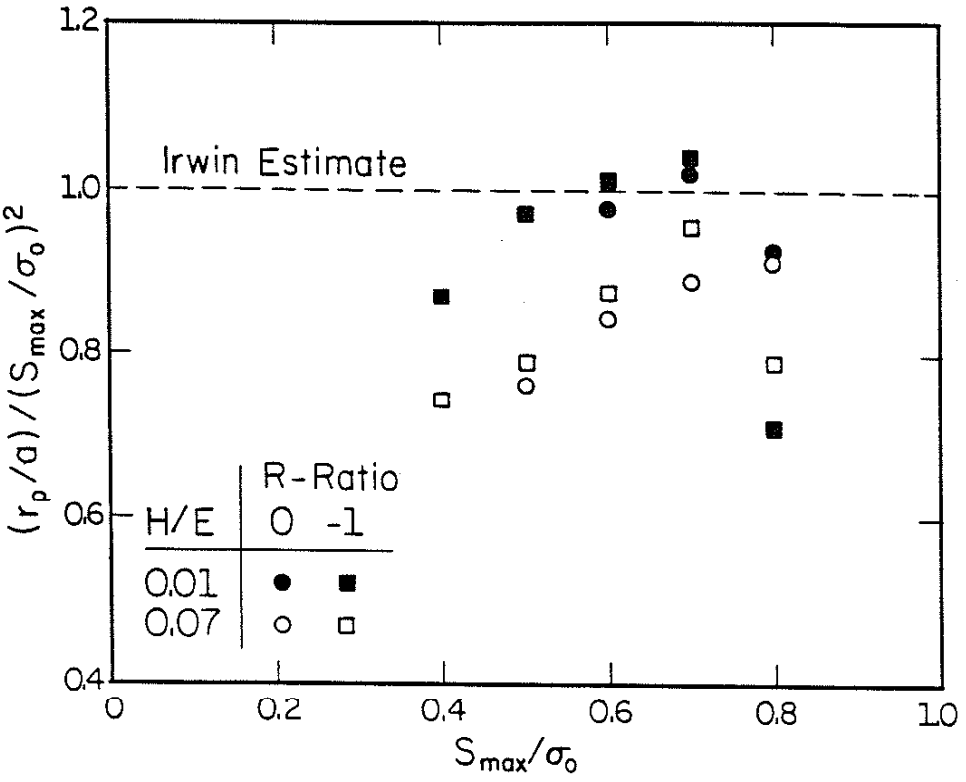

Figure 2.18 Normalized plastic zone widths for different maximum stresses, stress ratios, and hardening moduli.

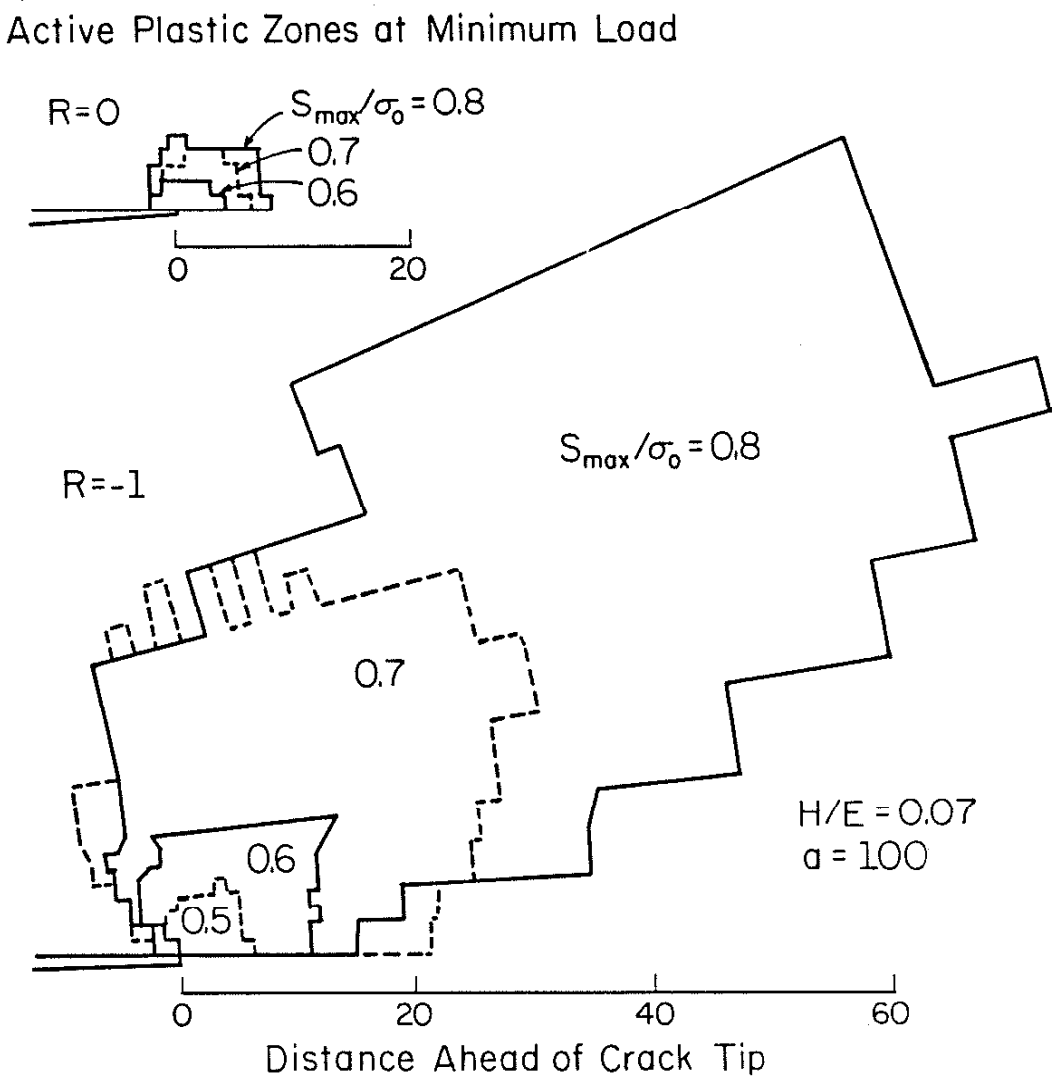

Figure 2.19 Active plastic zone shapes at minimum load for different maximum stresses and stress ratios.

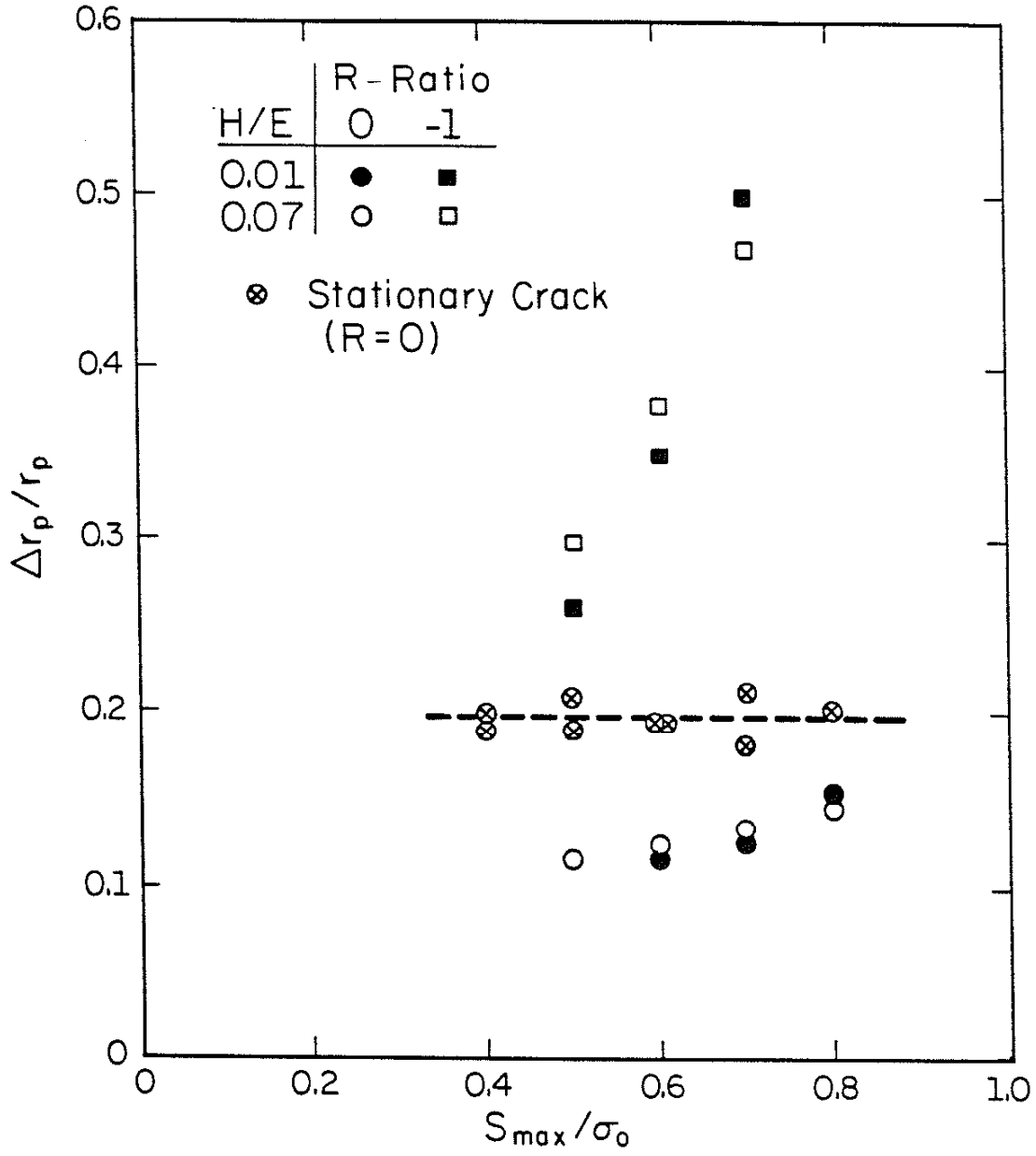

Figure 2.20 Ratio of reversed plastic zone width to forward plastic zone width for different maximum stresses, stress ratios, and hardening moduli, including both stationary and fatigue cracks.

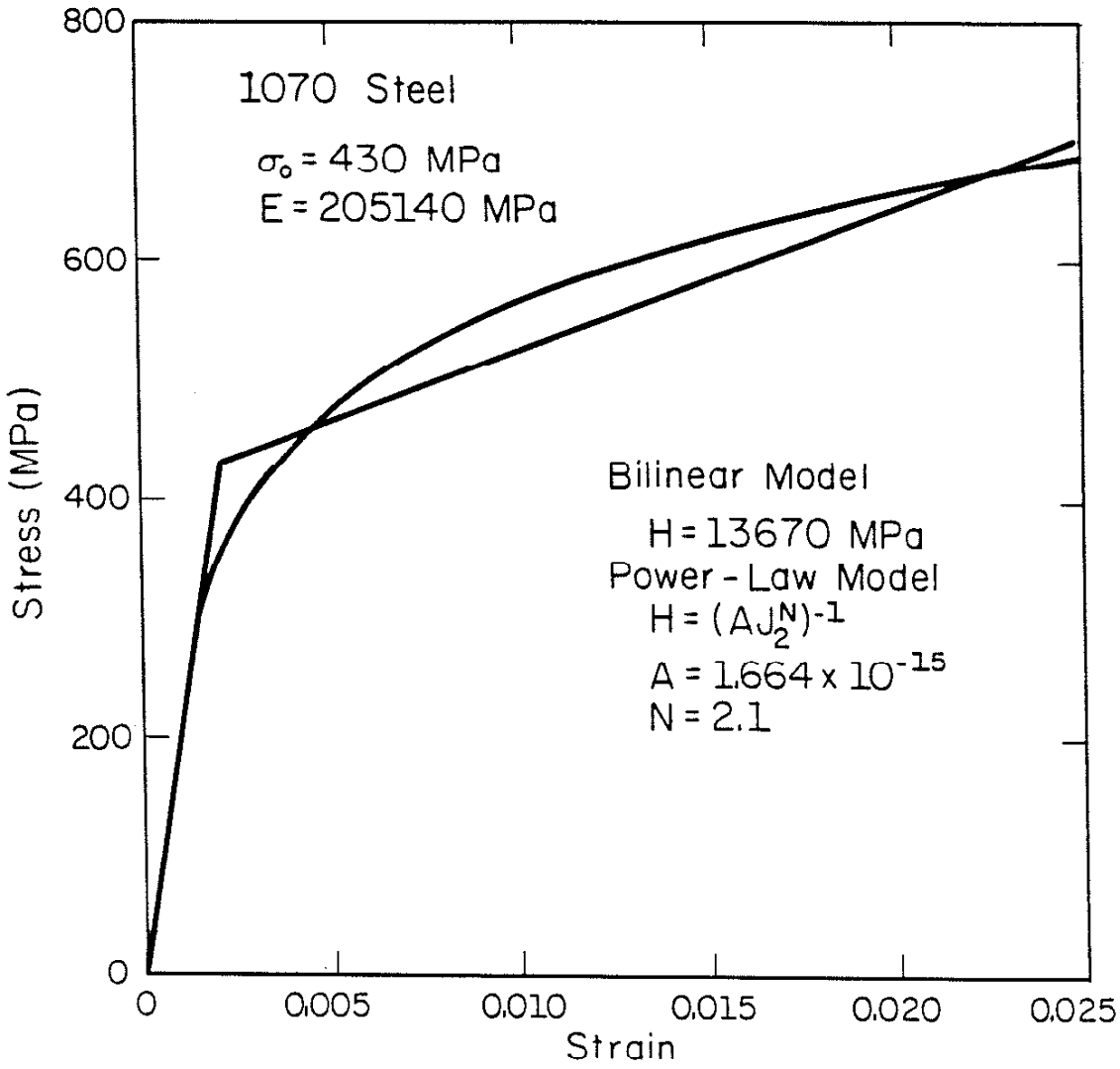

Figure 2.21 Two constitutive models for a 1070 steel.

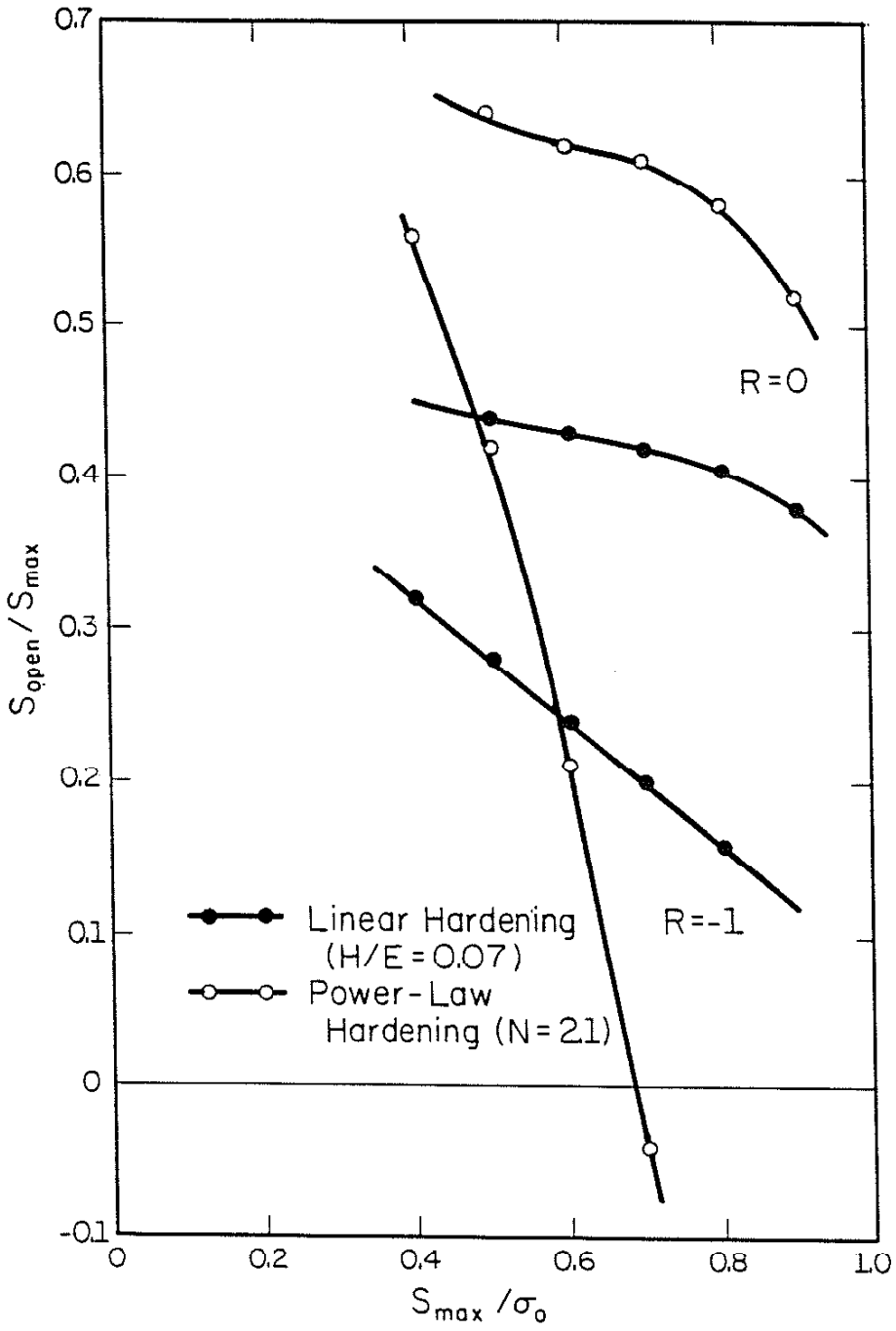

Figure 2.22 Normalized crack opening stresses as a function of maximum stress for two different constitutive models.

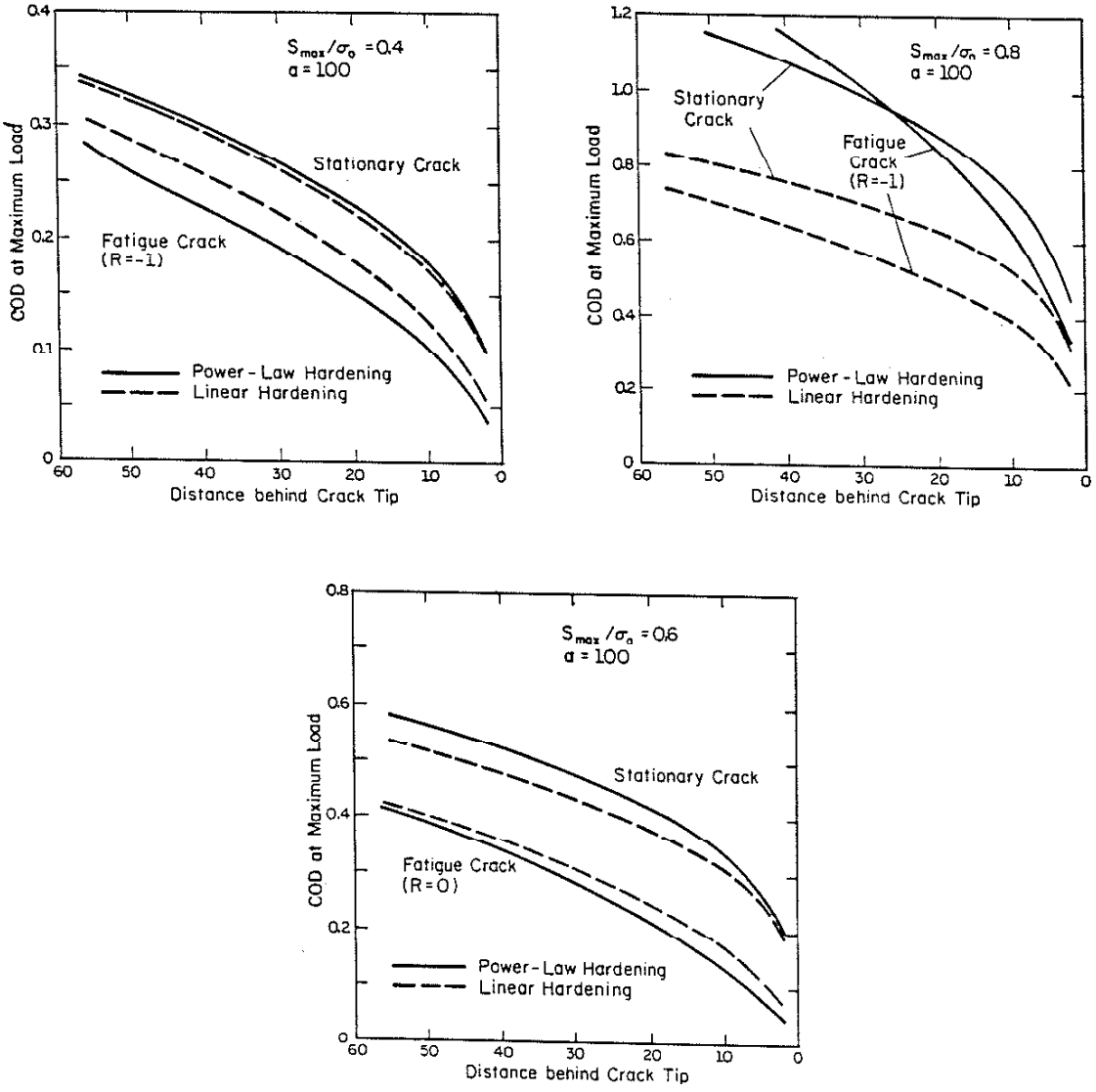

Figure 2.23 Crack opening displacements at maximum load for stationary and fatigue cracks with different constitutive models.
(bottom) R = 0, S_{max}/σ_o = 0.6
(upper left) R = -1, S_{max}/σ_o = 0.4
(upper right) R = -1, S_{max}/σ_o = 0.8

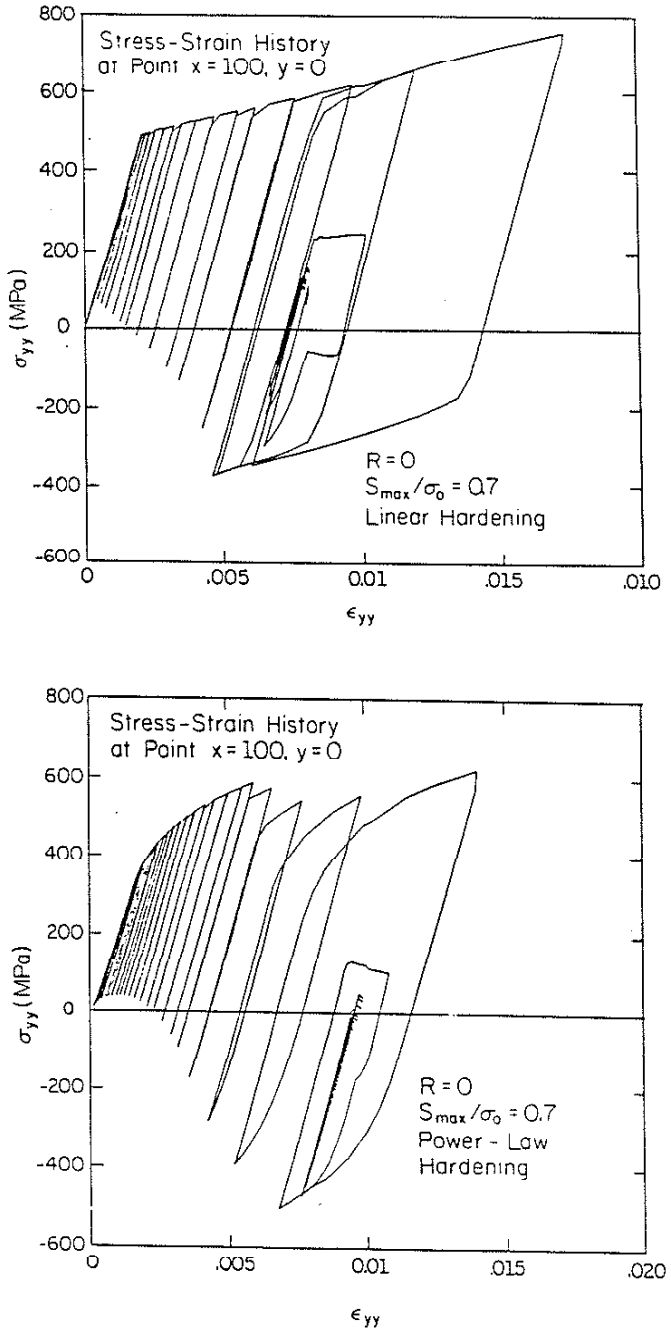

Figure 2.24 Stress-strain history at a point along the crack line as the crack tip approaches and passes.
(top) linear hardening model
(bottom) power-law hardening model

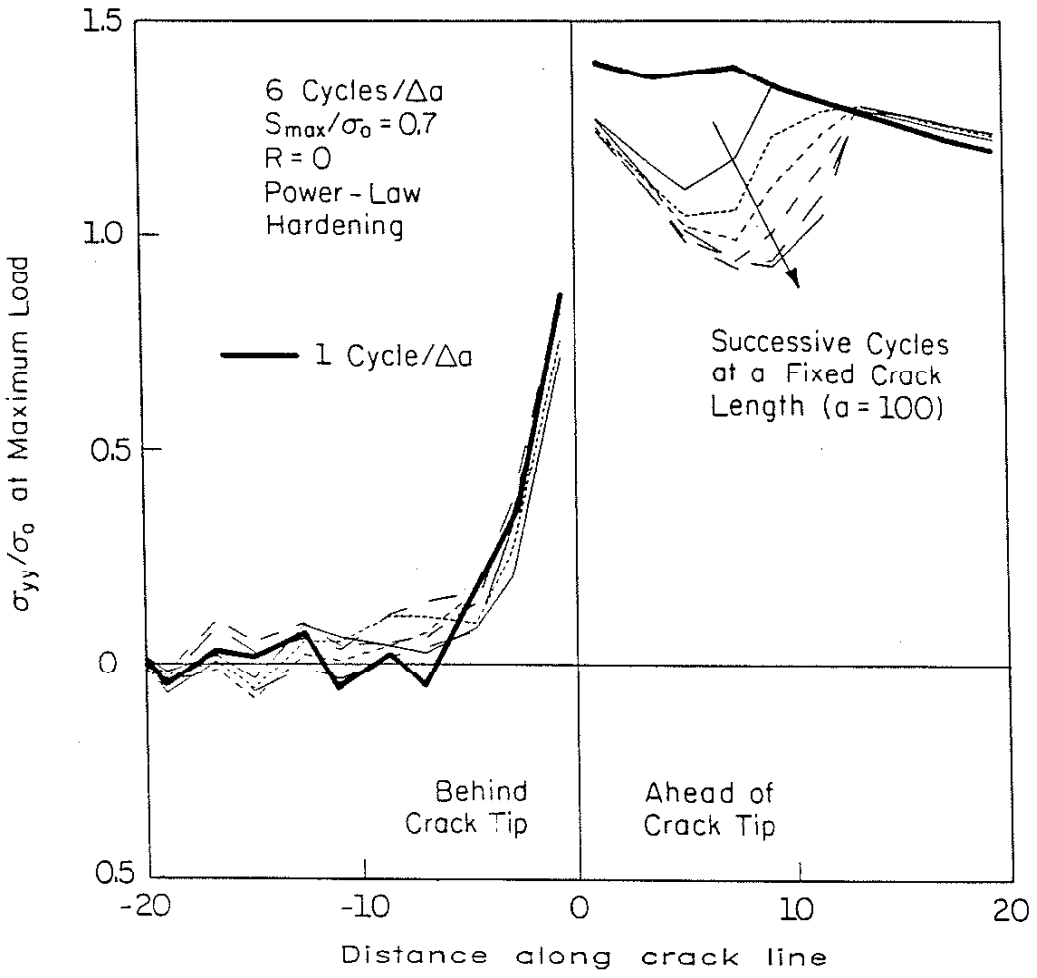

Figure 2.25 Stress distribution along the crack line at a single crack length, demonstrating mean stress relaxation with further cycling.

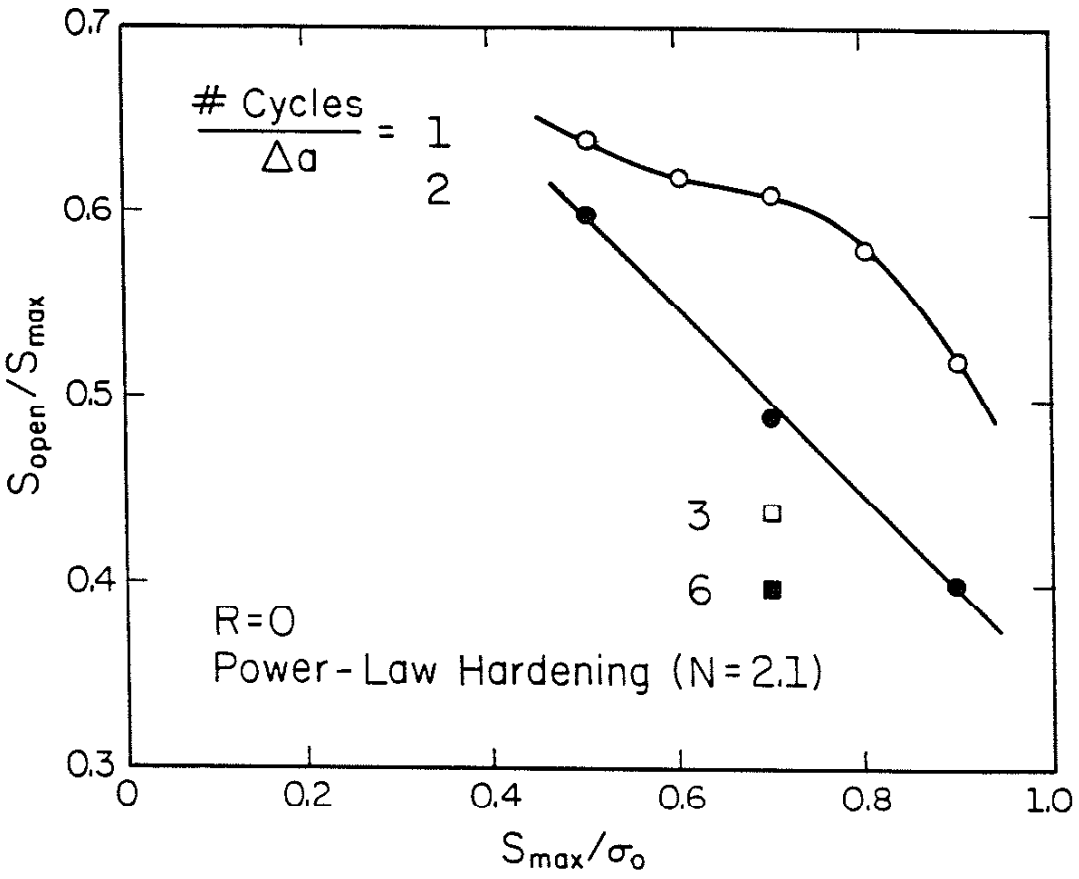

Figure 2.26 Normalized opening stresses corresponding to different crack advance rates with a power-law hardening model.

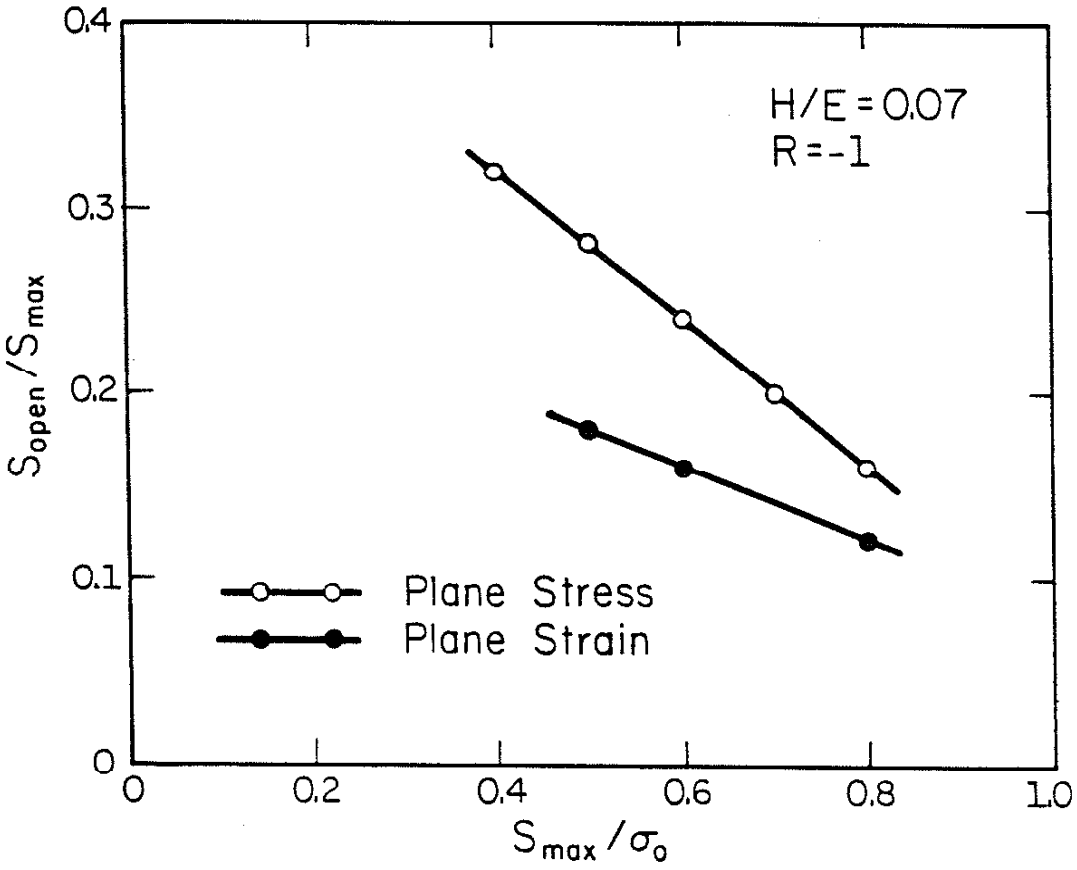

Figure 2.27 Normalized opening stresses as a function of maximum stress for plane stress and plane strain at R = -1.

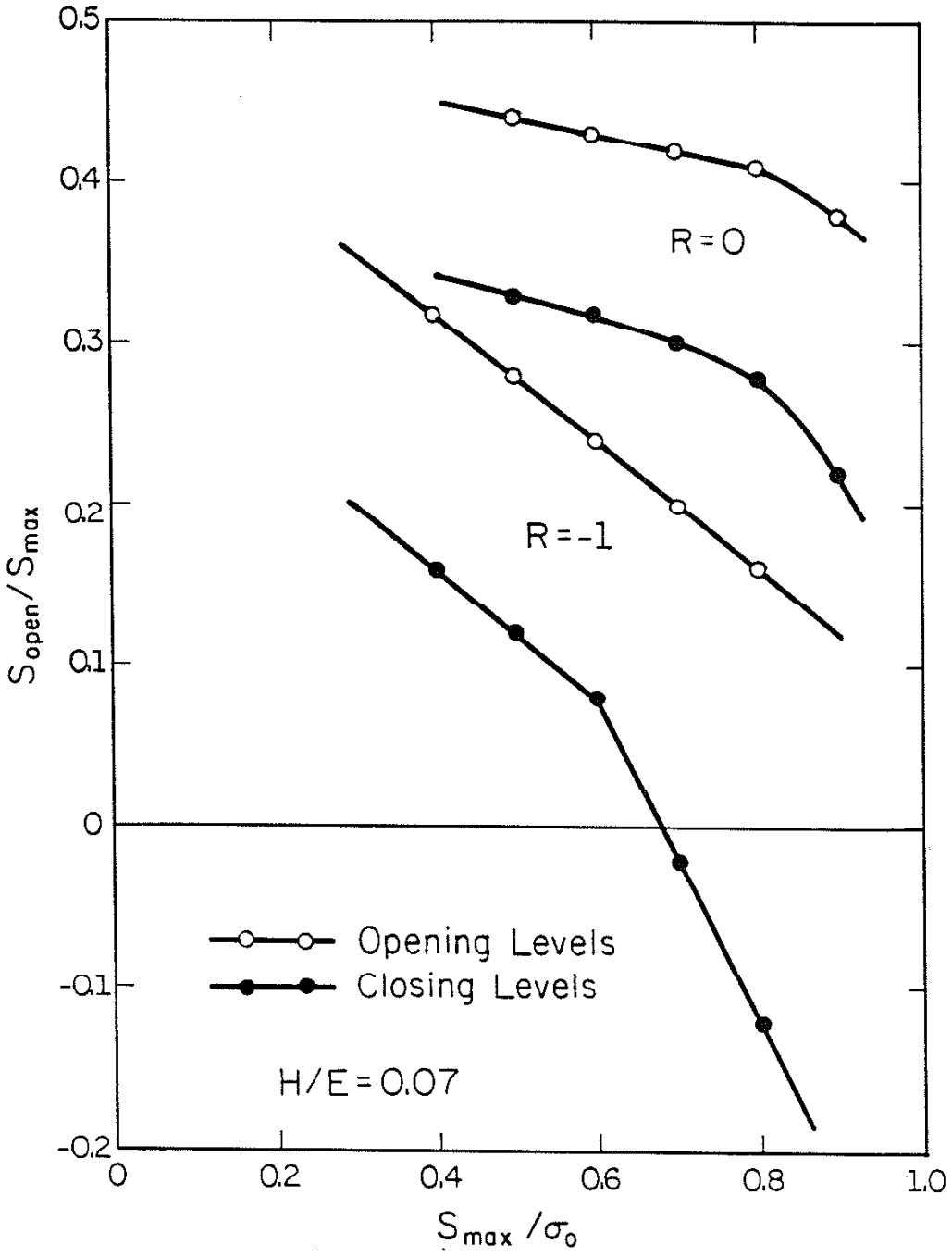

Figure 2.28 Comparison of crack opening stresses and crack closing stresses for different maximum stresses and stress ratios.

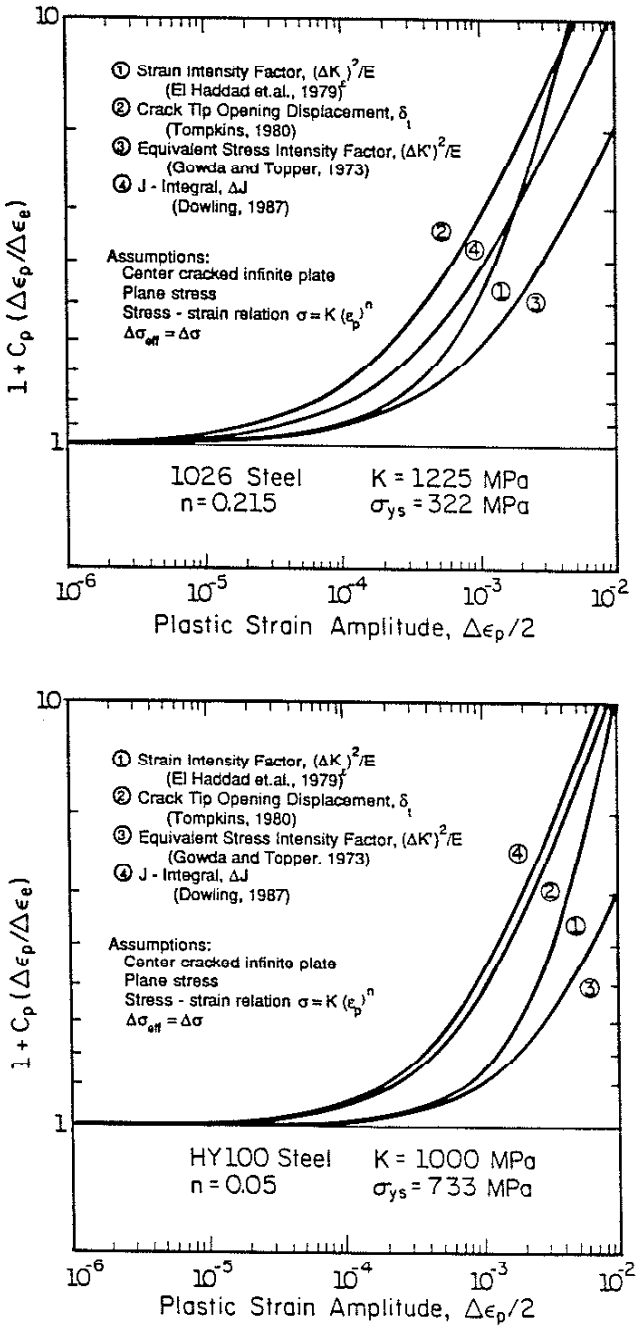

Figure 3.1 Comparisons of elastic-plastic fatigue crack growth parameters. (top) typical ductile steel (bottom) typical high-strength steel

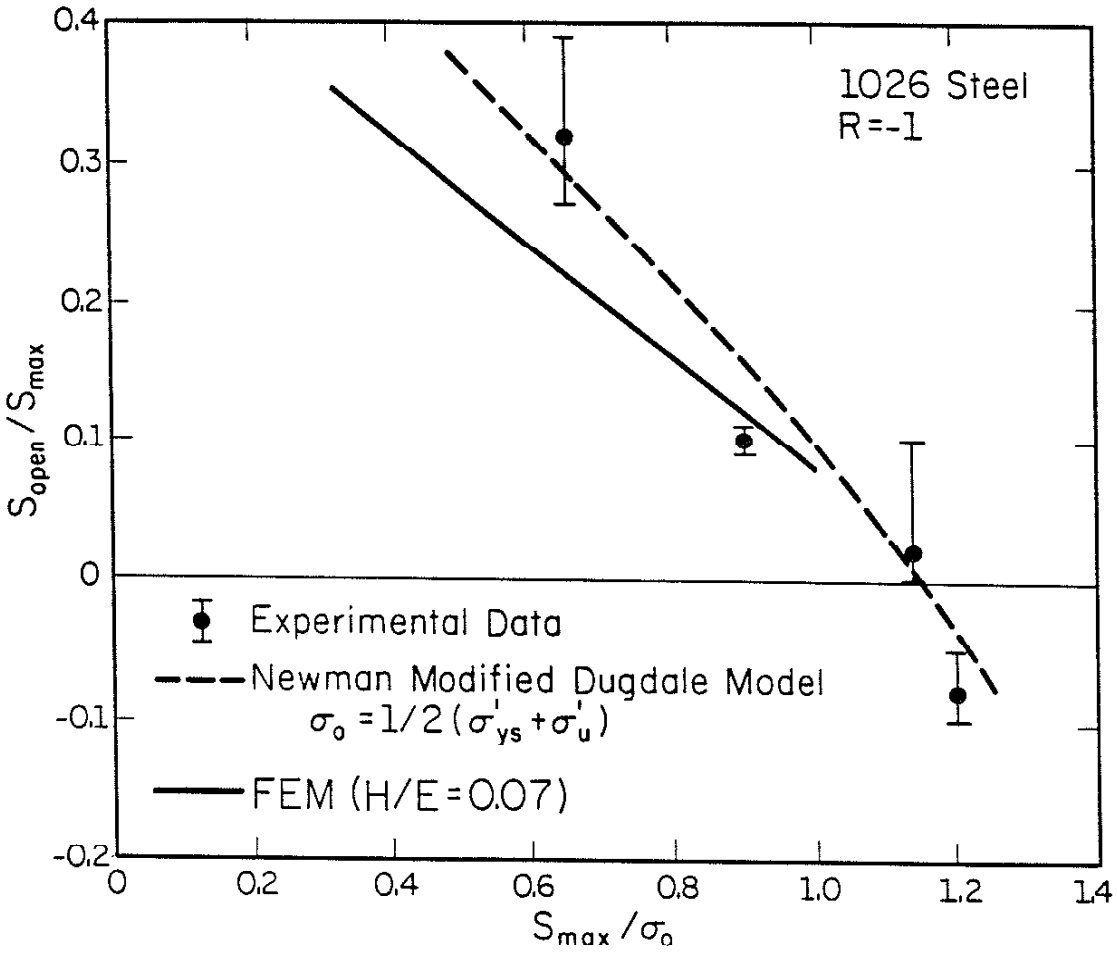

Figure 3.2 Experimental data and estimates based on two numerical models for crack opening stresses during low cycle fatigue in a 1026 steel.

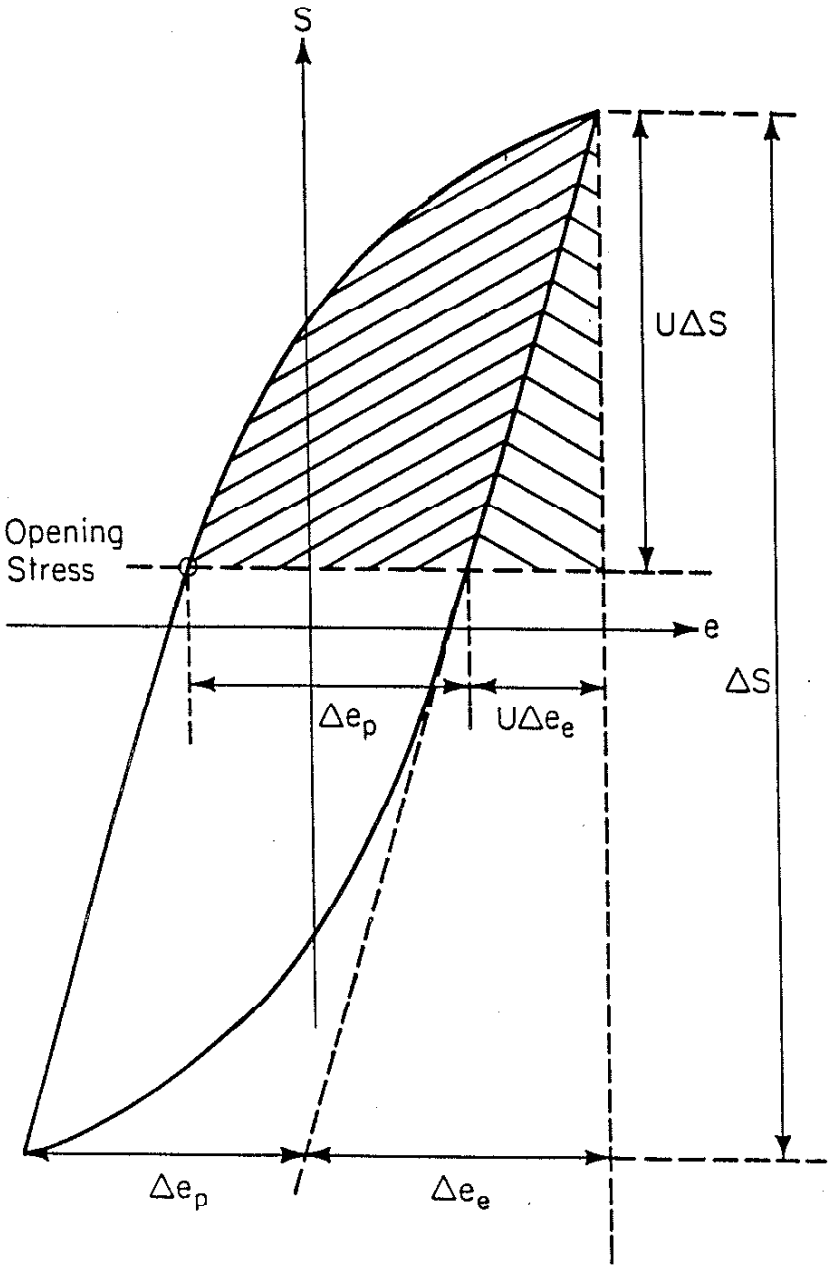

Figure 3.3 Schematic representation of hysteresis loop showing opening stress level and corresponding estimates of effective stress and strain ranges.

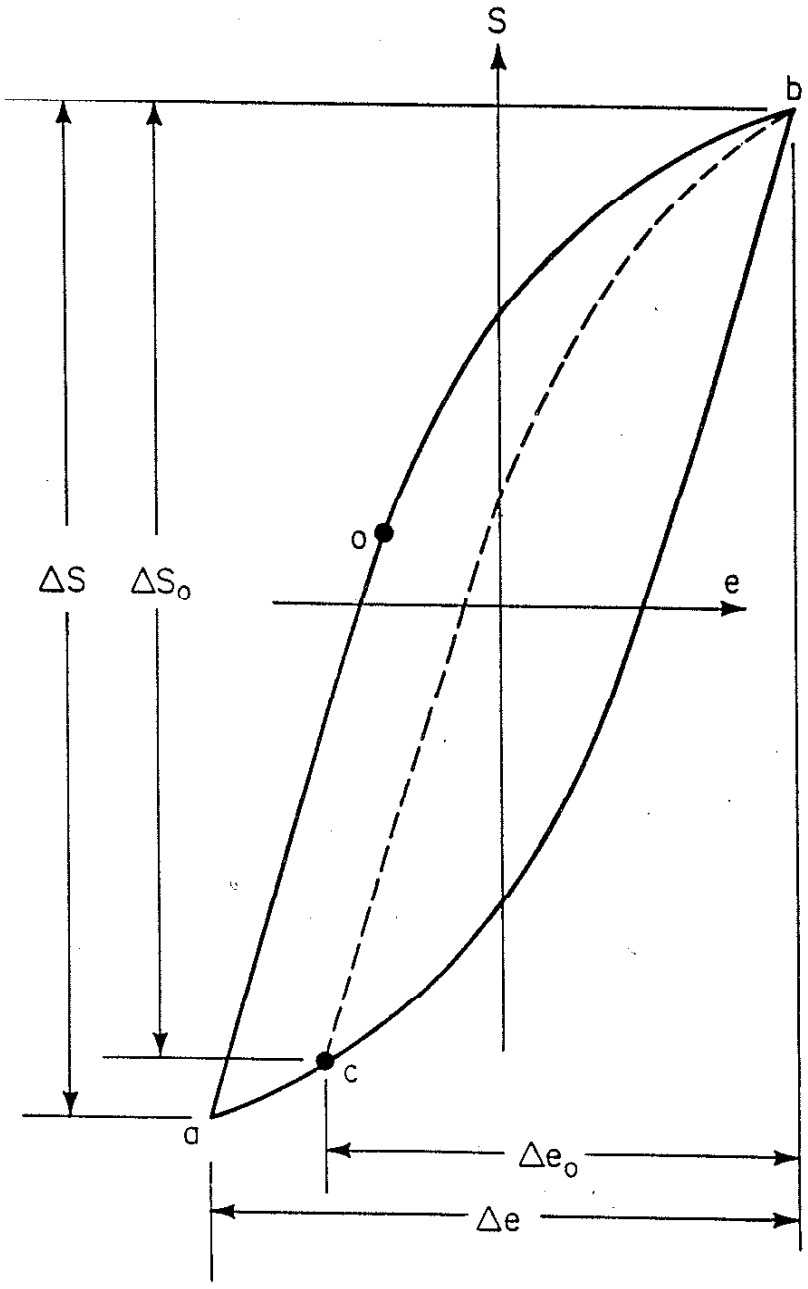

Figure 3.4 Schematic representation of hysteresis loop showing alternate scheme for estimating effective stress and strain ranges, as proposed by Dowling [110].

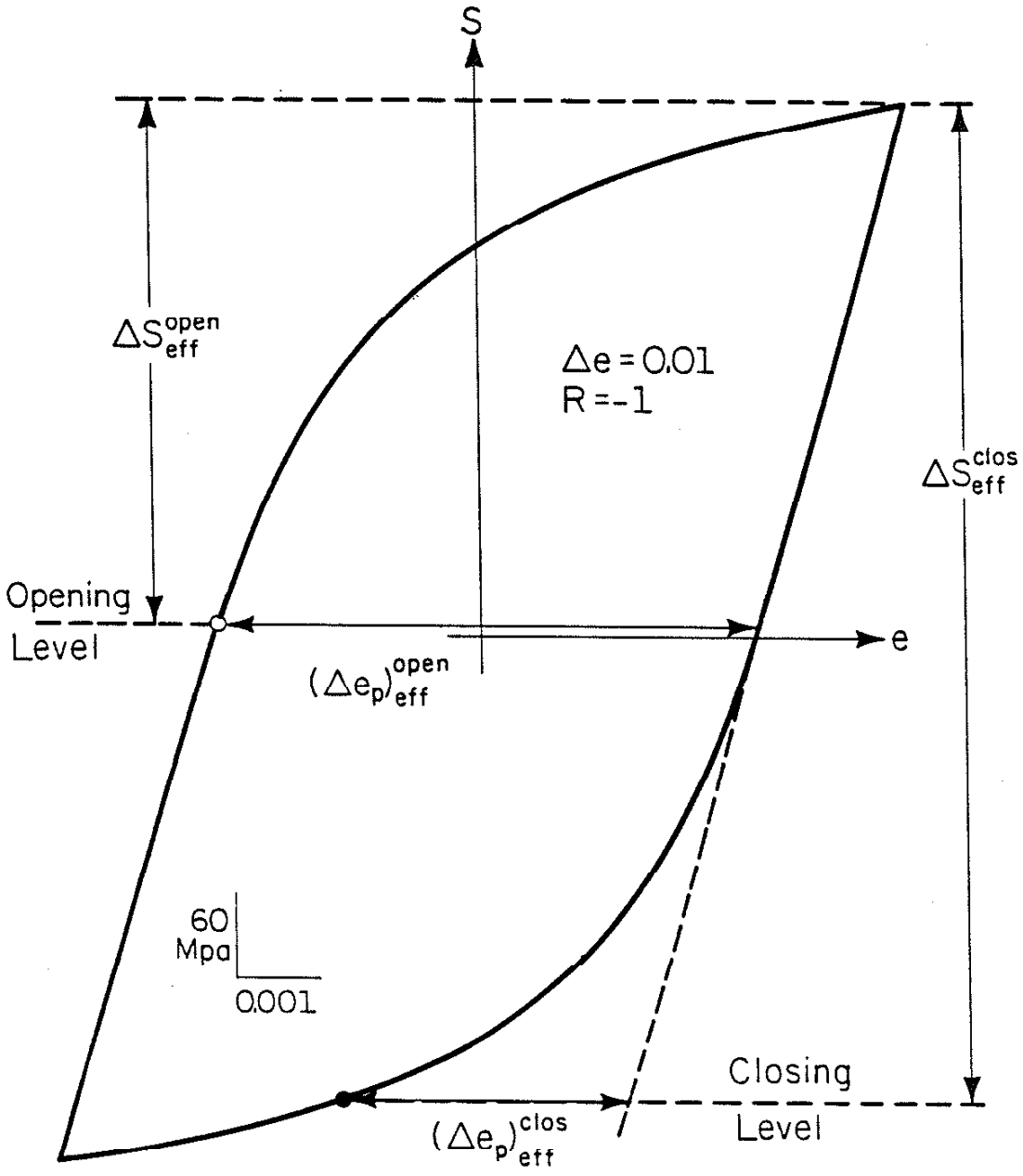

Figure 3.5 Hysteresis loop for 1026 steel, $\Delta\varepsilon = .01$, demonstrating probable equivalence of two schemes for estimating effective stress and strain ranges.

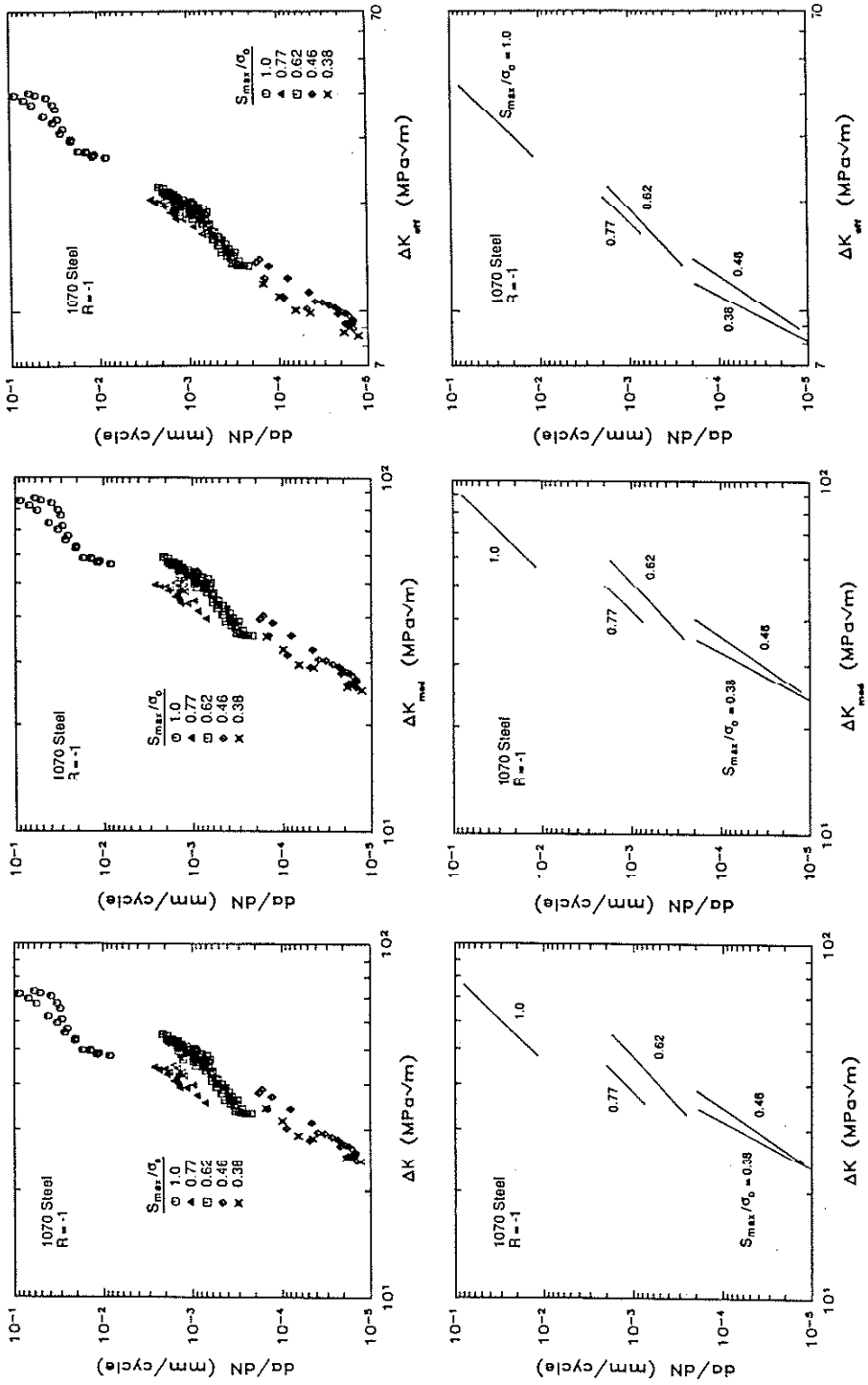

Figure 3.6 Crack growth rates at different maximum stresses (R = -1) in a 1070 steel, showing both individual data points and regression lines for each data set.
(left) correlated with simple ΔK
(middle) correlated with ΔK based on plasticity-modified crack lengths
(right) correlated with ΔK_{eff} based on plasticity-modified crack lengths and opening stresses determined from FEM results

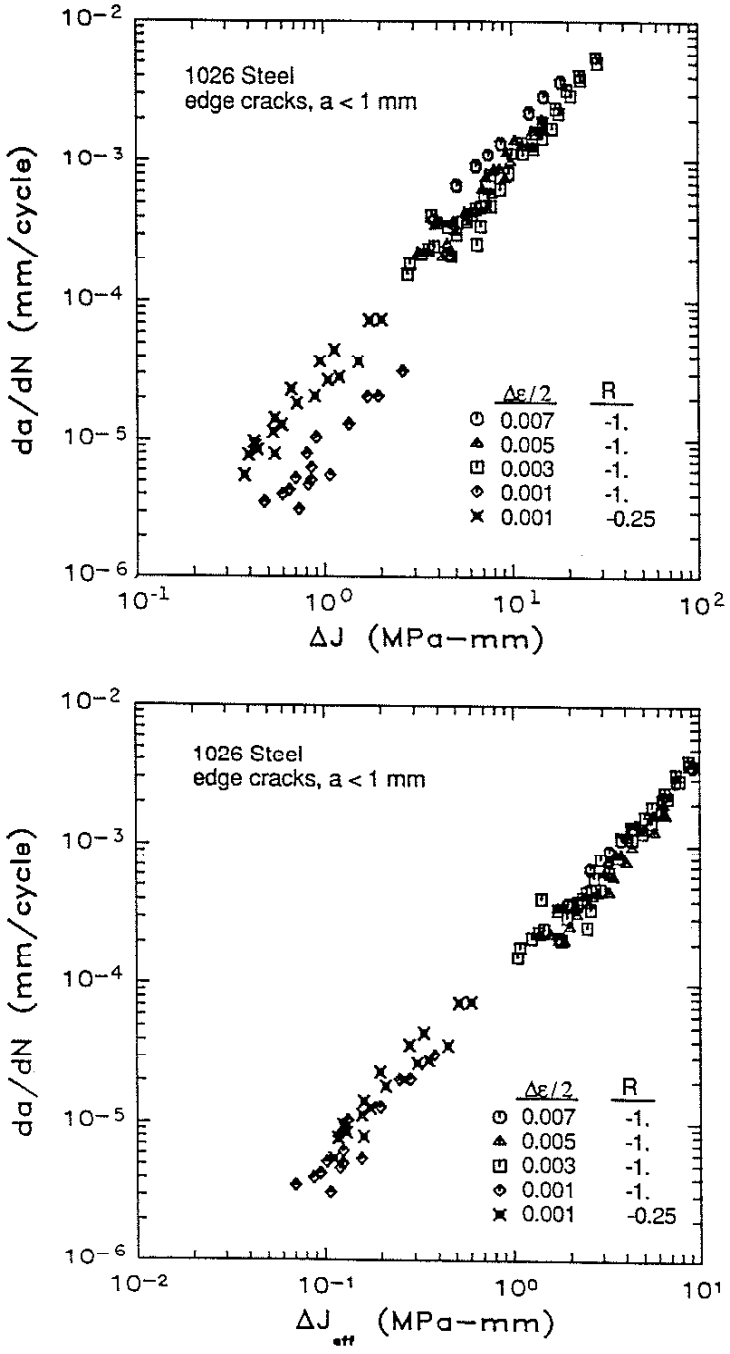

Figure 3.7 Growth rates for small cracks during low cycle fatigue in a 1026 steel.
(top) correlated with ΔJ
(bottom) correlated with ΔJ_{eff} based on experimentally measured opening stresses

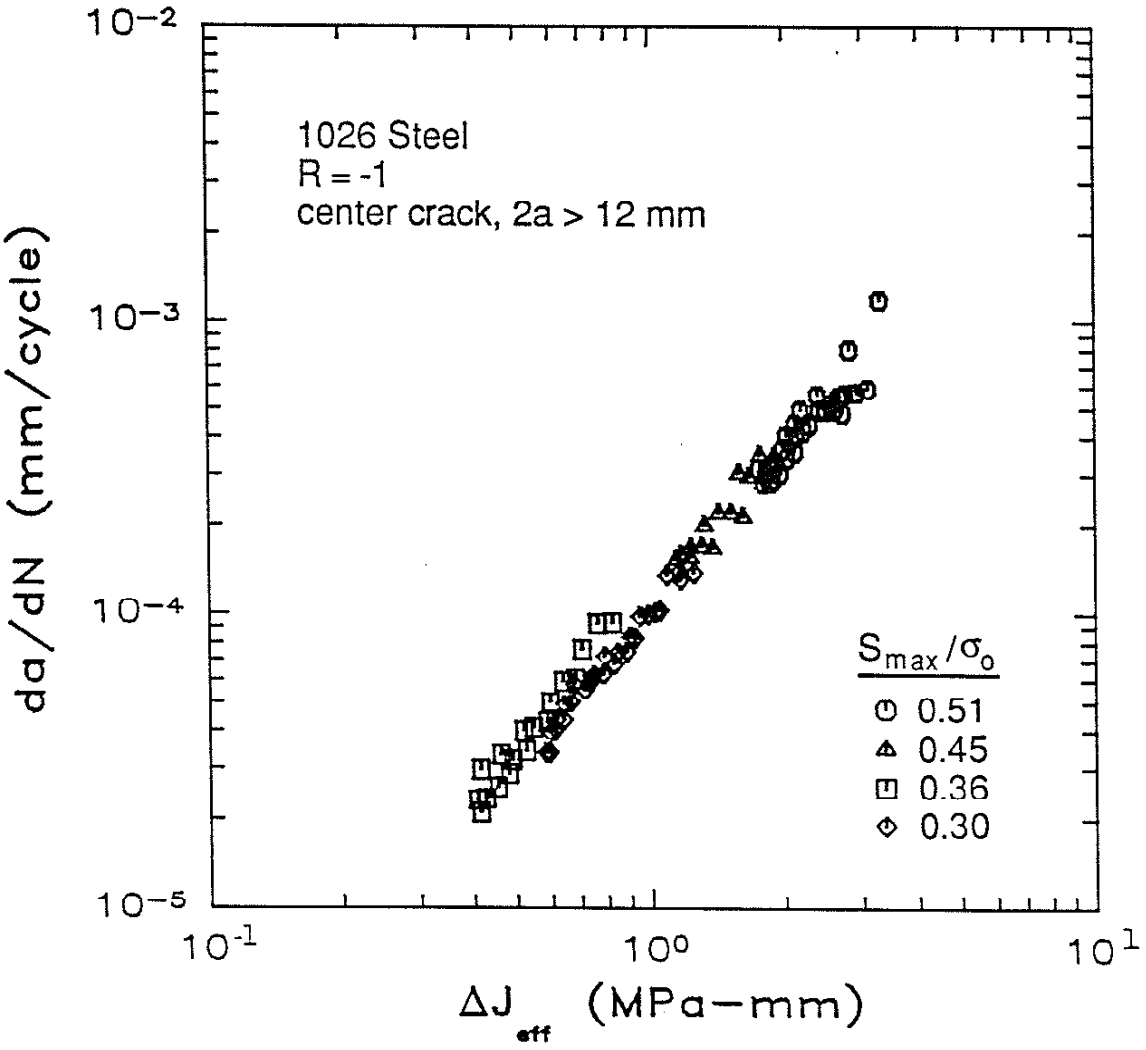

Figure 3.8 Growth rates for moderately long cracks during intermediate scale yielding in a 1026 steel, correlated with ΔJ_{eff}.

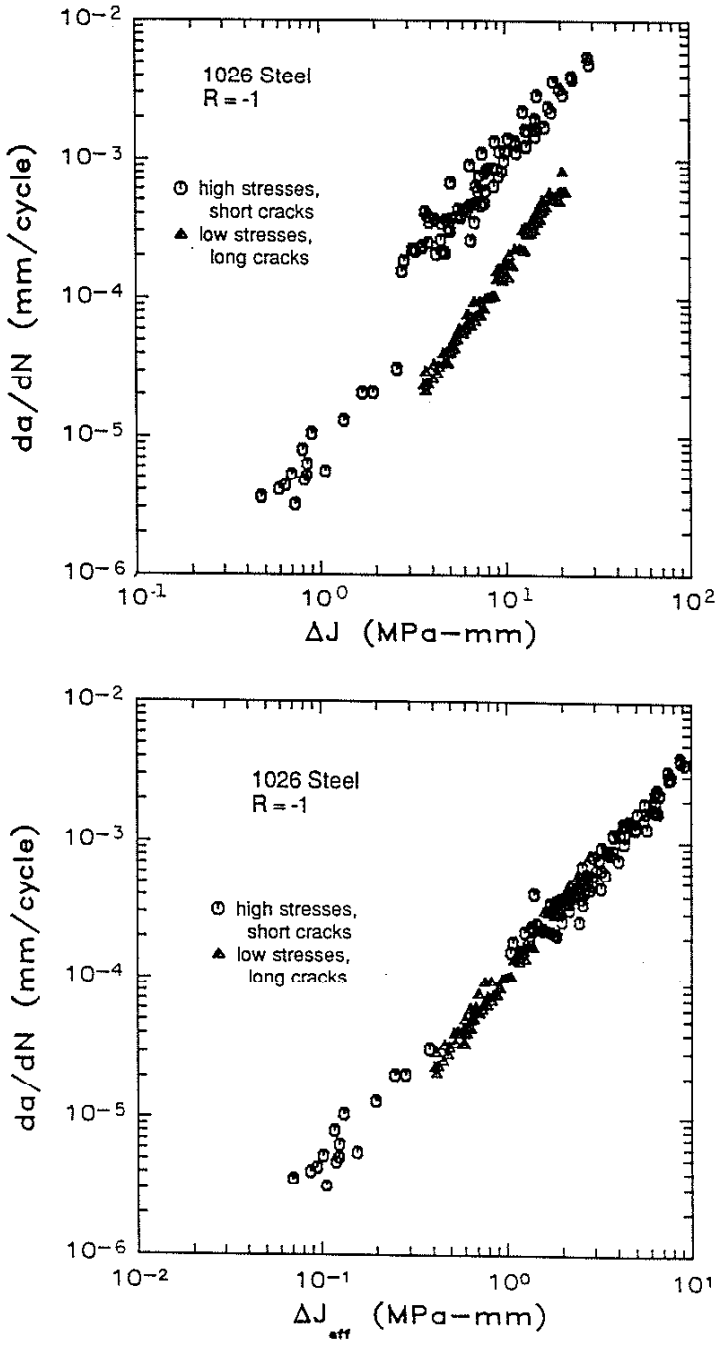

Figure 3.9 Crack growth rates at a wide range of maximum stresses and crack lengths in a 1026 steel.
(top) correlated with ΔJ
(bottom) correlated with ΔJ_{eff}

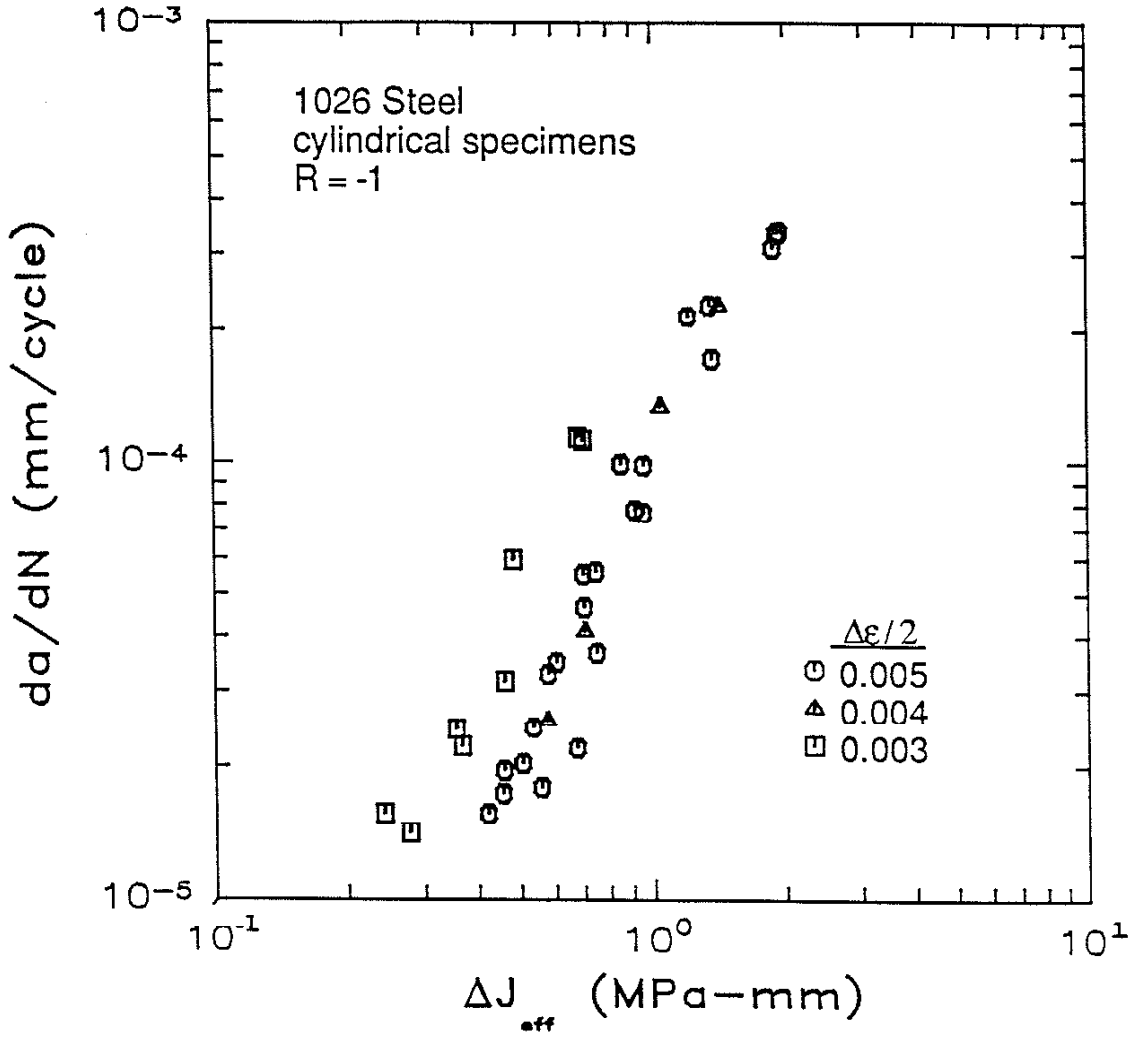

Figure 3.10 Crack growth rates at different maximum stresses (R = -1) during low cycle fatigue of smooth, cylindrical specimens of a 1026 steel, as correlated by ΔJ_{eff}.

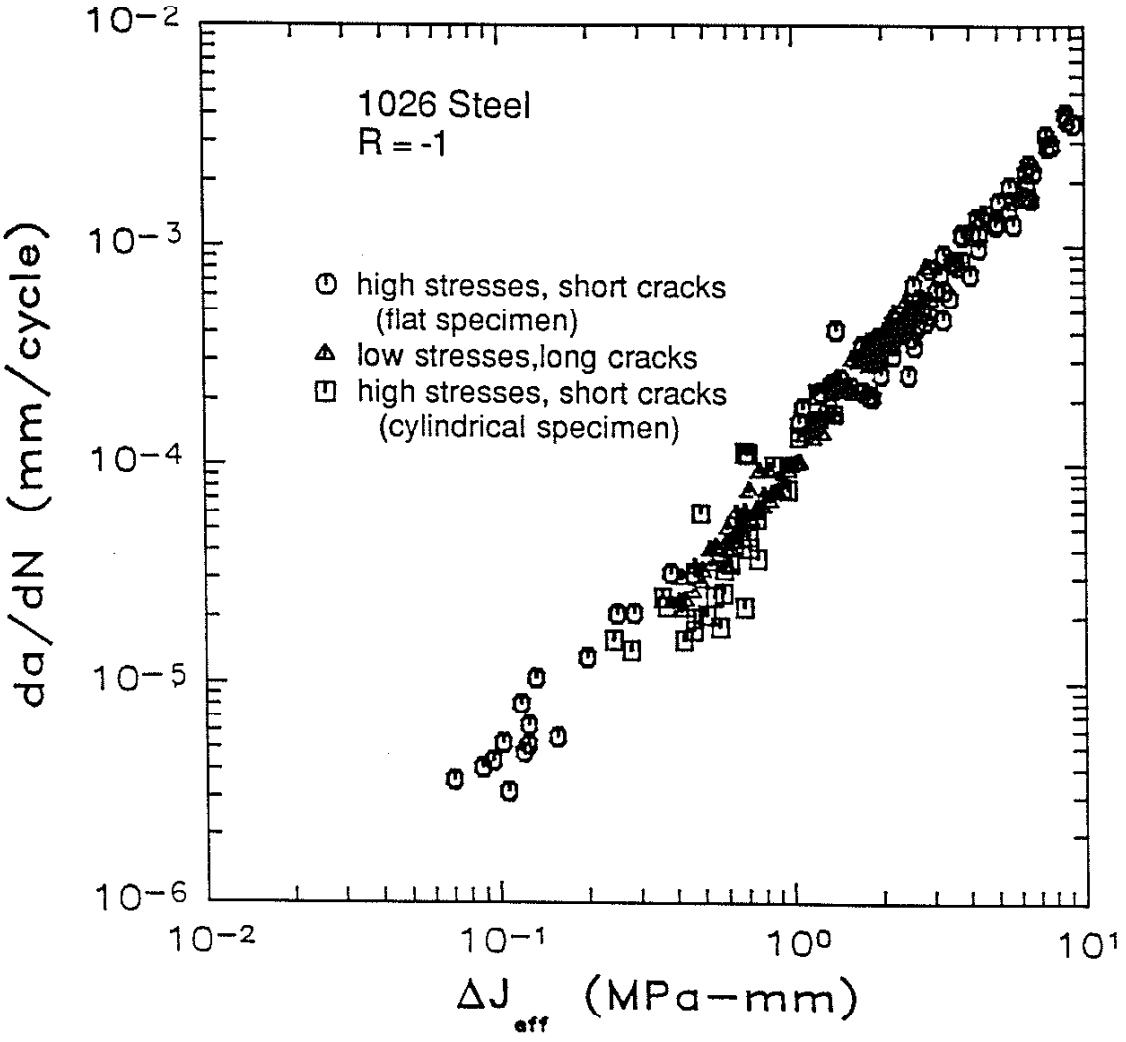

Figure 3.11 Crack growth rates for different maximum stresses (R = -1), crack lengths, and specimen geometries in a 1026 steel, as correlated by ΔJ_{eff}.

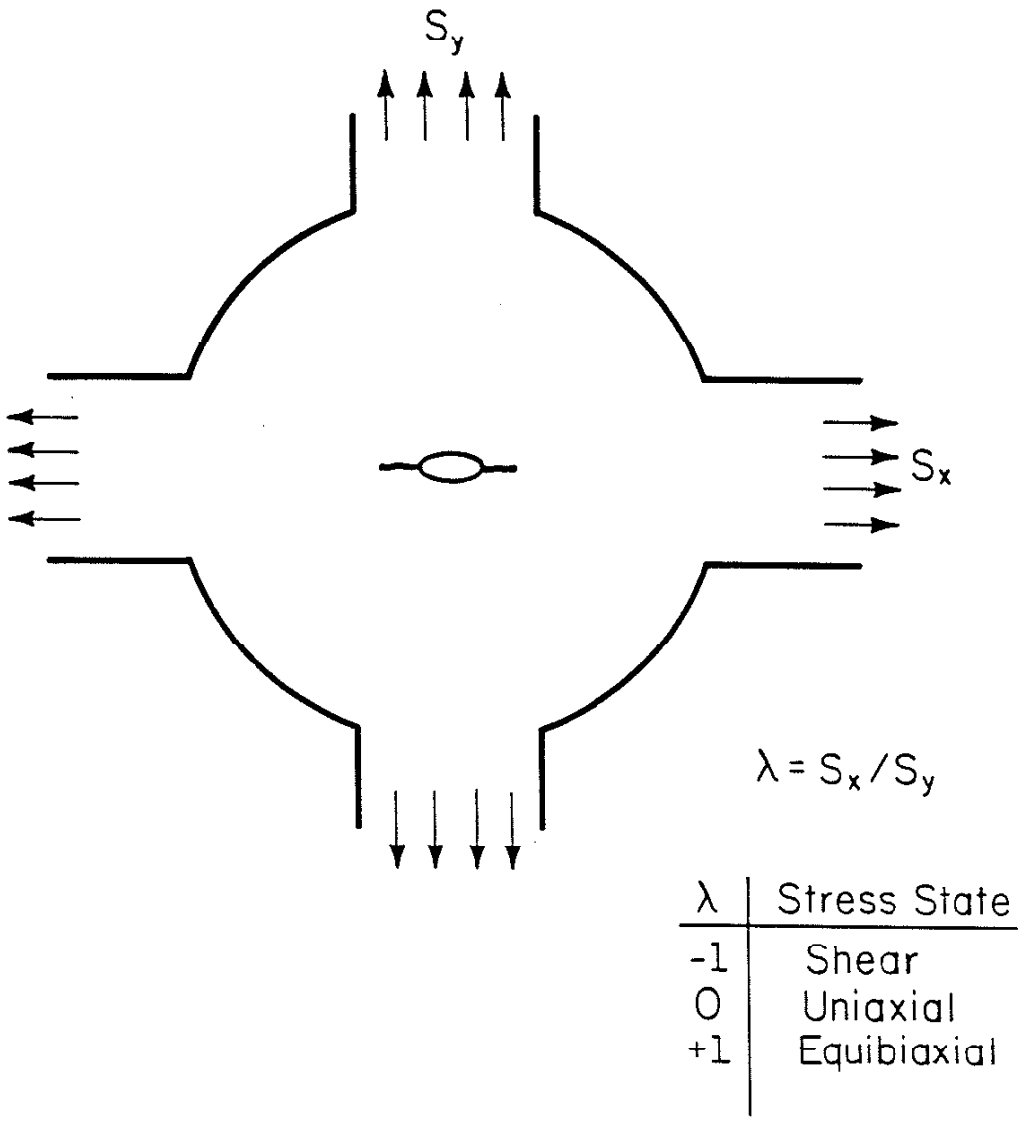

Figure 4.1 Schematic representation of a cruciform specimen for biaxial fatigue testing with associated nomenclature.

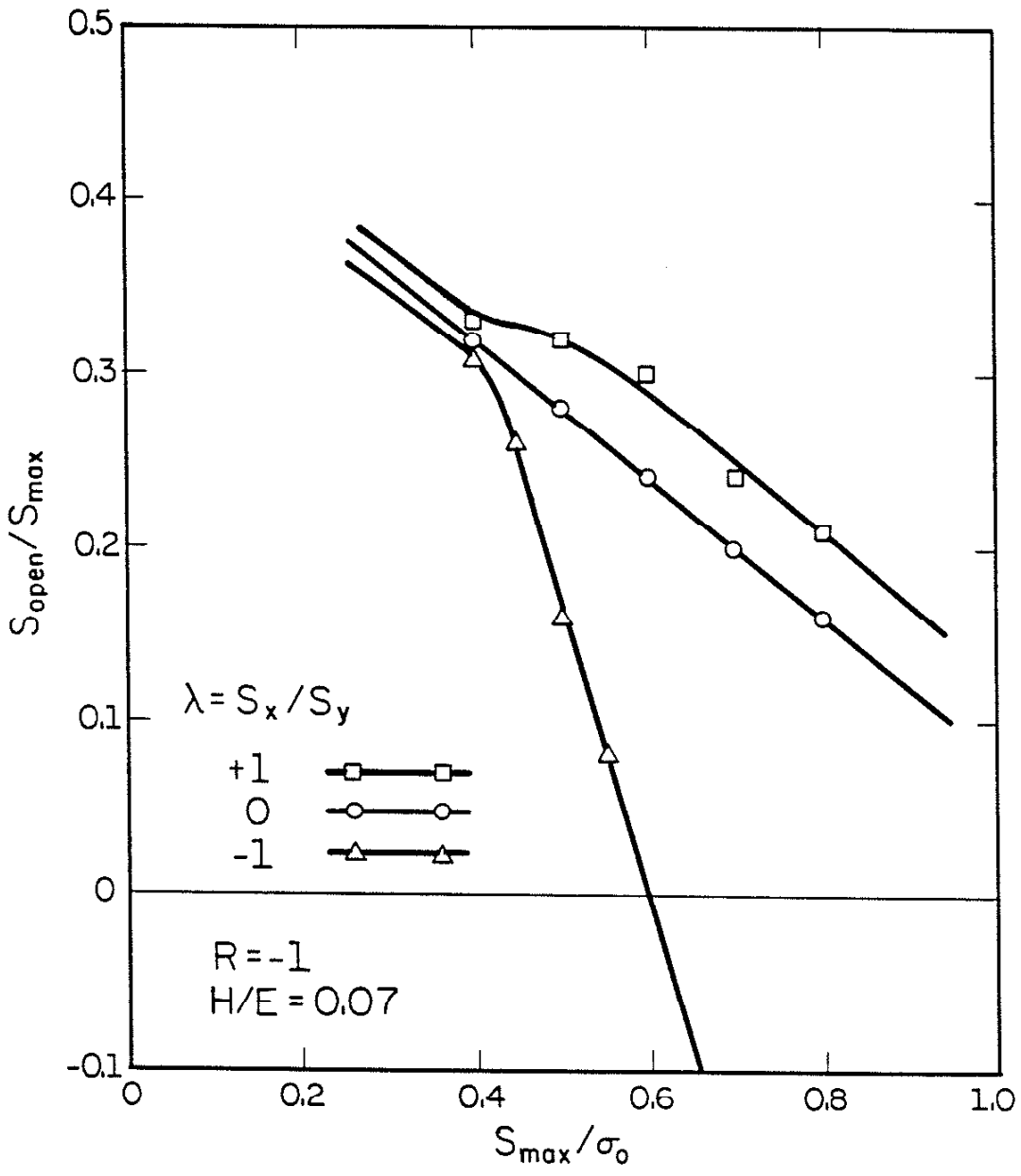

Figure 4.2 Normalized crack opening stresses as a function of maximum stress for three different biaxiality ratios.

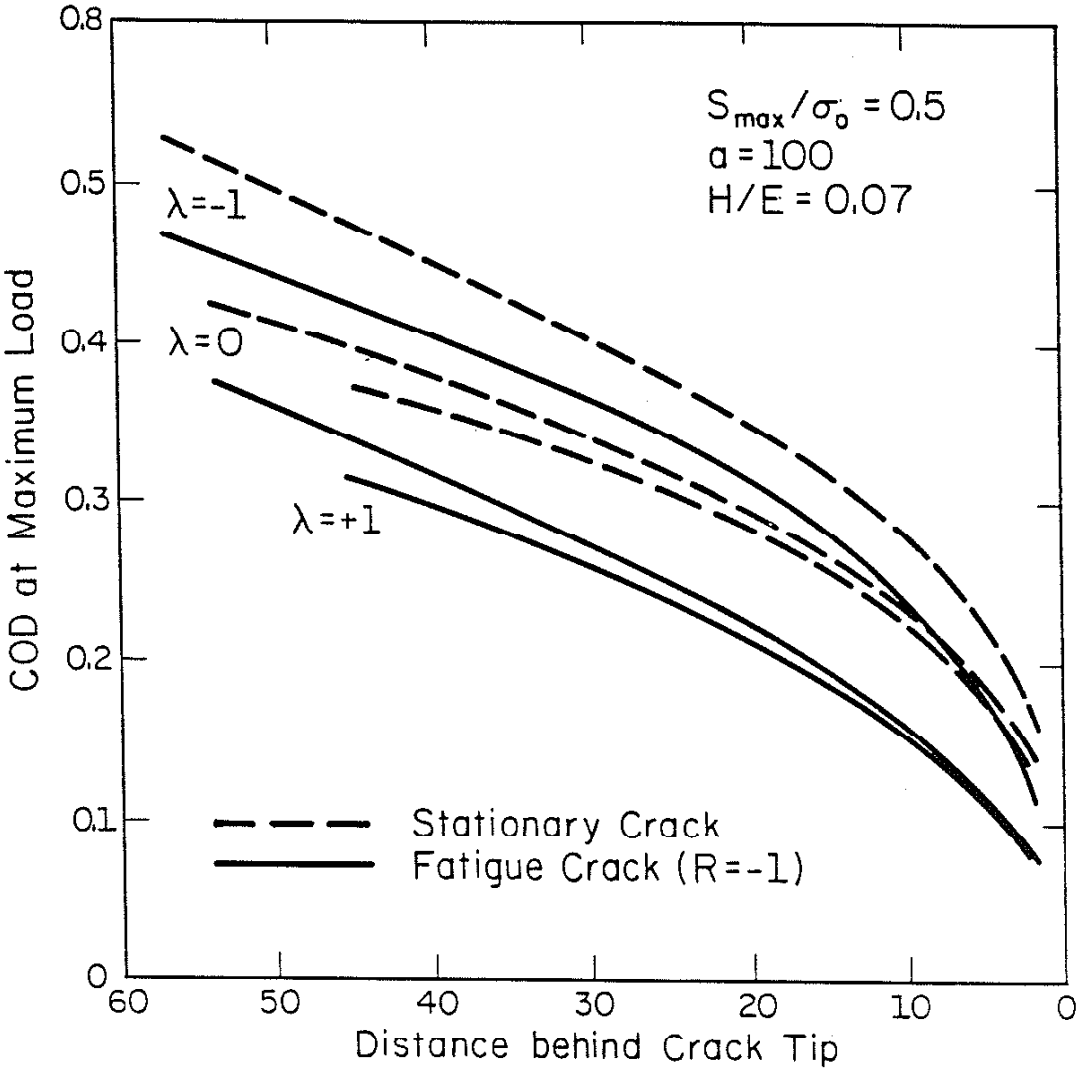

Figure 4.3 Crack opening displacements at maximum load for stationary and fatigue cracks at three different biaxiality ratios.

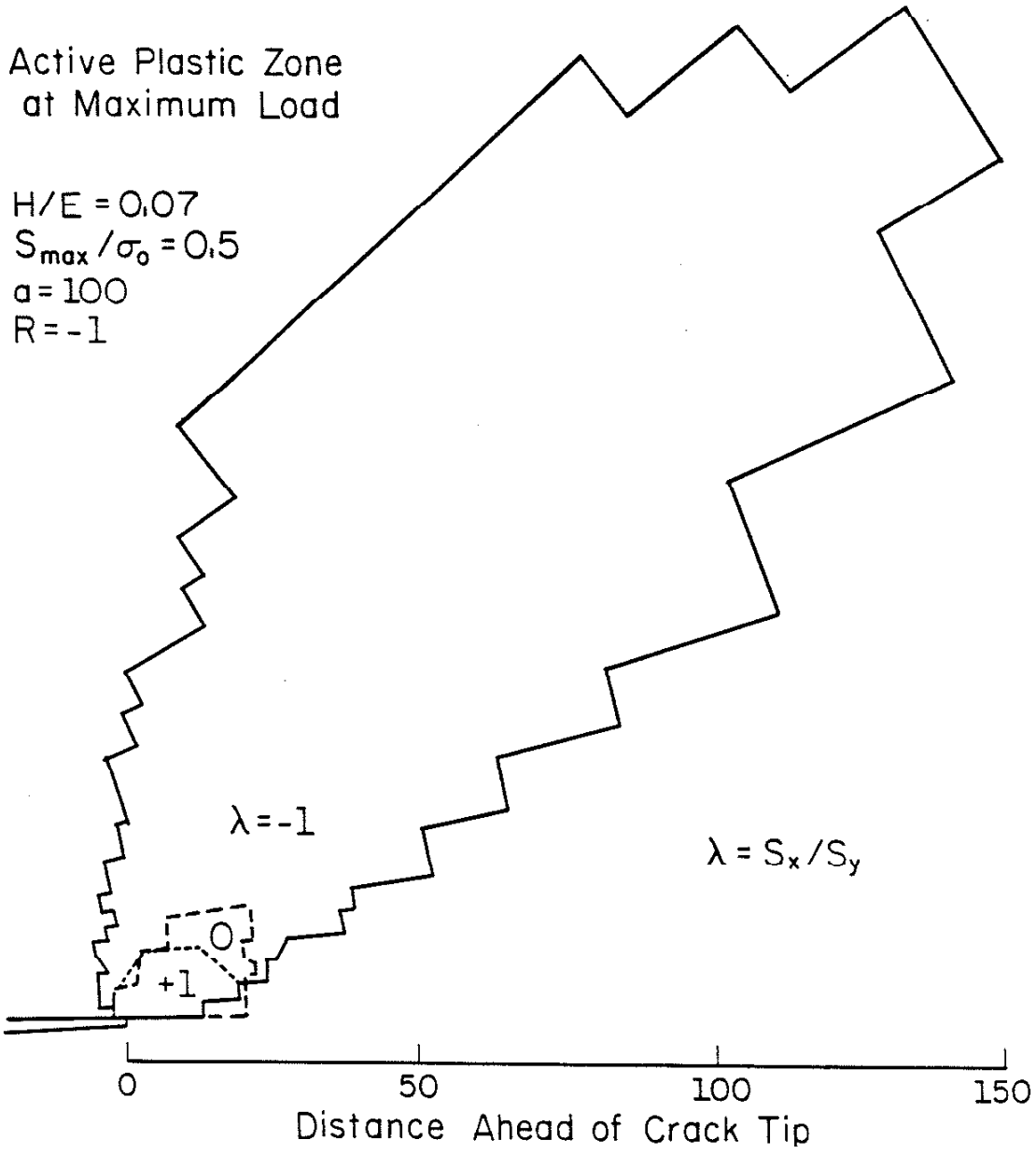

Figure 4.4 Active plastic zone shapes at maximum load for three different biaxiality ratios.

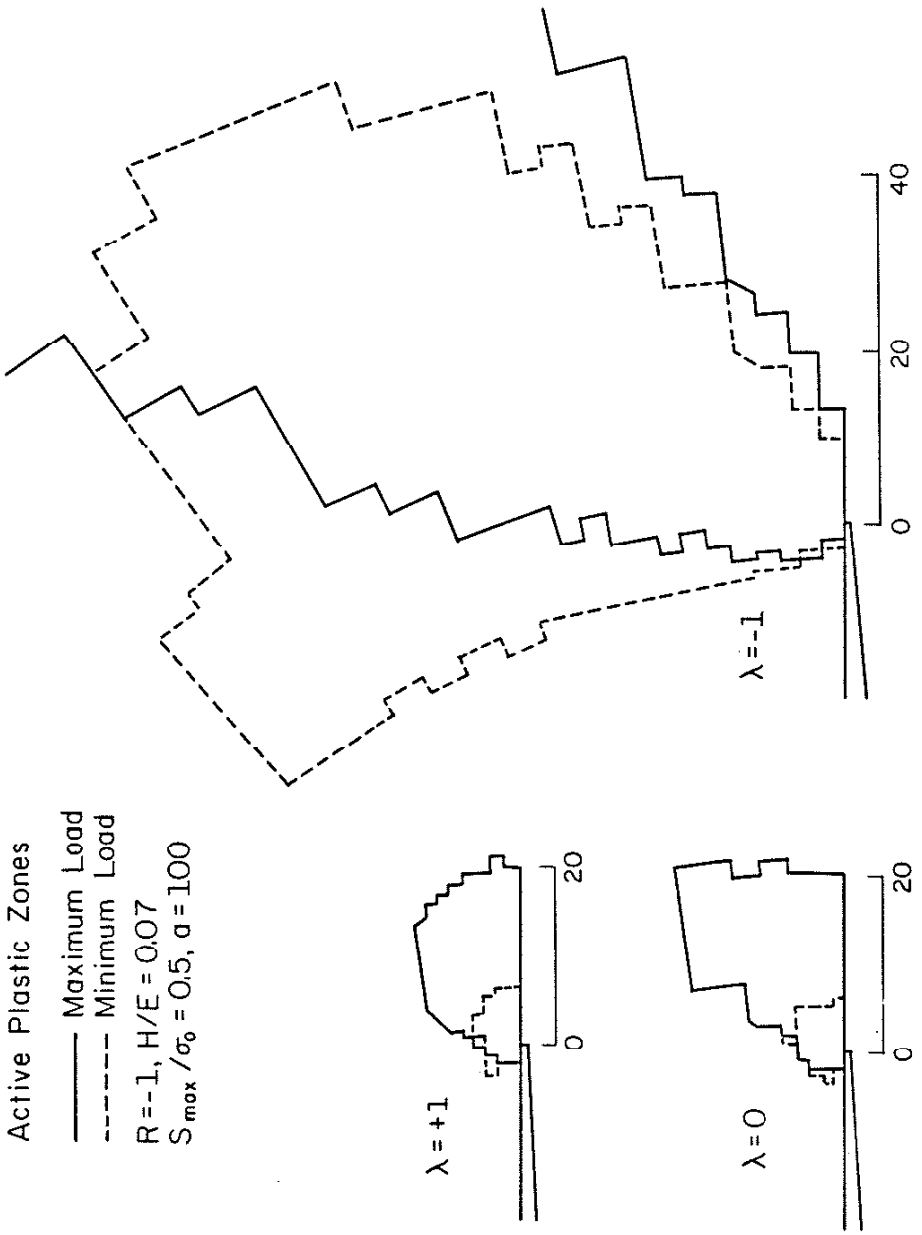

Figure 4.5 Comparisons of active plastic zones at maximum and minimum load (R = -1) for three different biaxiality ratios.

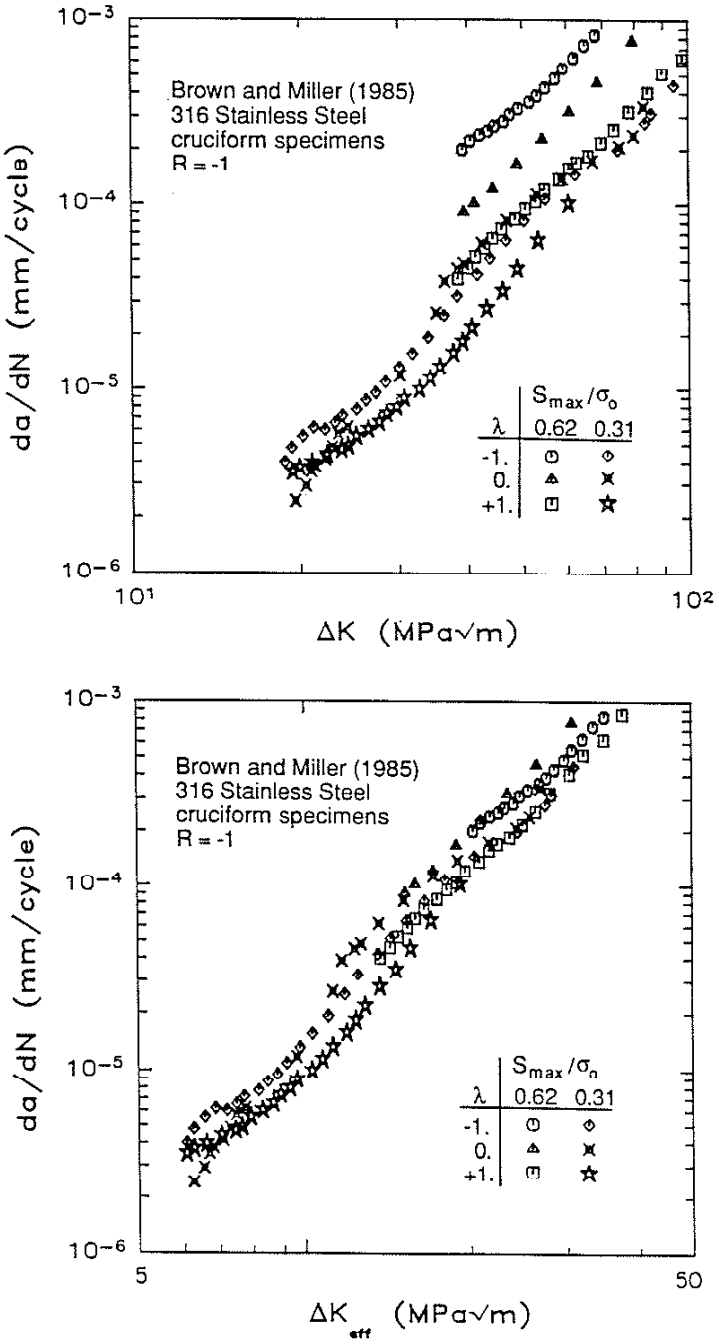

Figure 4.6 Crack growth rates for different biaxiality ratios and maximum stresses based on data of Brown and Miller for a 304 stainless steel [128].
(top) correlated with ΔK
(bottom) correlated with ΔK_{eff}

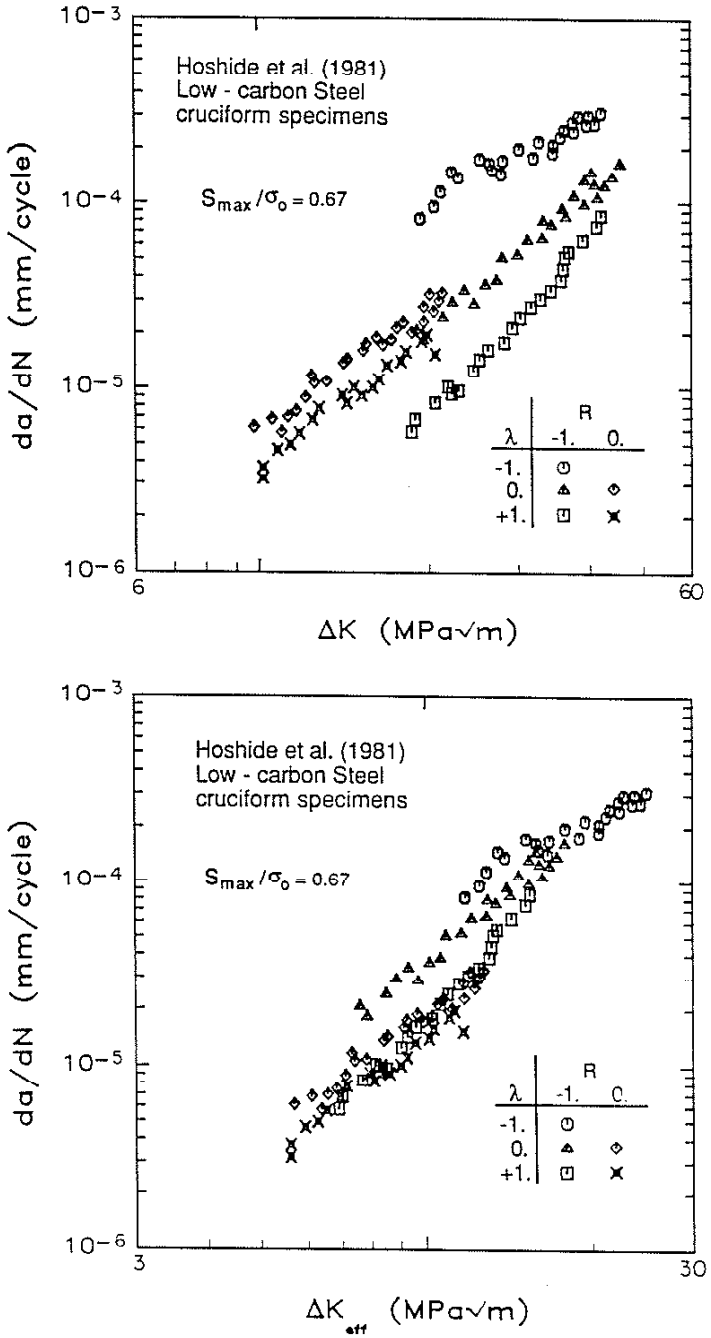

Figure 4.7 Crack growth rates for different biaxiality ratios and stress ratios, based on data of Hoshide, Tanaka, et al. for a low-carbon steel [124].
(top) correlated with ΔK
(bottom) correlated with ΔK_{eff}

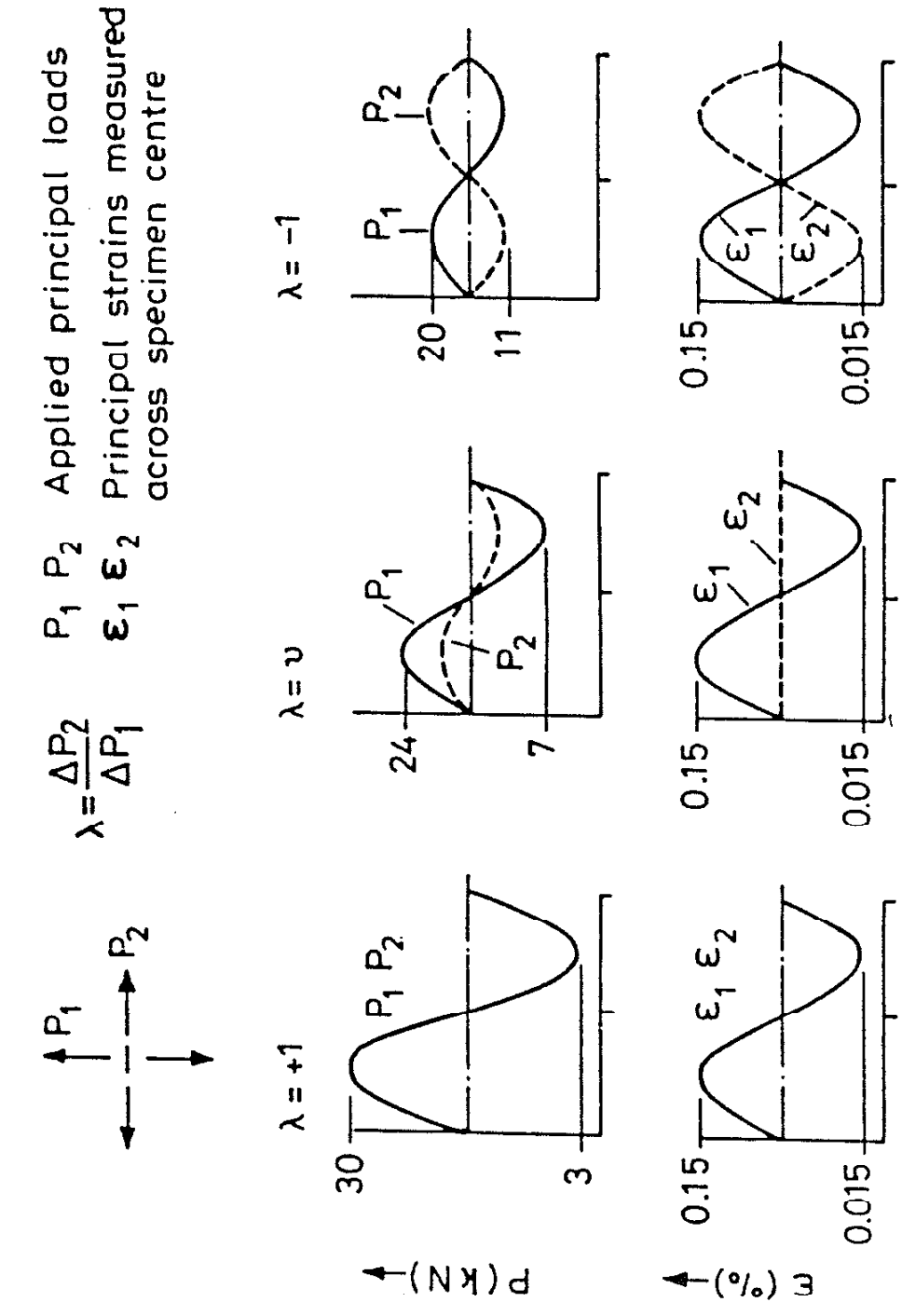

Figure 4.8 Summary of test conditions for Smith and Pascoe data, adapted directly from [127].

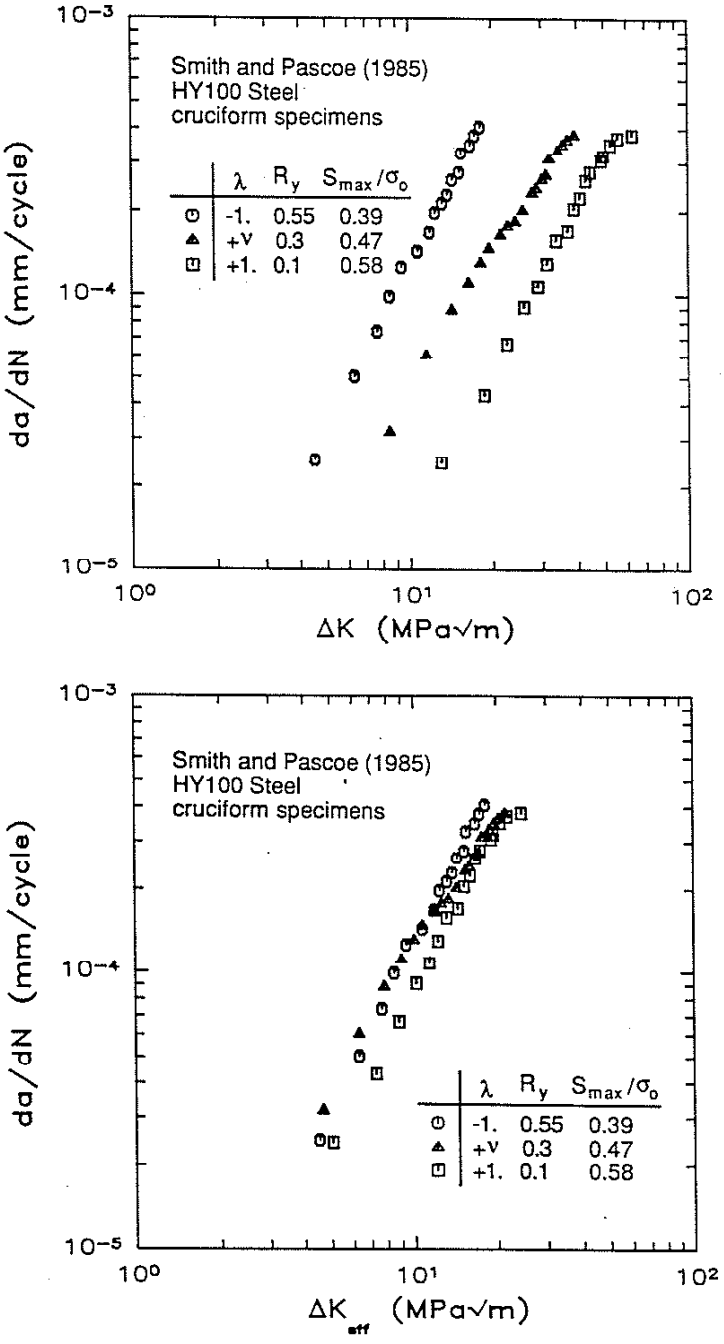

Figure 4.9 Crack growth rates for different biaxiality ratios and stress ratios, based on data of Smith and Pascoe for a high-strength steel [127].
(top) correlated with ΔK
(bottom) correlated with ΔK_{eff}

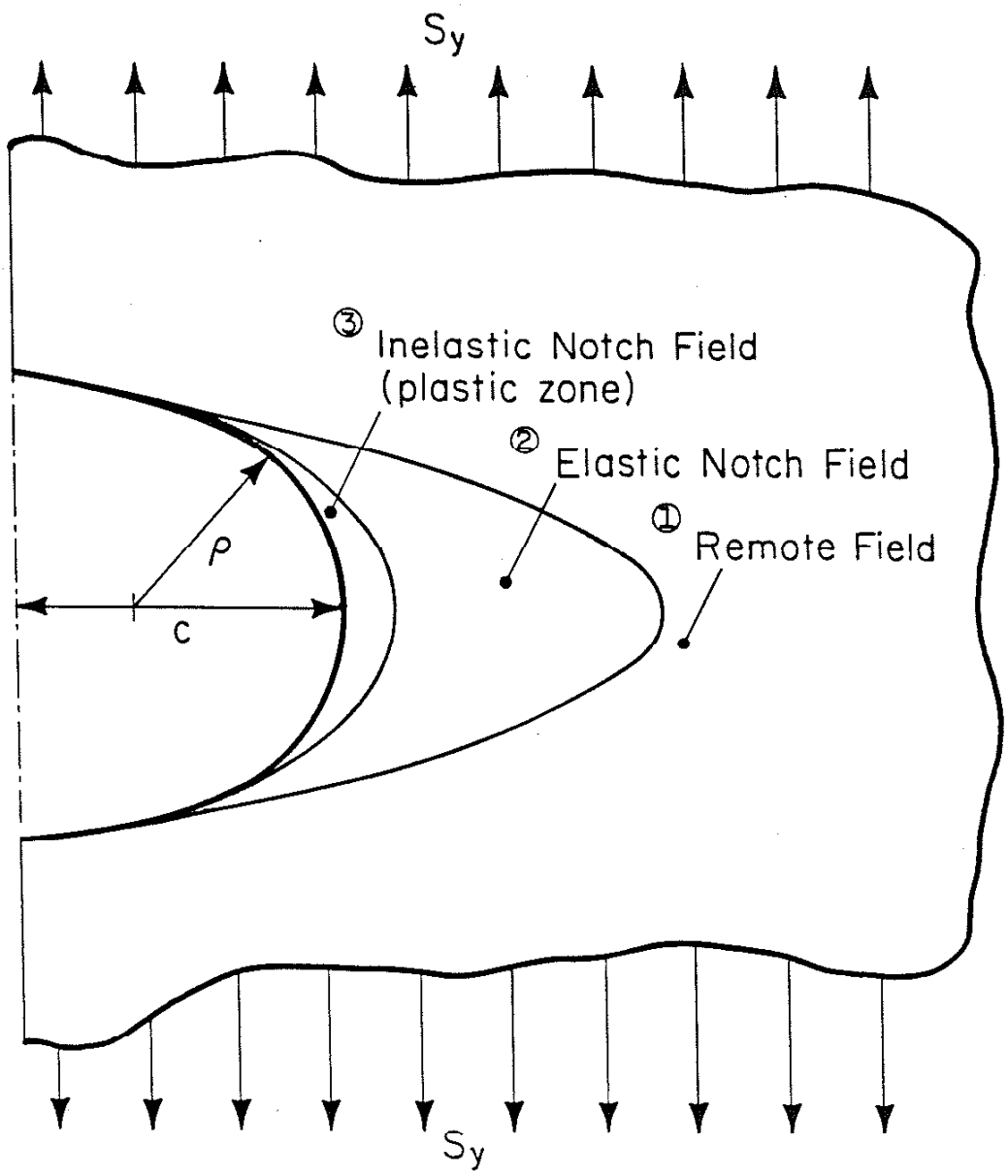

Figure 5.1 Schematic representation of the stress fields around a notch in a remotely stressed body.

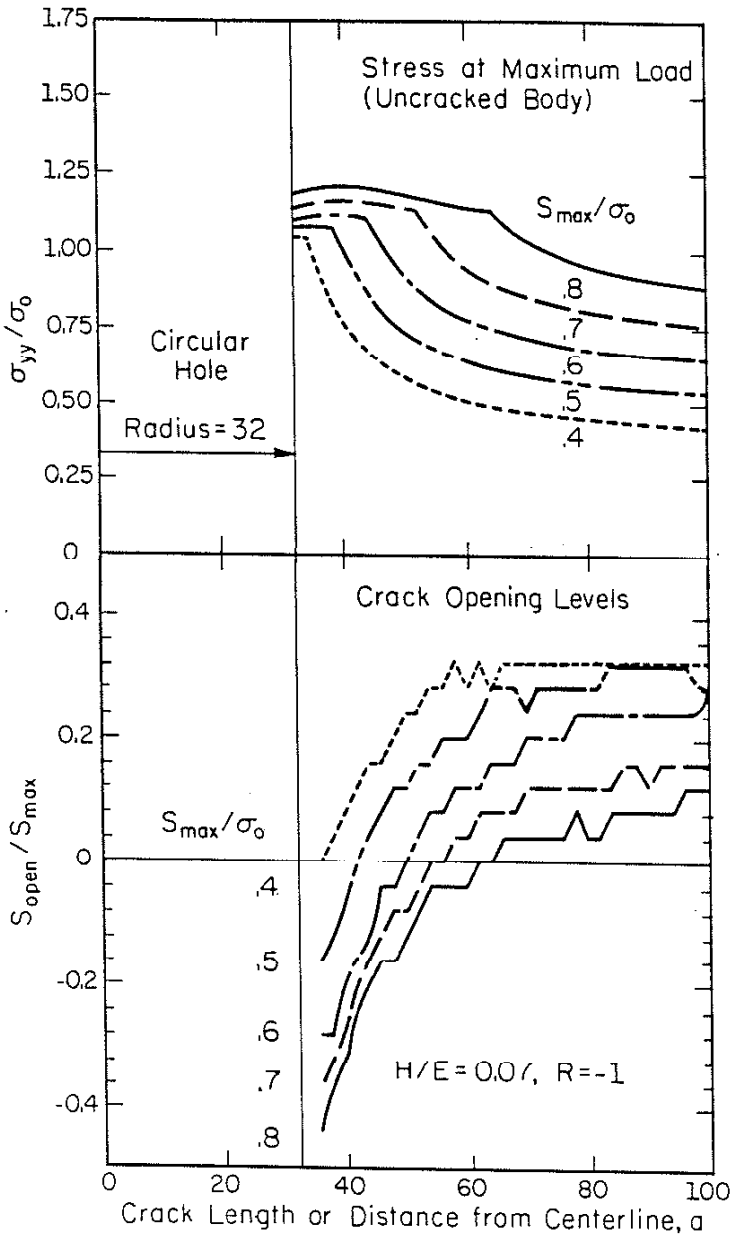

Figure 5.2 Stress distributions at maximum load for a circular notched, uncracked body (top), and changes in opening stresses for cracks growing from the notch (bottom).

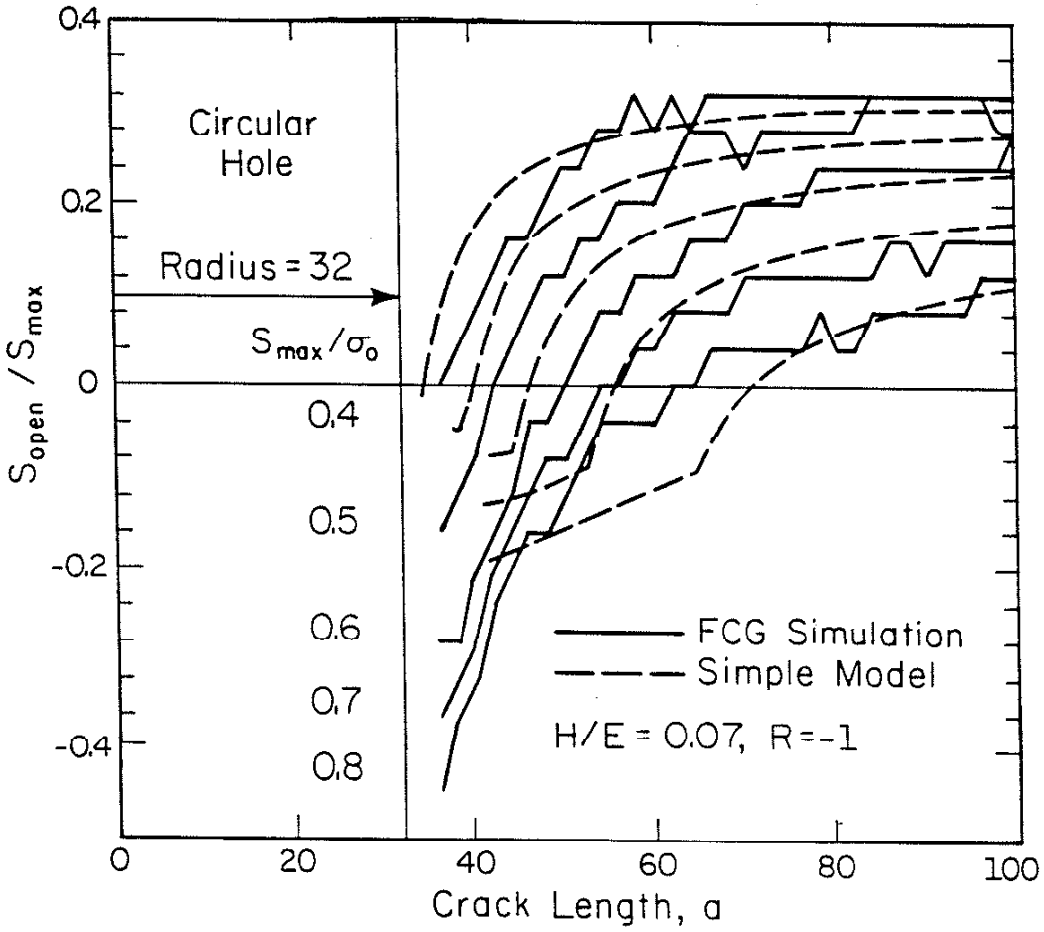

Figure 5.3 Changes in opening stresses for cracks growing from a circular hole, as determined from a complete finite element simulation and a simpler model.

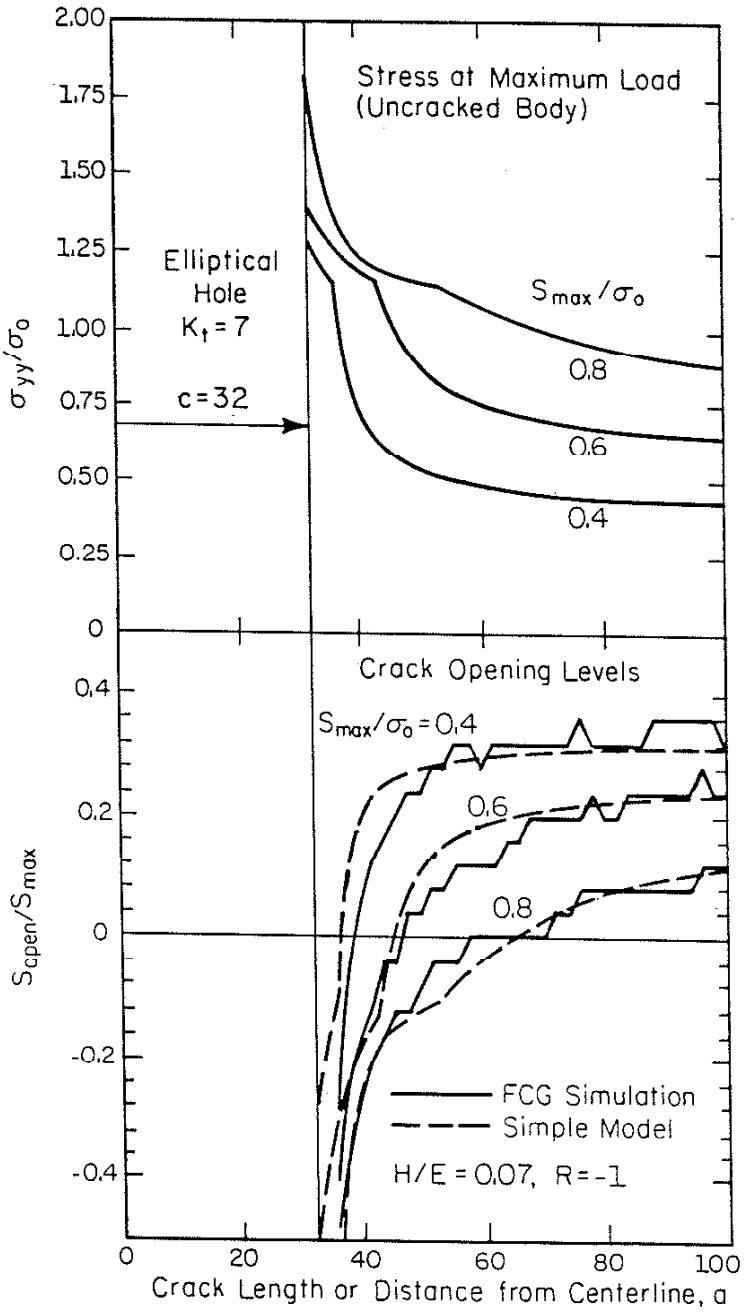

Figure 5.4 Stress distributions at maximum load for an elliptically notched, uncracked body (top), and changes in opening stresses for cracks growing from the notch, as determined by a complete finite element simulation and a simpler model.

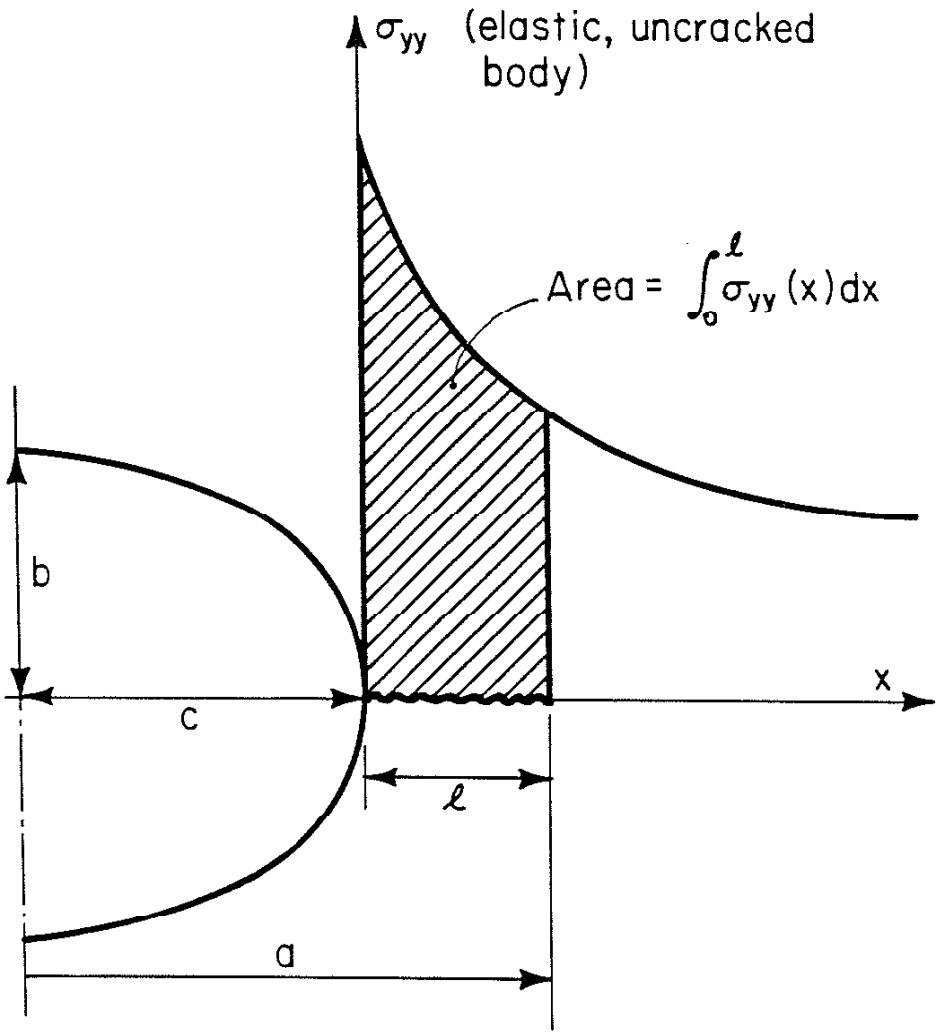

Figure 5.5 Nomenclature for the empirical expression for K at a notch.

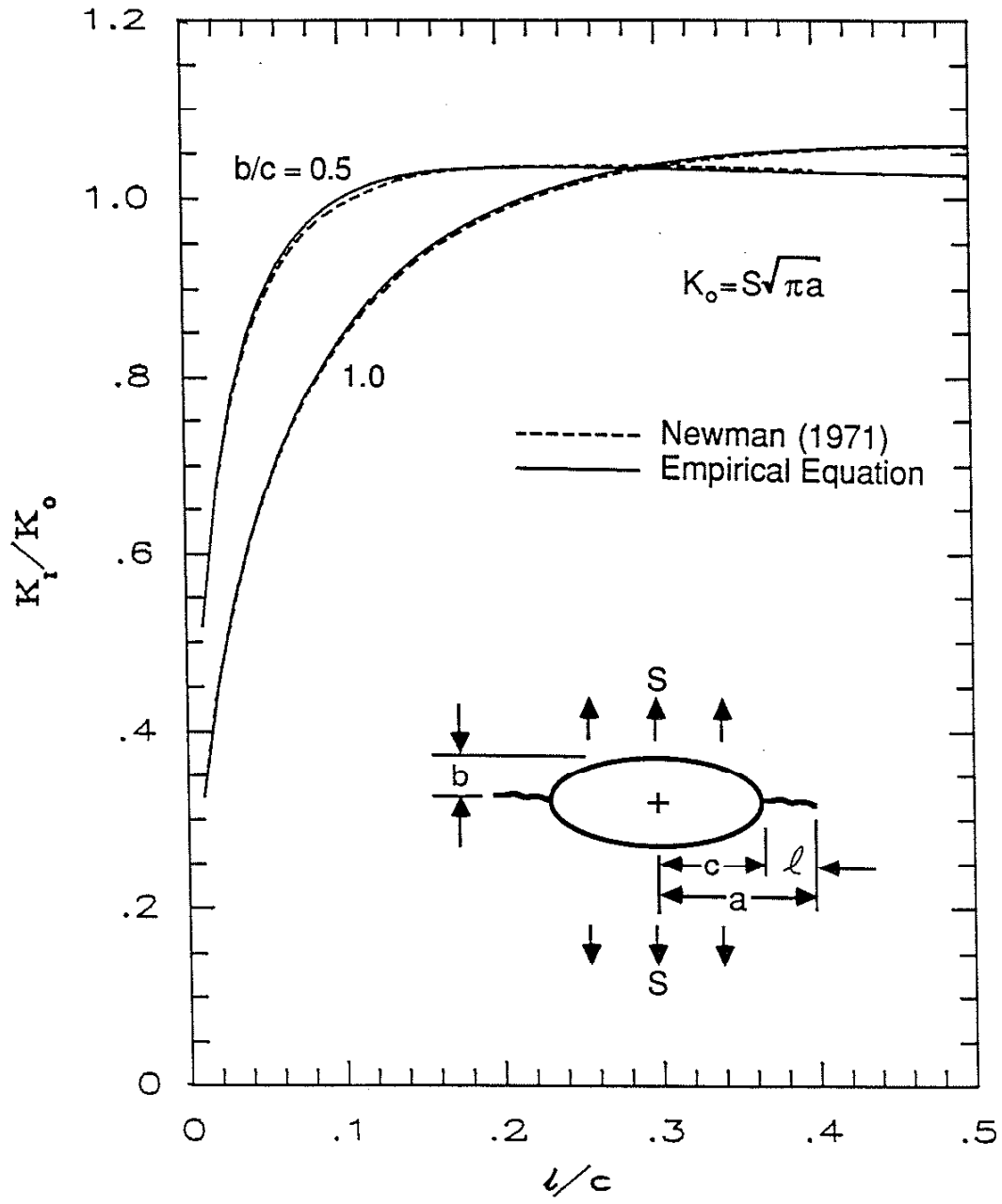

Figure 5.6 Comparison of the results of Newman [155] and the present empirical equation for the stress intensity factor of a crack growing from a notch.

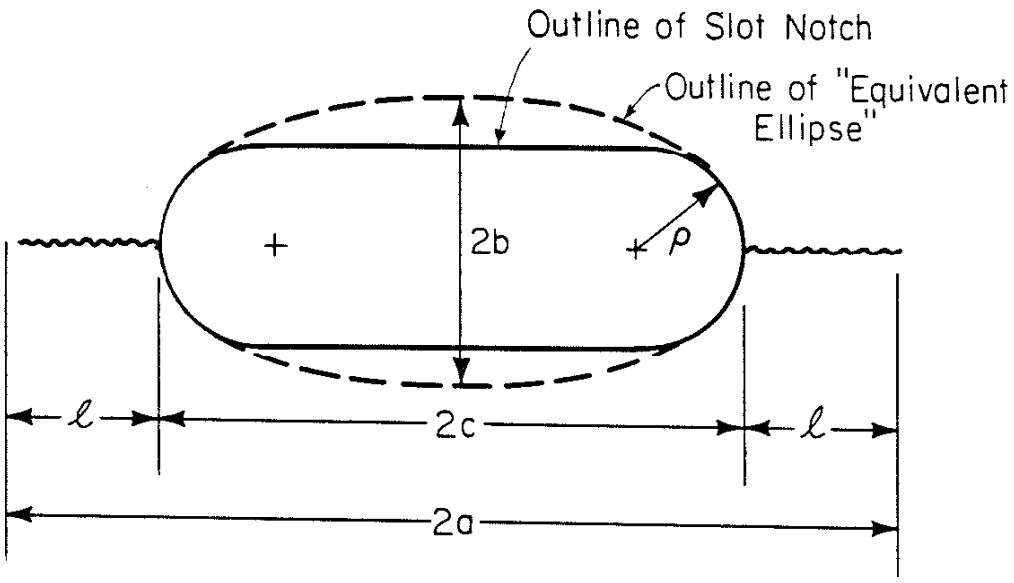

A few useful relationships:

Aspect ratio of equivalent ellipse = c/b

Theoretical stress concentration factor,

$K_t = 1 + 2\,(c/b)$

$\rho = b^2/c$

Figure 5.7 Nomenclature for a cracked slot notch and relationship to its "equivalent ellipse."

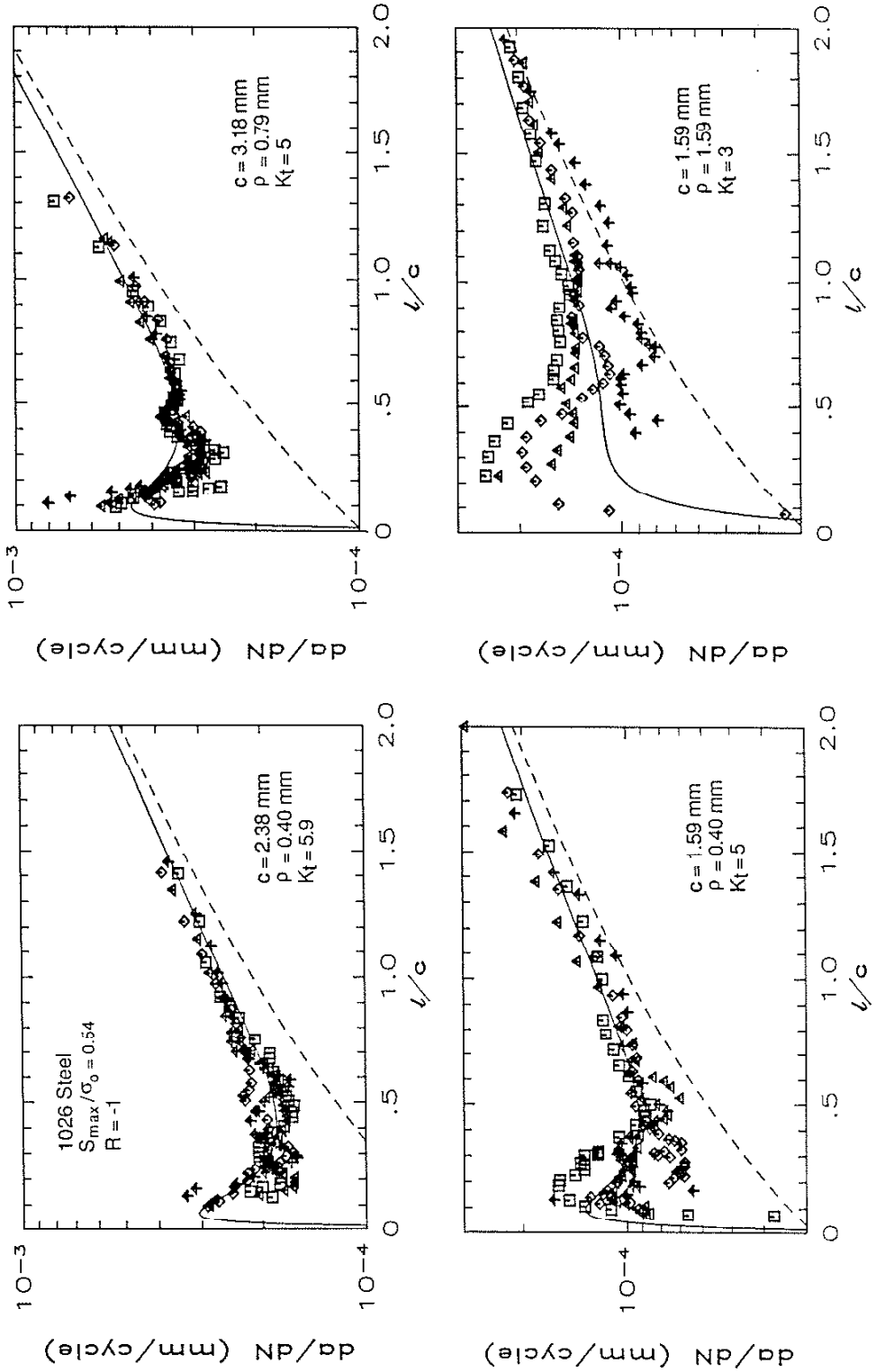

Figure 5.8 Experimental data for cracks growing from notches in a 1026 steel, compared with the predictions of a simple short crack model (solid line) and a long crack model (dashed line)

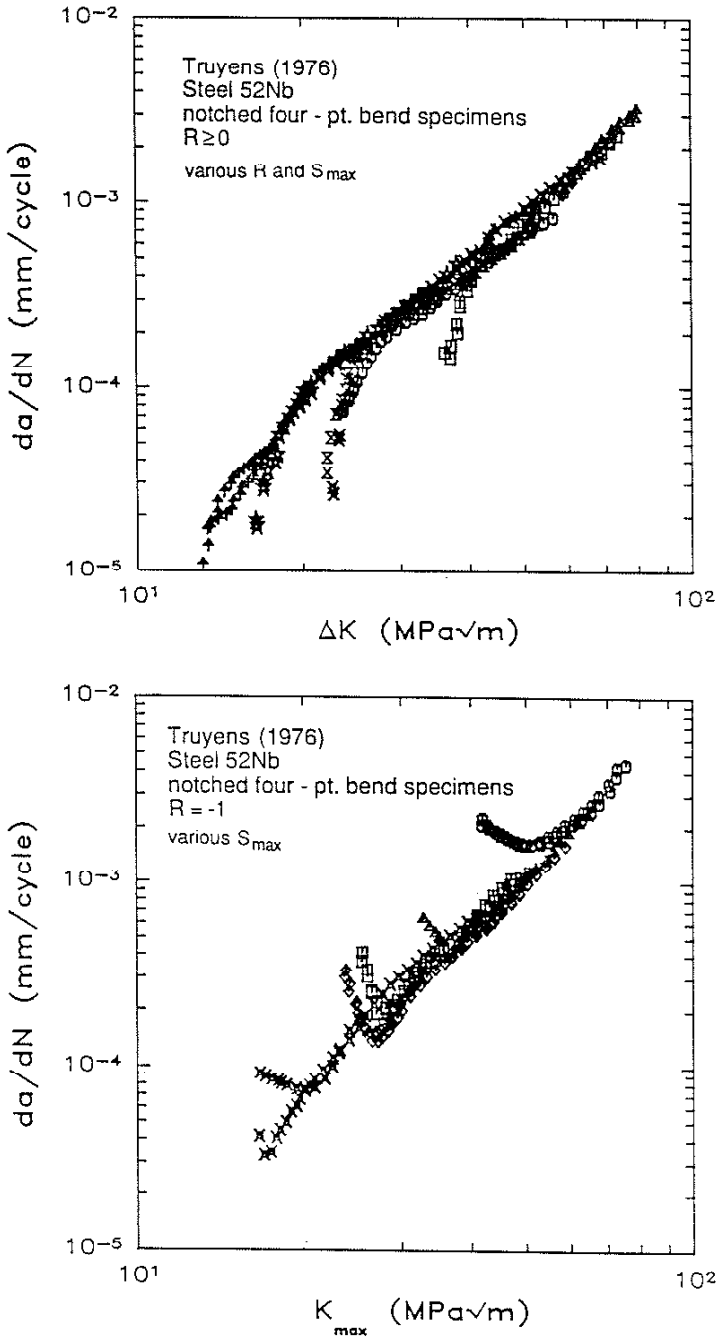

Figure 5.9 Crack growth data of Truyens [149] for four-point bending of a notched beam. (top) $R \geq 0$ (bottom) $R = -1$

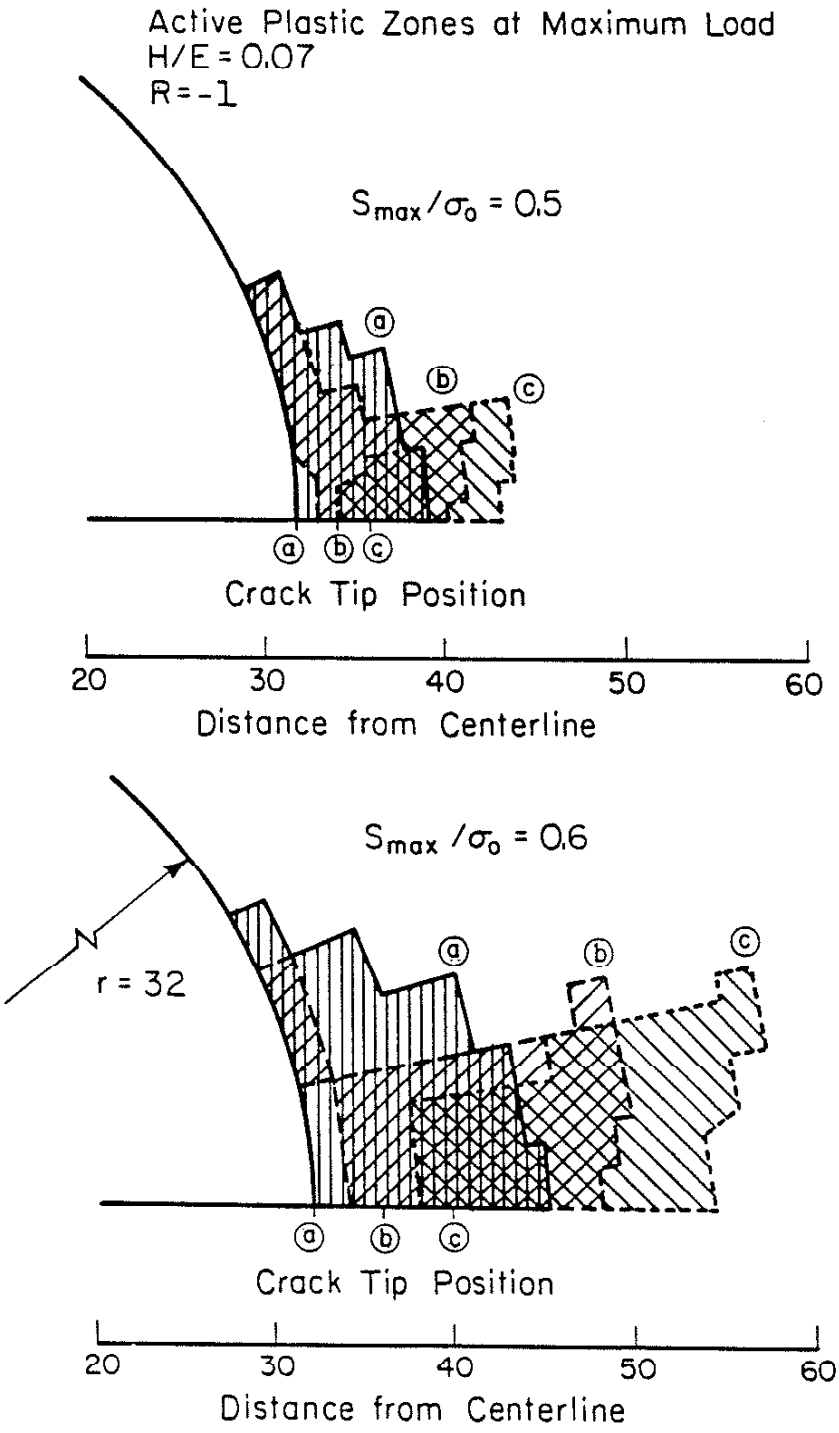

Figure 5.10 Plastic zones for short cracks near a notch in comparison to original notch plastic zone.

REFERENCES

1. Paris, P. C., M. P. Gomez, and W. E. Anderson, "A Rational Analytical Theory of Fatigue," The Trend in Engineering, Vol. 13, University of Washington, January 1961, pp. 9-14.

2. Paris, P. C., "The Fracture Mechanics Approach to Fatigue," Fatigue - An Interdisciplinary Approach, Tenth Sagamore Army Materials Research Conference, Aug. 1963, Syracuse University Press, 1964, pp. 107-132.

3. Elber, W., "Fatigue Crack Closure Under Cyclic Tension," Engineering Fracture Mechanics, Vol. 2, No. 1, July 1970, pp. 37-45.

4. Elber, W., "The Significance of Fatigue Crack Closure," Damage Tolerance in Aircraft Structures, ASTM STP 486, American Society for Testing and Materials, 1971, pp. 230-242.

5. Miyamoto, H., T. Miyoshi, and S. Fukuda, "An Analysis of Crack Propagation in Welded Structures," Significance of Defects in Welded Structures, Proc. of Japan-U.S. Seminar, Tokyo, University of Tokyo Press, 1973, pp. 189-202.

6. Ohji, K., K. Ogura, and Y. Ohkubo, "On the Closure of Fatigue Cracks Under Cyclic Tensile Loading," Int. J. Fracture, Vol. 10, 1974, pp. 123-124.

7. Ogura, K., K. Ohji, and Y. Ohkubo, "Fatigue Crack Growth Under Biaxial Loading," Int. J. Fracture, Vol. 10, 1974. pp. 609-610.

8. Ohji, K., K. Ogura, and Y. Ohkubo, "Cyclic Analysis of a Propagating Crack and its Correlation with Fatigue Crack Growth," Engineering Fracture Mechanics, Vol. 7, 1975, pp. 457-464.

9. Ogura, K., K. Ohji, and K. Honda, "Influence of Mechanical Factors on the Fatigue Crack Closure," Advances in Research on the Strength and Fracture of Materials (Fracture 1977), Fourth Int. Conf. Fracture, Waterloo, Canada, June 1977, Pergamon, Vol. 2, pp. 1035-1047.

10. Ogura, K., and K. Ohji, "FEM Analysis of Crack Closure and Delay Effect in Fatigue Crack Growth Under Variable Amplitude Loading," Engineering Fracture Mechanics, Vol. 9, No. 2, 1977, pp. 471-480.

11. Newman, J. C. Jr., "Finite Element Analysis of Fatigue Crack Propagation--Including the Effects of Crack Closure," Ph.D. Thesis, Virginia Polytechnic Institute and State University, Blacksburg, VA, May 1974.

12. Newman, J. C. Jr., and H. Armen, Jr., "Elastic-Plastic Analysis of a Propagating Crack Under Cyclic Loading," AIAA Journal, Vol. 13, No. 8, 1975, pp. 1017-1023.

13. Newman, J. C. Jr., "A Finite-Element Analysis of Fatigue Crack Closure," Mechanics of Crack Growth, ASTM STP 590, American Society for Testing and Materials," 1976, pp. 281-301.

14. Newman, J. C. Jr., "Finite-Element Analysis of Crack Growth Under Monotonic and Cyclic Loading," Cyclic Stress-Strain and Plastic Deformation Aspects of Fatigue Crack Growth, ASTM STP 637, American Society for Testing and Materials, 1977, pp. 56-80.

15. Shiratori, M., T. Miyoshi, and H. Miyamoto, "Analysis of the Crack Propagation and Closure Behavior in Fatigue," Trans. JSME, Vol. 43, No. 374, Oct. 1977, pp. 3577-3593 (in Japanese).

16. Socie, D. F., "Prediction of Fatigue Crack Growth in Notched Members Under Variable Amplitude Loading Histories," Engineering Fracture Mechanics, Vol. 9, 1977, pp. 849-865.

17. Nakagaki, M., and S. N. Atluri, "Fatigue Crack Closure and Delay Effects Under Mode I Spectrum Loading: An Effect Elastic-Plastic Analysis Procedure," Fatigue of Engineering Materials and Structures, Vol. 1, 1979, pp. 421-429.

18. Nakagaki, M., and S. N. Atluri, "Elastic-Plastic Analysis of Fatigue Crack Closure in Modes I and II," AIAA Journal, Vol. 18, No. 9, 1980, pp. 1110-1117.

19. Nakamura, H., H. Kobayashi, S. Yanase, and H. Nakazawa, "Finite Element Analysis of Fatigue Crack Closure in Compact Specimen," Mechanical Behavior of Materials (ICM4), Fourth Int. Conf. Mechanical Behavior of Materials, Stockholm, Aug. 1983, Pergamon, Vol. 2, pp. 817-823.

20. Kobayashi, H., and H. Nakamura, "Investigation of Fatigue Crack Closure (Analysis of Plasticity Induced Crack Closure)," Current Research on Fatigue Cracks, MRS Vol. 1, Society of Materials Science, Japan, 1985, pp. 201-215.

21. Blom, A. F., and D. K. Holm, "An Experimental and Numerical Study of Crack Closure," Engineering Fracture Mechanics, Vol. 22, No. 6, 1985, pp. 997-1011.

22. Fleck, N. A., "Finite Element Analysis of Plasticity-Induced Crack Closure Under Plane Strain Conditions," Engineering Fracture Mechanics, Vol. 25, No. 4, 1986, pp. 441-449.

23. Fleck, N. A., and J. C. Newman, Jr., "Analysis of Crack Closure Under Plane Strain Conditions," ASTM Int. Symp. on Fatigue Crack Closure, Charleston, SC, May 1986.

24. Chermahini, R. G., "Three-Dimensional Elastic-Plastic Finite Element Analysis of Fatigue Crack Growth and Closure," Ph.D. Thesis, Old Dominion University, August 1986.

25. Chermahini, R. G., and J. C. Newman, Jr., "Three-Dimensional Elastic-Plastic Finite Element Analysis of Fatigue Crack Growth and Closure," ASTM Int. Symp. on Fatigue Crack Closure, Charleston, SC, May 1986.

26. Nicholas, T., A. Palazotto, and E. Bednarz, "An Analytical Investigation of Plasticity Induced Closure Involving Short Cracks," ASTM Int. Sym. on Fatigue Crack Closure, Charleston, SC, May 1986.

27. Lalor, P., H. Sehitoglu, and R. C. McClung, "Mechanics Aspects of Small Crack Growth from Notches--The Role of Crack Closure," The Behavior of Short Fatigue Cracks, EGF Pub. 1, Mechanical Engineering Publications, London, 1986, pp. 369-386.

28. Lalor, P. L., and H. Sehitoglu, "Fatigue Crack Closure Outside Small Scale Yielding Regime," ASTM Int. Symp. on Fatigue Crack Closure, Charleston, SC, May 1986.

29. Lalor, P. L., "Mechanics Aspects of Crack Closure," M.S. Thesis, Department of Mechanical and Industrial Engineering, Univ. of Illinois at Urbana-Champaign, 1986. Also published as Materials Engineering-Mechanical Behavior Report No. 133, UILU-ENG 86-3610, College of Engineering, Univ. of Illinois at Urbana-Champaign, August 1986.

30. Marci, G., "Recent Advances in Fatigue Crack Growth Predictions," J. Aero. Soc. India, Vol. 36, No. 3,, August 1984, pp. 237-254.

31. Dugdale, D. S., "Yielding of Steel Sheets Containing Slits," J. of the Mechanics and Physics of Solids, Vol. 8, No. 2, 1960, pp. 100-104.

32. Bilby, B. A., A. H. Cottrell, and K. H. Swinden, "Plastic Yielding from Sharp Notches," Proc. Royal Society, Series A, Vol. 272, 1963, pp. 304-314.

33. Dill, H. D. and C. R. Saff, "Spectrum Crack Growth Prediction Method Based on Crack Surface Displacement and Contact Analysis," Fatigue Crack Growth Under Spectrum Loads, ASTM STP 595, American Society for Testing and Materials, 1976, pp. 306-319.

34. Shiratori, M., T. Miyoshi, H. Miyamoto, and T. Mori, "A Computer Simulation of Fatigue Crack Propagation Based on the Crack Closure Concept," Adv. in Research on the Strength and Fracture of Materials (Fracture 1977), Fourth Int. Conf. Fracture, Waterloo, Canada, June 1977, Pergamon, Vol. 2B, pp. 1091-1098.

35. Fuhring, H., and T. Seeger, "Dugdale Crack Closure Analysis of Fatigue Cracks Under Constant Amplitude Loading," Engineering Fracture Mechanics, vol. 11, 1979, pp. 99-122.

36. Budiansky, B., and J. W. Hutchinson, "Analysis of Closure in Fatigue Crack Growth," J. Applied Mechanics, Trans. ASME, Vol. 45, June 1978, pp. 267-276.

37. Newman, J. C., Jr., "A Crack-Closure Model for Predicting Fatigue Crack Growth Under Aircraft Spectrum Loading," Methods and Models for Predicting Fatigue Crack Growth Under Random Loading, ASTM STP 748, American Society for Testing and Materials, 1981, pp. 53-84.

38. Newman, J. C., Jr., "A Nonlinear Fracture Mechanics Approach to the Growth of Small Cracks," AGARD Specialists Meeting on Behavior of Short Cracks in Airframe Components, Toronto, Sept. 1982.

39. Newman, J. C., Jr., "A Crack Opening Stress Equation for Fatigue Crack Growth," Int. J. Fracture, Vol. 24, 1984, pp. R131-R135.

40. Sehitoglu, H., "Crack Opening and Closure in Fatigue," Engineering Fracture Mechanics, Vol. 21, No. 2, 1985, pp. 329-339.

41. Sehitoglu, H., "Characterization of Crack Closure," Fracture Mechanics: Sixteenth Symposium, ASTM STP 868, American Society for Testing and Materials, 1985, pp. 361-380.

42. Ibrahim, F. K., J. C. Thompson, and T. H. Topper, "A Study of the Effect of Mechanical Variables on Fatigue Crack Closure and Propagation," Int. J. Fatigue, Vol. 8, No. 3, July 1986, pp. 135-142.

43. Irwin, G. R., "Plastic Zone Near a Crack and Fracture Toughness," Mechanical and Metallurgical Behavior of Sheet Materials, Seventh Sagamore Ordnance Materials Research Conference, Aug. 1960, pp. IV-63-IV-78.

44. Rice, J. R., "Mechanics of Crack Tip Deformation and Extension by Fatigue," Fatigue Crack Propagation, ASTM STP 415, American Society for Testing and Materials, 1967, pp. 247-309.

45. Shih, C. F., "J Integral Estimates for Strain Hardening Materials in Antiplane Shear Using Fully Plastic Solution," Mechanics of Crack Growth, ASTM STP 590, American Society for Testing and Materials, 1976, pp. 3-22.

46. Chan, K. S., and J. Lankford, "A Crack-Tip Strain Model for the Growth of Small Fatigue Cracks," Scripta Met., Vol. 17, No. 4, 1983, pp. 529-532.

47. Lankford, J., and D. L. Davidson, "The Micromechanisms of Small Fatigue Crack Growth and the Influence of Metallurgical Factors," Third Int. Conf. on Fatigue and Fatigue Thresholds (Fatigue '87), Charlottesville, VA, June-July 1987.

48. Drucker, D. C., and L. Palgen, "On Stress-Strain Relations Suitable for Cyclic and Other Loadings," J. Applied Mechanics, Trans. ASME, Vol. 48, No. 3, Sept. 1981, pp. 479-485.

49. Sehitoglu, H., "Material Behavior Under Thermal Loading," J. Pressure Vessel Technology, Trans. ASME, Vol. 108, February 1986, pp. 113-119.

50. Slavik, D., and H. Sehitoglu, "Constitutive Models Suitable for Thermal Loading," J. Eng. Materials and Technology, Trans. ASME, Vol. 108, Oct. 1986, pp. 303-312.

51. Lankford, J., D. L. Davidson, and K. S. Chan, "The Influence of Crack Tip Plasticity in the Growth of Small Fatigue Cracks," Met. Trans. A, Vol. 15A, Aug. 1984, pp. 1579-1588.

52. Davidson, D. L., "Plasticity Induced Fatigue Crack Closure," ASTM Int. Symp. on Fatigue Crack Closure, Charleston, SC, May 1986.

53. Nisitani, H., and K. Takao, "Influence of Mean Stress on Crack Closure Phenomenon and Fatigue Crack Propagation," Bull. JSME, Vol. 20, No. 141, March 1977, pp. 264-270.

54. Macha, D. E., D. M. Corbly, and J. W. Jones, "On the Variation of Fatigue-Crack-Opening-Load with Measurement Location," Experimental Mechanics, Vol. 19, No. 6, June 1979, pp. 207-213.

55. Dodds, R. H., and D. T. Read, "Experimental and Analytical Estimates of the J-Integral for Tensile Panels Containing Short Center Cracks," Int. J. Fracture, Vol. 28, 1985, pp. 39-54.

56. McClung, R. C., and H. Sehitoglu, "Closure Behavior of Small Cracks Under High Strain Fatigue Histories," ASTM Int. Symp. on Fatigue Crack Closure, Charleston, SC, May 1986.

57. Paris, P. C., "Twenty Years of Reflection on Questions Involving Fatigue Crack Growth--Part I: Historical Observations and Perspectives," First Int. Conf. Fatigue and Fatigue Thresholds, Stockholm, June 1981, EMAS, Warley, U.K., Vol. 1, pp. 3-10.

58. Kumar, V., and C. F. Shih, "Fully Plastic Crack Solutions, Estimation Scheme, and Stability Analyses for the Compact Specimen," Fracture Mechanics: Twelfth Conference, ASTM STP 700, American Society for Testing and Materials, 1980, pp. 406-438.

59. Kumar, V., M. D. German, and C. F. Shih, An Engineering Approach for Elastic-Plastic Fracture Analysis, NP-1931, Research Project 1237-1, Topical Report, Electric Power Research Institute, July 1987.

60. Dowling, N. E., "J-Integral Estimates for Cracks in Infinite Bodies," Engineering Fracture Mechanics, Vol. 26, No. 3, 1987, pp. 333-348.

61. Boettner, R. C., C. Laird, and A. J. McEvily, Jr., "Crack Nucleation and Growth in High Strain-Low Cycle Fatigue," Trans. Met. Soc. AIME, Vol. 233, Feb. 1965, pp. 279-387.

62. McEvily, A. J., "Fatigue Crack Growth and the Strain Intensity Factor," Air Force Conf. on Fatigue and Fracture of Aircraft Structures and Materials, Miami Beach, Dec. 1969, AFFDL-TR-70-144, pp. 451-458.

63. Solomon, H. D., "Low Cycle Fatigue Crack Propagation in 1018 Steel," J. Materials, Vol. 7, No. 3, Sept. 1972, pp. 299-306.

64. El Haddad, M. H., K. N. Smith, and T. H. Topper, "A Strain Based Intensity Factor Solution for Short Fatigue Cracks Initiating from Notches," Fracture Mechanics, ASTM STP 677, American Society for Testing and Materials, 1979, pp. 274-289.

65. El Haddad, M. H., K. N. Smith, and T. H. Topper, "Fatigue Crack Propagation of Short Cracks," J. Eng. Materials and Technology, Trans. ASME, Vol. 101, 1979, pp. 42-46.

66. Haigh, J. R., and R. P. Skelton, "A Strain Intensity Approach to High Temperature Fatigue Crack Growth and Failure," Materials Science and Engineering, Vol. 36, 1978, pp. 133-137.

67. Starkey, M. S., and R. P. Skelton, "A Comparison of the Strain Intensity and Cyclic J Approaches to Crack Growth," Fatigue of Engineering Materials and Structures, Vol. 5, No. 4, 1982, pp. 329-341.

68. Skelton, R. P., "Growth of Short Cracks During High Strain Fatigue and Thermal Cycling," Low-Cycle Fatigue and Life Prediction, ASTM STP 770, American Society for Testing and Materials, 1982, pp. 337-381.

69. Tomkins, B., "Fatigue Crack Propagation--An Analysis," Philosophical Magazine, Eighth Series, Vol. 18, No. 155, 1968, pp. 1041-1066.

70. Tomkins, B., "Fatigue Failure in High Strength Metals," Philosophical Magazine, Eighth Series, Vol. 23, No. 183, 1971, pp. 687-703.

71. Donahue, R. J., H. McI. Clark, P. Atanmo, R. Kumble, and A. J. McEvily, "Crack Opening Displacement and the Rate of Fatigue Crack Growth," Int. J. Fracture Mechanics, Vol. 8, No. 2, 1972, pp. 209-219.

72. Lardner, R. W., "A Dislocation Model for Fatigue Crack Growth in Metals," Philosophical Magazine, Eighth Series, Vol. 17, No. 145, 1968, pp. 71-82.

73. Pelloux, R. M. N., "Crack Extension by Alternating Shear," Engineering Fracture Mechanics, Vol. 1, No. 4, 1970, pp. 697-704.

74. McMillan, J. C., and R. M. Pelloux, "Fatigue Crack Propagation Under Programmed Loads and Crack Tip Opening Displacements," Engineering Fracture Mechanics, Vol. 2, No. 1, 1970, pp. 81-84.

75. McEvily, A. J., D. Beukelmann, and K. Tanaka, "On Large-Scale Plasticity Effects in Fatigue Crack Propagation," Symp. Mechanical Behavior of Materials, Kyoto, Japan, 1974, Society of Materials Science, Japan, Vol. 1, pp. 269-281.

76. Tomkins, B., "The Development of Fatigue Crack Propagation Models for Engineering Applications at Elevated Temperatures," J. Eng. Materials and Technology, Trans. ASME, Vol. 97, No. 4, 1975, pp. 289-297.

77. Tomkins, B., G. Sumner, and J. Wareing, "Factors Affecting Crack Propagation in Low Cycle Fatigue," Int. Symp. Low Cycle Fatigue Strength and Elasto-Plastic Behavior of Materials, Stuttgart, Oct. 1979, Deutscher Verband für Materialprüfung e.V., pp. 495-507.

78. Tomkins, B., "Micromechanisms of Fatigue Crack Growth at High Stress," Metal Science, Vol. 14, Nos. 8-9, Aug.-Sept. 1980, pp. 408-417.

79. Tanaka, K., T. Hoshide, and N. Sakai, "Mechanics of Fatigue Crack Propagation by Crack-Tip Plastic Blunting," Engineering Fracture Mechanics, Vol. 19, No. 5, 1984, pp. 805-825.

80. Brown, M. W., E. R. de los Rios, and K. J. Miller, "A Critical Comparison of Proposed Parameters for High Strain Fatigue Crack Growth," ASTM Conf. on Fundamental Questions and Critical Experiments in Fatigue, Dallas, Oct. 1984 (to be published as an ASTM STP).

81. Gowda, C. V. B., and T. H. Topper, "Crack Propagation in Notched Mild Steel Plates Subjected to Cyclic Inelastic Strains," Cyclic Stress-Strain Behavior--Analysis, Experimentation, and Failure Prediction, ASTM STP 519, American Society for Testing and Materials, 1973, pp. 170-184.

82. Neuber, H., "A Physically Nonlinear Notch and Crack Model," J. Mech. Phys. Solids, Vol. 16, 1968, pp. 289-294.

83. Bhanderi, S., S. Charif D'Ouazzane, and C. Faidy, "Establishment of Governing Parameters for Fatigue Crack Growth Analysis in Areas of High Nominal Strain," ASME Paper 84-PVP-20, 1984.

84. Dowling, N. E., and J. A. Begley, "Fatigue Crack Growth During Gross Plasticity and the J-Integral," Mechanics of Crack Growth, ASTM STP 590, American Society for Testing and Materials, 1976, pp. 82-103.

85. Dowling, N. E., "Geometry Effects and the J-Integral Approach to Elastic-Plastic Fatigue Crack Growth," Cracks and Fracture, ASTM STP 601, American Society for Testing and Materials, 1976, pp. 19-32.

86. Dowling, N. E., "Crack Growth During Low-Cycle Fatigue of Smooth Axial Specimens," Cyclic Stress-Strain and Plastic Deformation Aspects of Fatigue Crack Growth, ASTM STP 637, American Society for Testing and Materials, 1977, pp. 97-121.

87. Shih, C. F., and J. W. Hutchinson, "Fully Plastic Solutions and Large Scale Yielding Estimates for Plane Stress Crack Problems," J. Eng. Materials and Technology, Trans. ASME, Vol. 98, No. 4, 1976, pp. 289-295.

88. Huang, J. S., and R. M. Pelloux, "Low Cycle Fatigue Crack Propagation in Hastelloy-X at 25 and 760°C," Met. Trans. A, Vol. 11A, 1980, pp. 899-904.

89. Reger, M., and L. Rémy, "Influence of Environment on Microcrack Propagation in High Temperature Low Cycle Fatigue," Fracture and the Role of Microstructure, Fourth European Conf. Fracture, Leoben, Austria, Sept. 1982, EMAS, Warley, UK, Vol. 2, pp. 531-538.

90. Okazaki, M., and T. Koizumi, "Crack Propagation of Steels during Low Cycle Thermal-Mechanical and Isothermal Fatigue at Elevated Temperatures," Met. Trans. A, Vol. 14A, 1983, pp. 1641-1648.

91. Heitmann, H. H., H. Vehoff, and P. Neumann, "Life Prediction for Random Load Fatigue Based on the Growth Behavior of Microcracks," Advance in Fracture Research (Fracture 84), Sixth Int. Conf. Fracture, New Delhi, India, Dec. 1984, Pergamon, Vol. 5, pp. 3599-3605.

92. Starkey, M. S., and P. E. Irving, "Prediction of Fatigue Life of Smooth Specimens of SG Iron by Using a Fracture Mechanics Approach," Low-Cycle Fatigue and Life Prediction, ASTM STP 770, American Society for Testing and Materials, 1982, pp. 382-398.

93. Sehitoglu, H., "Fatigue Life Prediction of Notched Members Based on Local Strain and Elastic-Plastic Fracture Mechanics Concepts," Engineering Fracture Mechanics, Vol. 18, No. 3, 1983, pp. 609-621.

94. Dowling, N. E., "Growth of Small Fatigue Cracks in an Alloy Steel," Paper No. 83-PVP-94, ASME 4th Nat. Cong. on Pressure Vessel and Piping Technology, Portland, OR, June 1983. Also circulated as Westinghouse Scientific Paper 82-1D7-STINE-P1, Nov. 1982.

95. Mowbray, D. F., "Use of a Compact-Type Strip Specimen for Fatigue Crack Growth Rate Testing in the High-Rate Regime," Elastic-Plastic Fracture, ASTM STP 668, American Society for Testing and Materials, 1979, pp. 736-752.

96. El Haddad, M. H., and B. Mukherjee, "Elastic-Plastic Fracture Mechanics Analysis of Fatigue Crack Growth," Elastic-Plastic Fracture: Second Symposium, Vol. II, ASTM STP 803, American Society for Testing and Materials, pp. II-689-II-707.

97. Tanaka, K., T. Hoshide, and M. Nakata, "Elastic-Plastic Crack Propagation Under High Cyclic Stresses," Elastic-Plastic Fracture: Second Symposium, Vol. II, ASTM STP 803, American Society for Testing and Materials, pp. II-708-II-722.

98. Leis, B. N., and A. Zahoor, "Cyclic Inelastic Deformation Aspects of Fatigue-Crack-Growth Analysis," Fracture Mechanics: Twelfth Conference, ASTM STP 700, American Society for Testing and Materials, 1980, pp. 65-96.

99. Landgraf, R. W., J. Morrow, and T. Endo, "Determination of the Cyclic Stress-Strain Curve," J. Materials, Vol. 4, No. 1, March 1969, pp. 176-188.

100. Koibuchi, K., and S. Kotani, "The Role of Cyclic Stress-Strain Behavior on Fatigue Damage Under Varying Load," Cyclic Stress-Strain Behavior--Analysis, Experimentation, and Failure Prediction, ASTM STP 519, American Society for Testing and Materials, 1973, pp. 229-245.

101. Polák, J., M. Klesnil, and P. Lukás, "On the Cyclic Stress-Strain Curve Evaluation in Low Cycle Fatigue," Materials Science and Engineering, Vol. 28, 1977, pp. 109-117.

102. McClung, R. C., "Behavior of Short Cracks Under Low Cycle Block Loading Fatigue Histories," M.S. Thesis, Department of Theoretical and Applied Mechanics, University of Illinois at Urbana-Champaign, 1984.

103. Iyyer, N. S., and N. E. Dowling, "Opening and Closing of Cracks at High Cyclic Strains," Small Fatigue Cracks, Second Engineering Foundation Int. Conf., Met. Society of AIME, 1986, pp. 213-223.

104. Iyyer, N. S., and N. E. Dowling, "Closure of Fatigue Cracks at High Strains," NASA CR-175021, Dec. 1985.

105. Rie, K.-T., and R. Schubert, "Note on the Crack Closure Phenomenon in Low-Cycle Fatigue," Second Int. Conf. Low Cycle Fatigue and Elastic-Plastic Behavior of Materials, Munich, Sept. 1987, pp. 575-580.

106. Hatanaka, K., T. Fujimitsu, and S. Shiraishi, "Effect of Mean Stress on Closure and Growth of Short Cracks in Low Cycle Fatigue," Trans. JSME, Ser. A., Vol. 53, No. 488, April 1987, pp. 740-747 (in Japanese).

107. Hatanaka, K., T. Fujimitsu, and H.Ichiyama, "Effects of Mean Stress and Strain on Crack Growth and Crack Closure in Low Cycle Fatigue," Trans. JSME, Ser. A., Vol. 53, No. 488, April 1987, pp. 748-754 (in Japanese).

108. Vormwald, M., and T. Seeger, "Crack Initiation Life Predictions based on Elastic-Plastic Fracture Mechanics of Short Cracks," Second Int. Conf. Low Cycle Fatigue and Elastic-Plastic Behavior of Materials, Munich, Sept. 1987, pp. 562-568.

109. Dowling, N. E., and N. S. Iyyer, "Fatigue Crack Growth and Closure at High Cyclic Strains," Second Int. Conf. Low Cycle Fatigue and Elastic-Plastic Behavior of Materials, Munich, Sept. 1987, pp. 569-574.

110. Dowling, N. E., and N. S. Iyyer, "Fatigue Crack Growth and Closure at High Cyclic Strains," submitted to Materials Science and Engineering, May 1987.

111. Sehitoglu, H., "Characterization of Thermo-Mechanical Fatigue," Ph.D. Thesis, Department of Theoretical and Applied Mechanics, University of Illinois at Urbana-Champaign, 1984.

112. Kibler, J. J., and R. Roberts, "The Effect of Biaxial Stresses on Fatigue and Fracture," J. Eng. for Ind., Trans. ASME, Vol. 92, 1970, pp. 727-733.

113. Joshi, S. R., and J. Shewchuk, "Fatigue-crack Propagation in a Biaxial-stress Field," Experimental Mechanics, Vol. 10, No. 12, 1970, pp. 529-533.

114. Roberts, R., and S. Pothiraj, "The Effect of Biaxial Stresses and Combined Stresses on Fatigue and Fracture," Second Int. Conf. Structural Mechanics in Reactor Technology, Berlin, Sept. 1973, Vol. 5, Part L, paper L8/3.

115. Adams, N. J. I., "Fatigue Crack Growth in Pure Shear," Third Int. Conf. Fracture, Munich, April 1973, Vol. 6, paper V-522/A.

116. Zamrik, S. Y., and M. A. Shabara, "The Application of Fracture Mechanics Analysis to Crack Growth Rate in a Biaxial Stress Field," IV Interamerican Conf. on Materials Technology, Caracas, Venezuela, June-July 1975, pp. 472-477.

117. Hopper, C. D., and K. J. Miller, "Fatigue Crack Propagation in Biaxial Stress Fields," J. Strain Analysis, Vol. 12, No. 1, 1977, pp. 23-28.

118. Miller, K. J., "Fatigue under Complex Stress," Metal Science, Vol. 11, No. 8-9, Aug.-Sept. 1977, pp. 432-438.

119. Anstee, R. F. W., and S. M. Morrow, "The Effects of Biaxial Loading on the Propagation of Cracks in Integrally Stiffened Panels," Tenth Symp., Int. Comm. on Aeronautical Fatigue, Brussels, Belgium, May 1979, paper 3.9.

120. Charvat, I. J. H., and G. G. Garrett, "The Development of a Closed-Loop, Servo-Hydraulic Test System for Direct Stress Monotonic and Cyclic Crack Propagation Studies Under Biaxial Loading," J. Testing and Evaluation, Vol. 8, No. 1, 1980, pp. 9-17.

121. Taira, S., K. Tanaka, S. Ogawa, and M. Kan, "Fatigue Crack Propagation in Medium Carbon Steel Under Biaxial Stress Cycling," 21st Japan Congress on Materials Research, Tokyo, Oct. 1977, Society of Materials Science, Japan, 1978, pp. 50-55.

122. Taira, S., K. Tanaka, M. Kan, and A. Yamada, "Effect of Non-Singular Stress on Fatigue Crack Propagation in Biaxial Stress Fields," 22nd Japan Congress on Materials Research, Kyoto, Sept. 1978, Society of Materials Science, Japan, 1979, pp. 130-137.

123. Tanaka, K., T. Hoshide, A. Yamada, and S. Taira, "Fatigue Crack Propagation in Biaxial Stress Fields," Fatigue of Engineering Materials and Structures, Vol. 2, 1979, pp. 181-194.

124. Hoshide, T., K. Tanaka, and A. Yamada, "Stress-Ratio Effect of Fatigue Crack Propagation in a Biaxial Stress Field," Fatigue of Engineering Materials and Structures, Vol. 4, No. 4, 1981, pp. 355-366.

125. Kitagawa, H., R. Tuuki, and K. Tohgo, "A Fracture Mechanics Approach to High-Cycle Fatigue Crack Growth Under In-Plane Biaxial Loads," Fatigue of Engineering Materials and Structures, Vol. 2, 1979, pp. 195-206.

126. Kitagawa, H., R. Yuuki, K. Tohgo, and M. Tanabe, "ΔK-Dependency of Fatigue Growth of Single and Mixed Mode Cracks Under Biaxial Stress," Multiaxial Fatigue, ASTM STP 853, American Society for Testing and Materials, 1985, pp. 164-183.

127. Smith, E. W., and K. J. Pascoe, "Fatigue Crack Initiation and Growth in a High-Strength Ductile Steel Subject to In-Plane Biaxial Loading," Multiaxial Fatigue, ASTM STP 853, American Society for Testing and Materials, 1985, pp. 111-134.

128. Brown, M. W., and K. J. Miller, "Mode I Fatigue Crack Growth under Biaxial Stress at Room and Elevated Temperature," Multiaxial Fatigue, ASTM STP 853, American Society for Testing and Materials, 1985, pp. 135-152.

129. Liu, A. F., J. E. Allison, D. F. Dittmer, and J. R. Yamane, "Effect of Biaxial Stresses on Crack Growth," Fracture Mechanics, ASTM STP 677, American Society for Testing and Materials, 1979, p. 5-22.

130. Truchon, M., M. Amestoy, and K. Dang-Van, "Experimental Study of Fatigue Crack Growth Under Biaxial Loading," Advances in Fracture Research (Fracture 81), Fifth Int. Conf. Fracture, Cannes, France, March-April 1981, Pergamon, Vol. 4, pp. 1841-1849.

131. Smith, E. W., and K. J. Pascoe, "The Behavior of Fatigue Cracks Subject to Applied Biaxial Stress: A Review of Experimental Evidence," Fatigue of Engineering Materials and Structures, Vol. 6, No. 3, 1983, pp. 201-224.

132. Miller, K. H., and A. P. Kfouri, "An Elastic-Plastic Finite Element Analysis of Crack Tip Fields under Biaxial Loading Conditions," Int. J. Fracture, Vol. 10, No. 3, 1974, pp. 393-404.

133. Smith, E. W., and K. J. Pascoe, "Fatigue Crack Initiation and Growth in HY100 Steel Subject to In-Plane Biaxial Loading," Report CUED/C-MAT/Tr.95, Cambridge University Engineering Department, Sept. 1982.

134. Clark, W. G. Jr., "Effect of Temperature and Section Size on Fatigue Crack Growth in Pressure Vessel Steel," J. Materials, Vol. 6, No. 1, March 1971, pp. 134-149.

135. McGowan, J. J., and H. W. Liu, "The Role of Three-Dimensional Effects in Constant Amplitude Fatigue Crack Growth Testing," J. Eng. Materials and Technology, Trans. ASME, Vol. 102, Oct. 1980, pp. 341-346.

136. Daiuto, R. A., and B. M. Hillberry, "Effect of Thickness on Fatigue Crack Propagation in 7475-T731 Aluminum Alloy Sheet," NASA CR-172367, June 1984.

137. Shahinian, P., "Influence on Section Thickness on Fatigue Crack Growth in Type 304 Stainless Steel," Nuclear Technology, Vol. 30, No. 3, Sept. 1976, pp. 390-397.

138. Hertzberg, R. W., and P. C. Paris, "Application of Electron Fractography and Fracture Mechanics to Fatigue Crack Propagation," First Int. Conf. Fracture, Sendai, Japan, Sept. 1965, Vol. 1, pp. 459-478.

139. Broek, D., "The Propagation of Fatigue Cracks Emanating from Holes," Report NLR TR-72134C, National Aerospace Laboratory, Amsterdam, The Netherlands, 1972.

140. Leis, B. N., and T. P. Forte, "Fatigue Growth of Initially Physically Short Cracks in Notched Aluminum and Steel Plates," Fracture Mechanics: Thirteenth Conference, ASTM STP 743, American Society for Testing and Materials, 1981, pp. 100-124.

141. Leis, B. N., and R. D. Galliher, "Growth of Physically Short Corner Cracks at Circular Notches, Low-Cycle Fatigue and Life Prediction, ASTM STP 770, American Society for Testing and Materials, 1982, pp. 399-421.

142. Leis, B. N., "Fatigue Crack Propagation Through Inelastic Gradient Fields," Int. J. Pressure Vessels and Piping, Vol. 10, No. 2, March 1982, pp. 141-158.

143. Leis, B. N., "Microcrack Initiation and Growth in a Pearlitic Steel Experiments and Analysis," Fracture Mechanics: Fifteenth Symposium, ASTM STP 833, American Society for Testing and Materials, 1984, pp. 449-480.

144. Leis, B. N., "Displacement Controlled Fatigue Crack Growth in Inelastic Notch Fields: Implications for Short Cracks," Engineering Fracture Mechanics, Vol. 22, No. 2, 1985, pp. 279-293.

145. Ogura, K., Y. Miyoshi, and I. Nishikawa, "Fatigue Crack Growth and Closure of Small Cracks at the Notch Root," Current Research on Fatigue Cracks, MRS Vol. 1, Society of Materials Science, Japan, 1985, pp. 57-78.

146. Usami, S., "Short Crack Fatigue Properties and Component Life Estimation," Current Research on Fatigue Cracks, MRS Vol. 1, Society of Materials Science, Japan, 1985, pp. 57-78.

147. Tanaka, K., and Y. Nakai, "Propagation and Non-Propagation of Short Fatigue Cracks at a Sharp Notch," Fatigue of Engineering Materials and Structures, Vol. 6, No. 4, 1983, pp. 315-327.

148. Shin, C. S., and R. A. Smith, "Fatigue Crack Growth from Sharp Notches," Int. J. Fatigue, Vol. 7, No. 2, 1985, pp. 87-93.

149. Truyens, P., "Crack Growth under Variable Load in Ships," Ph.D. Thesis, State University of Ghent, Belgium, Nov. 1976 (in Dutch). Also see Nibbering, J. J. W., "Vermoeiing van gelaste constructies," Parts 1, 2, 3, Lastijdschrift nos. 1, 2, 3, 1978 (in Dutch).

150. Hammouda, M. M., and K. J. Miller, "Elastic Plastic Fracture Mechanics Analysis of Notches," Elastic-Plastic Fracture, ASTM STP 668, American Society for Testing and Materials, 1979, pp. 703-719.

151. Hammouda, M. M., R. A. Smith, and K. J. Miller, "Elastic-Plastic Fracture Mechanics for Initiation and Propagation of Notch Fatigue Cracks," Fatigue of Engineering Materials and Structure, Vol. 2, 1979, pp. 139-154.

152. Smith, R. A., and K. J. Miller, "Fatigue Cracks at Notches," Int. J. Mechanical Sciences, Vol. 19, 1977, pp. 11-22.

153. Dowling, N. E., "Notched Member Fatigue Life Predictions Combining Crack Initiation and Propagation," Fatigue of Engineering Materials and Structures, Vol. 2, No. 2, 1979, pp. 129-138.

154. Suresh, S., and R. O. Ritchie, "Propagation of Short Fatigue Cracks," International Metals Reviews, Vol. 29, No. 6, 1984, pp. 445-476.

155. Newman, J. C. Jr., "An Improved Method of Collocation for the Stress Analysis of Cracked Plates with Various Shaped Boundaries," NASA TN D-6376, Aug. 1971.

156. Peterson, R. E., Stress Concentration Factors. John Wiley, New York, 1974, see esp. pp. 130-131.

157. Inglis, C. E., "Stresses in a Plate due to the Presence of Cracks and Sharp Corners," Trans. Royal Institute of Naval Architects, London, Vol. 55, 1913, pp. 219-230.

158. Socie, D. F., N. E. Dowling, and P. Kurath, "Fatigue Life Estimation of Notched Members," Fracture Mechanics: Fifteenth Symposium, ASTM STP 833, American Society for Testing and Materials, 1984, pp. 284-299.